Spectral Enhancement of Quantum Well Laser Diode Bars for Spectroscopic Applications

Brian Sheehy, BSc.

A thesis submitted for the degree of

Master of Engineering

Dublin City University

School of Electronic Engineering

Supervisors:

Prof. Liam Barry (School of Electronic Engineering)

Prof. John Costello (School of Physical Sciences)

Dr. Rainer Bättig (II-VI Laser Enterprise)

September 2015

Declaration

I hereby certify that this material, which I now submit for assessment on the programme of study leading to the award of Master of Engineering is entirely my own work, that I have exercised reasonable care to ensure that the work is original, and does not to the best of my knowledge breach any law of copyright, and has not been taken from the work of others save and to the extent that such work has been cited and acknowledged within the text of my work.

Signed: _____ (Candidate) ID No.: 99316919 Date: _____

ACKNOWLEDGMENTS

Special thanks go to Professors Liam Barry and John Costello for showing the willingness to take me on as a research student and enabling me to “return” to DCU after 5 years away. They engaged and encouraged, advised and helped me develop my ideas. 4 years ago when the idea to pursue a research masters first formed, the journey seemed daunting but with guidance from them, despite working away from campus, they made my task simpler.

The work in this thesis would not have been possible without the help, support and good will of a number of people, firstly my employers, Laser Enterprise Gmbh Zurich, Switzerland, and specifically my direct manager at the time, Tim Kellner, who supported my application for time and resources to undertake this research. Dr. Rainer Baettig, who has been my mentor since I joined company in 2006, was available to answer technical questions and give advice when I needed it. I was given the freedom to explore the subject area, design test profiles and focus on the topic that interested me most. Appreciation also goes to the various colleagues who gave me the time and space to follow this project to its conclusion.

Various people supported and helped me over these years, family at home and but most importantly friends in Zurich who became my support network, without their encouragement, patience and understanding my task would’ve been a lot more difficult.

Contents

List of Figures

Abstract

Spectral Enhancement of Quantum Well Laser Diode Bars

For Spectroscopic Applications

Brian Sheehy (99316969)

Laser diode bars are notoriously poor at delivering narrow linewidth, fully phase coherent, high power laser beams. Over the width of a multiple emitter diode bar, a wavelength shift of several nanometres is normal since, in practice, the central wavelength varies from diode to diode. However, for applications in spectroscopy, emitters with a narrow wavelength band are required so that a particular transition in an atom or molecule can be excited to accurately detect particular gases or particles. This project investigates the possibility of controlling the spectral width of a laser diode bar by controlling the drive current to each individual emitter with the objective of bringing all emitter spectra as close as possible to a defined central output wavelength. Comparing the spectral output obtained by using a single power source for all emitters with that obtained by exercising drive control over each individual emitter, it is shown that the wavelengths of a group of emitters can be made to overlap with each other. It is also observed that by controlling the current inputs to the emitters, multiple wavelengths can be targeted and overlapped in this way. It is also observed that thermal crosstalk between neighbouring emitters has an effect on central wavelength overlapping. This work represents the first step in developing a high power, long range, infrared (IR) laser based spectrometer for applications in remote gas detection, e.g., from smoke stacks, furnaces, power plants, incinerators, landfill sites, etc.

1. Introduction

Spectroscopy takes advantage of the fact that all atoms and molecules absorb and emit light at well defined wavelengths. In the Bohr model of an atom, an electron in a particular orbit is associated with a specific amount of energy which is a minimum when the atom is in its ground state. To move from the ground state to an orbit farther away from the nucleus (i.e., to a higher energy excited state), an electron must absorb energy. They gain such energy in collisions with other electrons, atoms, ions or photons. Electrons can't remain in an excited state indefinitely, albeit some states can have very long lifetimes and are referred to as being metastable. In general, electrons in excited states return to the ground state on a time scale of nanoseconds for typical bound atomic states, a move that requires the release of the same amount of energy that enabled them to become excited in the first place. This energy can generally take the form of a photon, the exception being states lying above an ionization threshold that decay by electron emission (i.e., autoionising or Auger states). Each element has a unique set of Bohr orbits (or quantized energy states) that no other element shares so that the internal electronic structures of the elements are unique; hence they emit concomitantly specific wavelengths of light when their electrons get excited. In essence, every element and molecule has a unique atomic "fingerprint" that takes the form of a set of wavelengths, or a characteristic spectrum (1).

Named after the Indian scientist who first discovered the process, i.e., C. V. Raman, Raman spectroscopy measures the scattering of monochromatic light caused by a sample. The beam from a laser is directed by a system of mirrors to a lens, which focuses monochromatic light onto the sample. Most of the light bouncing off the sample scatters at the same wavelength as the incoming light (elastic or Rayleigh scattering), but some of the light is scattered at different wavelengths. This happens because the laser light interacts with vibrational modes present in the molecules. These vibrations cause the photons of the laser beam to gain or lose energy. The shift in energy gives information about the phonon modes in the system and ultimately about the molecules present in the sample. Laser sources are the key element in this and a number of other forms of spectroscopy (2).

Spectral lines cannot be infinitely sharp, even for motionless, isolated atoms. According to the Heisenberg Uncertainty Principle, as the time available for an energy measurement decreases, the inherent uncertainty in that energy measurement increases. An electron resides in an excited state for a brief time interval (usually on the nanosecond timescale) and therefore the energy of such a state cannot be precisely determined. This uncertainly results

in the natural broadening of a spectral line. Since naturally broadened lines in isolated atoms are usually very narrow, a highly precise and narrow probing laser mode is required to tune into the resonances of such gases. However, by using a laser source with a broader spectral range, one or more gaps will appear in the spectrum of transmitted light corresponding to absorption by the sample gas. (3)

The other externally influenced line broadening contributors are collisional (or pressure) broadening and Doppler broadening. A line broadening mechanism is referred to as homogenous when it results in identical broadening of the lines of each individual atom. Collisional broadening in a gas is due to the collision of an atom with other atoms, ions or free electrons in the gas or plasma. Broadening is referred to as inhomogeneous when it leads to the atomic resonance frequencies being distributed over a band of frequencies and therefore results in a broadened line for the system as a whole without necessarily broadening the line of individual atoms (4). It is more usual in solids where local inhomogeneities give rise to differential wavelength shifting and broadening. In collisional broadening, an atom in an excited state is forced to decay to a lower energy state when it collides with another particle in the gaseous sample thereby shortening the lifetime to a value below the natural one and hence broadening the line to a value above the natural linewidth. In plasmas, where such collisions occur predominantly with electrons, such collisional broadening is a major contributor to so-called Stark broadening (5).

Doppler broadening results from the differences in frequency measured for the radiation emitted from atoms as they travel away from or towards an observer. This is directly related to the kinetic temperature of the system as defined by the Maxwell-Boltzmann distribution function. As a system's temperature increases the velocity of the atoms or molecules increases, also in multiple directions so the spectral line width increases. The total line width as a result of natural, collisional and Doppler broadening is called the Voigt Profile (6). A good example of spectral line broadening is in plasmas where a spectral linewidth on the order of a few times 0.1 nm is typical and is hence within the scope of the lasers used in this thesis (7) (8).

Searching for faint traces of an unusual gas mixed in the air is called "trace gas sensing" (9). By far, the most common method to detect various dilute media such as gases (atomic, molecular or as nanoparticle plumes), is spectroscopy. The telltale pattern of dark absorption lines in a transmission (or absorption) spectrum indicates which gases are present in the mix. A perfect example of this is the solar spectrum. Accurately measuring the concentrations of relatively low-concentration gases from a distance, however, requires a lot of light, generated

by a laser that can be tuned to different wavelengths (10). In such cases the spectral fingerprints are measured from the laser light scattered from the distant target, e.g., smoke stack, atmosphere, etc.

The focus of this thesis is on the development of high average power laser diodes for potential use in remote spectroscopy and specifically gas detection. Knowing that atoms and molecules possess unique spectral signatures enables the use of lasers to detect various materials. Wavelength tuning can be achieved in the laser diode fabrication process and with the use of external wavelength filters, but this thesis aims to show the advantages of the individual tuneability of each of the 64 emitters in the laser diode bar, as opposed to a single current source powering all devices on the bar.

The ability to grow special structures one atomic layer at a time by liquid phase epitaxy (LPE), molecular beam epitaxy (MBE), and metal-organic chemical vapour deposition (MOCVD) has led to an explosive growth of activity and numerous new laser structures and configurations, meaning far greater control over laser characteristics such as wavelength range and spectral width (11). However, laser diode bars are notorious for their poor beam shape, collimation and broad spectral width of the central peak. Multiple emitter devices are also affected by heating due to high fill factors (ratio of active lasing region to passive substrate) which affects the spectrum (12). In order to selectively detect particular atoms or molecules, a narrow spectrum optical source is required (13) (14) (15). Although narrow spectrum laser diodes are available (16)**,** they are relatively low power and hence are not a practical option for applications outside the laboratory, e.g., in standoff detection of hazardous or greenhouse gases. A perfect example of such an instrument is a LIDAR (a combination of "**LI**ght and ra**DAR**). Active LIDAR remote sensing instruments provide information about the three-dimensional distribution of clouds and aerosols by emitting a laser pulse of light and measuring the elapsed time of the return signal.

For the purpose of this thesis, examination of thermal effects as a contributor to wavelength instability and drifts will be addressed. When this thermal interference comes from neighbouring lasers it is known as *Thermal Crosstalk* (17). The heating effects of neighbouring lasers on an individual emitter can be quite significant, with large wavelength shifts being one deleterious consequence. Typically, the output wavelength of a laser increases by ≈0.3 nm for every 1 °C increase in temperature (18). The motivation for this thesis comes from this idea of narrowing the ensemble spectrum of a laser diode array or bar, the spectrum of which is normally very broad and not suited to laser spectroscopy. To date, most molecular gas detection is carried out in a confined chamber with multiple passes of laser light through the

material under examination. With a suitably sensitive detection apparatus, longer range remote detection may become a reality. Currently this is achieved with LIDAR systems using expensive pulsed solid state (e.g. Nd-YAG) or Carbon Dioxide (CO2) lasers (19).

The simple ramping up of the injected current, with a view to increasing laser output power, results in higher junction temperatures and therefore an actual reduction in efficiency when the laser reaches thermal rollover, a reduction in output power and also a shift in the wavelength. When dealing with a multi-emitter laser, these effects are exacerbated due to the increased power output in a confined area. The thermal load on the cooler body is increased, especially at higher powers. Above certain limits (approximately 100 W) actively cooled devices are required to maintain a laser's output potential and are reliable in terms of maintaining output power and their specified wavelength for the duration of their lifespan. Slight differences in chip characteristics or defects in the wafer will also affect the ultimate optical performance of any one emitter in comparison to its neighbours. With the ability to control the operating current of each individual emitter, the output wavelength could be fine-tuned to take into account differential thermal effects between neighbouring emitters. Aligning a single fibre in front of each individual laser emitter while all are active is necessary in order to capture the true impact of thermal crosstalk on each emitter and adjust the input parameters accordingly. To select, measure, and ultimately adjust the spectral central wavelength and distribution of each emitter, an automated fibre scanning system is required along with a feedback loop to adjust the injection current to overlap each emitter central wavelength in turn. In a further development of this proposal, a multi-fibre array would permit the design and manufacture of a multichannel emitter control system so that all feedback channels could be operated in real-time. This thesis aims to show that a relatively narrow line width can be achieved with electronic circuitry and an appropriate laser design including cooler body to enhance thermal stability.

The basic structure of this thesis is as follows. Chapter 2 contains a review of laser diodes with particular focus on the laser diode bar and the parameters affecting performance, specifically spectral performance. Chapter 3 focuses on spectroscopy and the use of laser diodes in the advancement of this area. Chapter 4 provides an insight into the lasers used in the experiments, how they were mounted on their packages, and introduces the test equipment. Chapter 5 discusses the testing at the initial characterisation stage, looking at basic parameters of the modules such as Power-Current-Wavelength, while Chapter 6 goes into a more in depth analysis of how individual emitters behave in the laser array in relation

to their position on the laser bar, how to control them and eventually combine multiple emitters' spectra into a usable narrow line width.

2. Laser Diodes

This chapter introduces the basic concepts and characteristics of the laser diode, the idea behind quantum well lasers, the formation of modes, how to control them and the form factors used for single chip and multi-emitter devices. Also included is a section on the molecular beam epitaxy process and the standard fabrication of laser diodes.

2.1 Laser Diode Fundamentals

The laser is a very important optical tool that has found widespread use in science, engineering, medicine and industry, from high resolution and ultra-fast spectroscopy, to precise, high power welding. The basic element of any laser is a gain medium (20). This gain medium, which can be solid, liquid, or gas, contains atoms or molecules in excited states that emit light over a range of wavelengths. In order for lasing to occur, the lasing host material must be excited, either through electrical means or another optical source, to create a population inversion between the upper and lower quantum states of the active atomic or molecular species of the host laser material. Of all the lasers commercially available, semiconductor laser diodes demonstrate the following characteristics, which make them extremely suitable for many applications:

- the best wall plug efficiency (in the region of 85%) compared to gas, liquid and other solid state lasers
- high life expectancy (20,000 hours in continuous mode) depending on operating conditions
- cooling requirements are greatly reduced because electrical to light conversion is high – little heat waste
- low weight and small volume of individual devices and arrays make them attractive for integration into many measuring instruments and systems

Many issues remain with using laser diodes, including sensitivity to electrostatic discharge, the fact that multimode emission is normal without more complex cavity designs, and the output from the facet is poorly collimated and presents problems with external alignment optics (21).

Laser action in semiconductor laser diodes, in contrast to other solid state lasers, is associated with radiative recombination of electrons and holes at the junction of a n-type material (excess electrons) and a p-type material (excess holes). Figure 2-1 shows graphically how this happens; excess charge is injected into the active region via an external electric field

applied across a simple p-n junction (homojunction), or in a heterostructure consisting of several layers of semiconductor materials that have different band gap energies but are lattice matched.

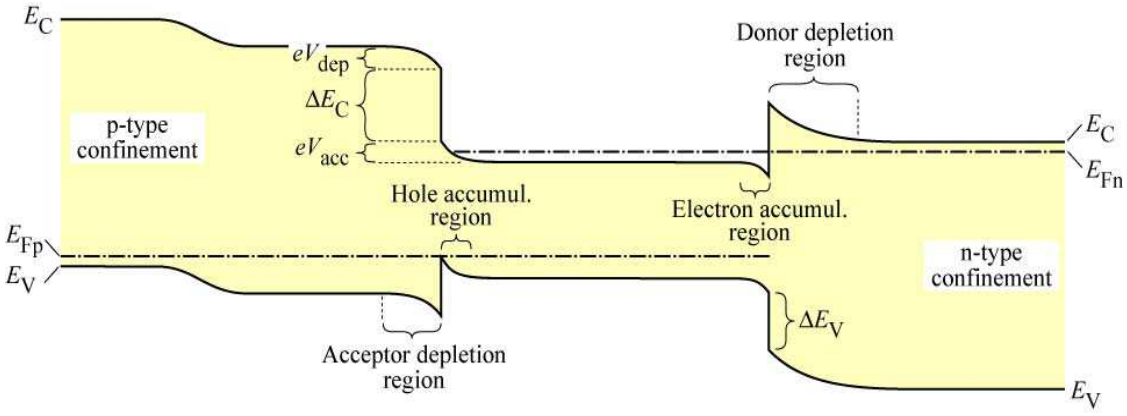

Figure 2-1: Electron-hole recombination in a heterostructure material (22), where E_c is Conduction band energy of material, E_v is the Valence band energy, E_{FP} is the Fermi energy of the holes, E_{Fn} is the Fermi energy of the electrons.

When the dimensions of the semiconductor material reach <100 nm, quantum effects modify the band gap. Quantum wells result from confinement in one dimension, quantum wires from confinement in two dimensions, and quantum dots or boxes from confinement in three dimensions. The wavelength of quantum well lasers can be changed by varying the quantum well thickness or the composition of the active material. By using materials of different lattice constants, thereby effectively straining the materials, one can further engineer the band gap (23). Figure 2-2 gives an overview of the wavelength ranges of different materials and compounds used in laser diode fabrication.

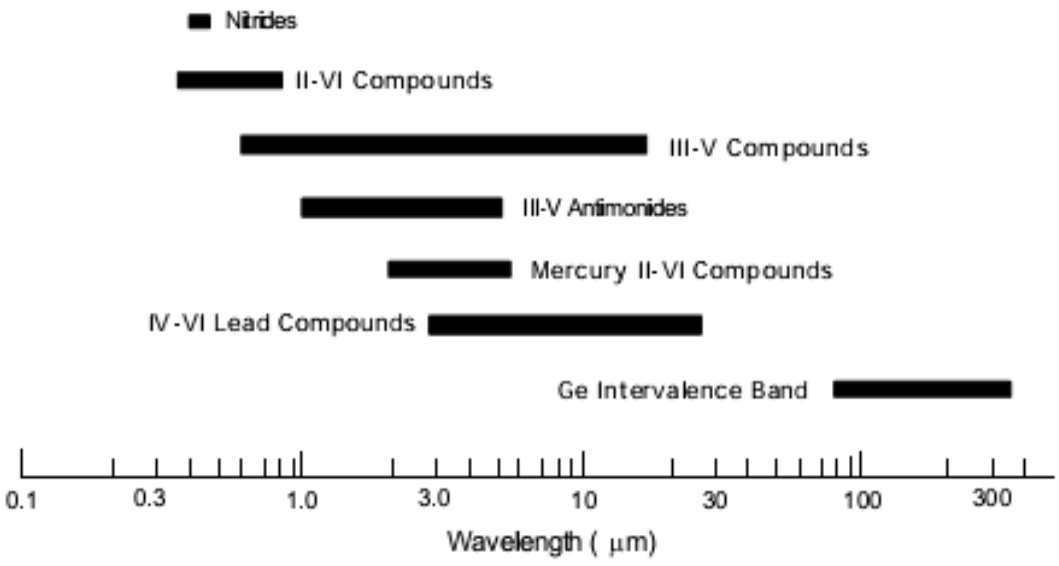

Figure 2-2: Ranges of reported output wavelengths for various types of semiconductor lasers (21).

2.1.1 Quantum Well Lasers

A quantum well (QW) laser diode is a double heterostructure laser diode whose active layer contains a QW in contrast to a conventional double heterostructure laser diode whose active layer is so thick (more than 50nm) that quantum size effects are not expected. The first demonstration was achieved by van der Ziel *et al.* (24), but with limited success due to the early development stage in epitaxial technology at that time. Quantum well semiconductor lasers offer the advantages of low threshold current density and high-power capability with good efficiency. This principal feature of the QW laser, i.e., extremely high optical gain obtained in the QW for low current input, results in part from greater population inversion at a given carrier density because of the lower quantised density of states, but also from the aforementioned high carrier density in the QW because of its small width.

Equally important in determining laser properties is the modal gain which is determined by the optical confinement factor and the ability to collect injected carriers efficiently. These factors prevent the improvement of laser performance at arbitrarily-thin QW dimensions unless additional design features are added e.g. multiple QWs, and addition of waveguide layers to increase the optical confinement factor and carrier collection (25).

The lasing material may be elemental but more generally is a binary, ternary, or quaternary compound semiconductor. Gallium-arsenide and indium-phosphide lasers are commercially made from the III–V group of semiconductor materials. Semiconductor laser diodes emit from the visible to near-infrared wavelengths from 0.63 to 1.55 μm including the InGaAsP/InP 1.3–1.55 μm optical communication lasers, as well as the GaAs/AlGaAs 0.78 and 0.83 μm lasers.

2.2 Laser Modes

A laser cavity contains lateral, transverse, and longitudinal modes - orientation relative to the diode. Longitudinal modes are in the direction of the propagation of the light, transverse is perpendicular to the diode/substrate, while lateral refers to the direction parallel to the diode/substrate. The mode is the volume/shape of light within the cavity. The cavity is defined by the facets of the cavity in the longitudinal direction and waveguides in the lateral and transverse directions.

Some important properties of laser diodes are determined by the geometry of the optical cavity. Generally, in the vertical direction, the light is contained in a very thin layer, and the structure supports only a single optical mode in the direction perpendicular to the layers. In the transverse direction, if the waveguide is wide compared to the wavelength of light, then

the waveguide can support multiple transverse optical modes, and the laser is known as 'multi-mode'. These transversely multi-mode lasers are adequate in cases where one needs a very large amount of power, but not a small diffraction-limited beam.

In applications where a small focused beam is needed, the waveguide must be made narrow on the order of the optical wavelength. This way, only a single transverse mode is supported and one achieves a diffraction-limited beam. Such single spatial mode devices are used for optical storage, laser pointers, and fibre optic applications. Note that these lasers may still support multiple longitudinal modes, and thus can lase at multiple wavelengths simultaneously.

The separation distance of the mirrors L is usually much greater than the wavelength of light λ, so the relevant values of q (mode integer) are large. The frequency separation between any two adjacent modes, q and q+1, in a material that is transparent at the laser wavelength, are given (for an empty linear resonator of length L) by Δv: To calculate the frequency (mode) spacing in a cavity, the following formula is used:

$$\Delta \boldsymbol{\upsilon} = \frac{\boldsymbol{c}}{\boldsymbol{2nL}} \tag{2.1}$$

where c is the speed of light, n is the refractive index of the material and L is the cavity length. The dimensions of the cavity determine the number of supported modes.

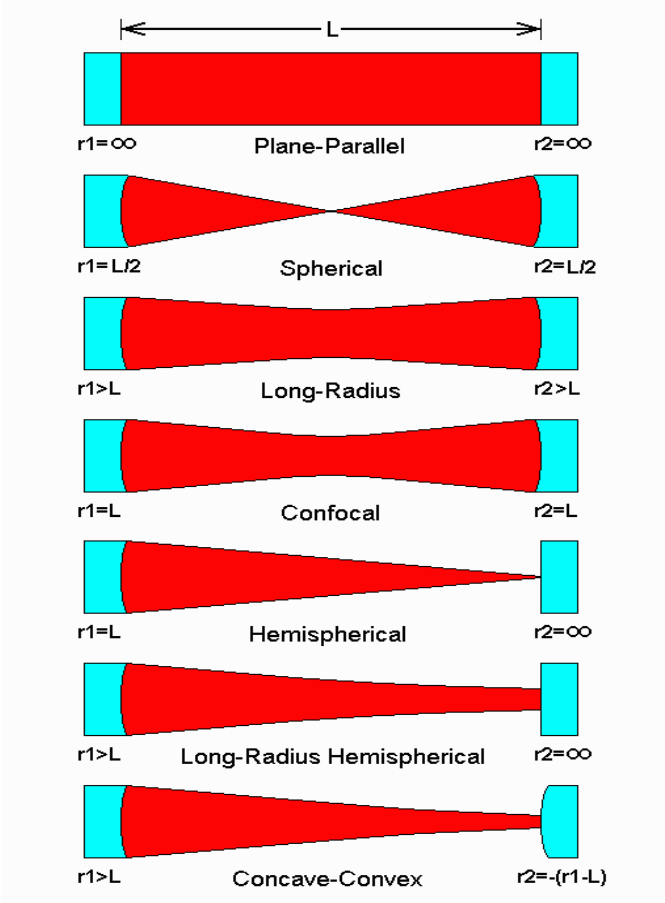

Figure 2-3: The different resonator configurations are shown above. The plane parallel laser resonator design is used in this thesis (26).

The modes within the resonator are electric field distributions that maintain their complex amplitude distribution after a complete resonator round trip, apart from a possible loss of optical power.

The simplest resonator mode is referred to as a Gaussian, with a focal point on one laser mirror (shown as “hemispherical” in Figure 2-3), where the beam radius at the focus is such that the wave front curvature matches that of the curved mirror. In addition, a stable resonator has higher order transverse modes with structured intensity distributions. In cases with cavity aberrations there are Hermite Gaussian modes where the electric field is proportional to the product of the Gaussian function and the Hermite polynomial (27). Hermite-Gaussian modes are a convenient description for the output of lasers whose cavity design is not radially symmetric. Some examples of the optical field distributions, computed using Hermite-Gaussian functions, are shown in Figure 2-4 below. Along with their intensity profiles, it shows the shape of different mode configurations. In a single transverse mode laser, only TEM_{00} modes oscillate.

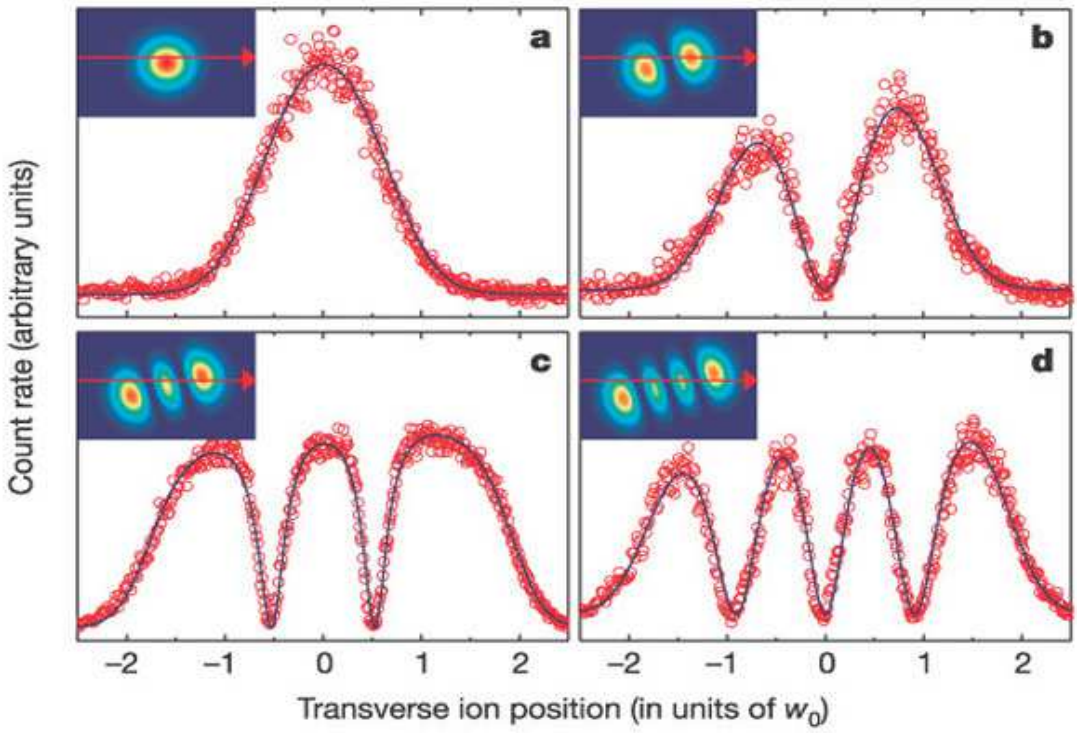

Figure 2-4: Computed Hermite-Gaussian functions to simulate mode (field) profiles in a resonator. The solid line is a fit including saturation of the transition. The inset shows the calculated intensity distribution of the mode and indicates the scan path. The modes are TEM00 (a), TEM01 (b), TEM02 (c) and TEM03 (d) (28).

For transverse electromagnetic modes (TEM), the mode frequencies can be calculated as:

$$\boldsymbol{\nu_{nmq} = \nu_0 + q\Delta\nu + (n+m)\delta\upsilon} \qquad (2.2)$$

where q is the axial mode index, $\Delta\nu$ is the free spectral range and $\delta\upsilon$ is the transverse mode spacing. As an example of longitudinal single and multimode lasers, Figure 2-5 shows the characteristics of the spectra of 2 such devices. The precision of the central peak is very clear to note.

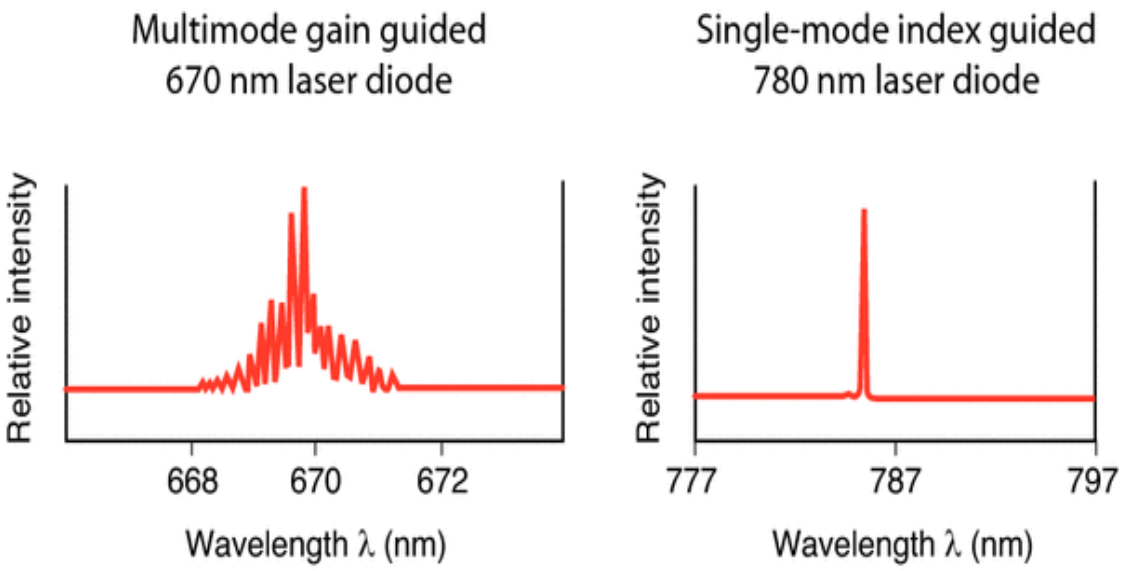

Figure 2-5: Examples of longitudinal multimode and single mode laser spectra (29)

2.3 Types of Laser Diode

A laser diode's characteristics predominantly come from the material from which it is manufactured. For the wavelength range under discussion in this thesis, 830 nm, gallium arsenide is the compound of choice.

2.3.1 Gallium Arsenide (GaAs)

Gallium arsenide (GaAs) is a solid state compound of the elements gallium and arsenic. It is a III-V direct band gap semiconductor with a zinc blende crystal structure (30). GaAs is often used as a substrate material for the epitaxial growth of other III-V semiconductors including: Indium gallium arsenide, aluminium gallium arsenide and others.

Some electronic properties of gallium arsenide are superior to those of silicon. It has a higher saturated electron velocity and higher electron mobility, allowing gallium arsenide transistors to function at frequencies in excess of 250 GHz. Unlike silicon junctions, GaAs devices are relatively insensitive to heat owing to their wider band gap. This is a result of higher carrier mobilities and lower resistive device parasitics. This also adds to their benefits for spectroscopic applications enabling laser diodes to be used in more extreme environments. Also, GaAs devices tend to have less noise than silicon devices, especially at high frequencies. These properties result in the employment of GaAs circuitry in mobile phones, satellite communications, microwave point-to-point links and higher frequency radar systems. It is also used in the manufacture of Gunn diodes for the generation of microwaves (31). Another advantage of GaAs is that it has a direct band gap, which means that it can be used to absorb and emit light efficiently. Silicon has an indirect band gap and so is relatively poor at emitting light.

2.3.2 Laser Diode - Single Emitters

Laser diodes can be created as a single emitter, an array or multiple arrays, known as a stack. Individual laser diodes soldered to a submount or directly to a cooling block are the most common type of laser diode device. These devices are used for solid-state laser pumping, medical, analytical, and printing applications. Laser diodes have extremely low threshold currents and high power intensities. *Dong Zhen et al.* (32) demonstrated an 8mA threshold current on a ridge wave-guided laser diode in November 2013. 76 mW was achieved with 100 mA drive current in single mode operation at room temperature. The maximum power reached was 450 mW.

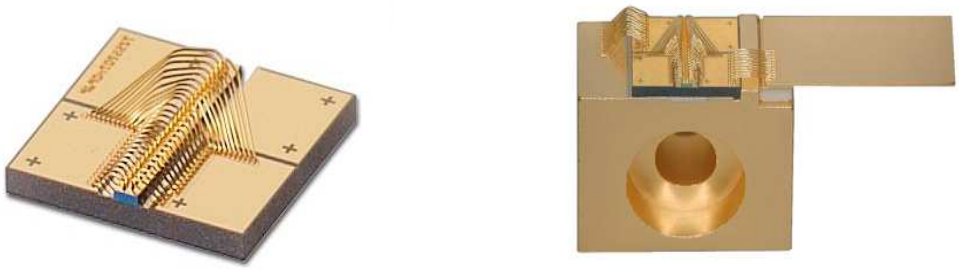

(a) (b)

Figure 2-6: (a) A single emitter laser on a submount, with anode contacts to the left and right of the chip (b) a submounted laser on a C-Mount with anode contact coming via the isolated "wing" on the right and the cathode to the back left (33).

2.3.3 Laser Diode - Bars

Diode bars are high-power semiconductor lasers containing a one-dimensional array of broad-area emitters. They typically contain between 20 and 50 emitters, each being approximately 100 µm wide. A typical commercial device has a laser resonator length of the order of 1 mm. The devices used in this thesis have a resonator length of 1.2 mm.

Important design parameters for diode bars are the number of emitters, their width and their spacing (referred to as pitch). With respect to beam quality and brightness, it is ideal to get the output power from a small number of closely spaced emitters. However, the optical intensity at the output facet is limited by the risk of catastrophic optical damage to the mirror coatings and by the active lasing volume. In addition, closely spaced emitters may be too difficult to cool, at least in continuous-wave operation; such diode bars are sometimes used only in quasi-continuous-wave operation with short (<microsecond) pump pulses (34).

The semiconductor chip of a diode bar is usually soldered to a thin submount, which also forms one of the electrical connections; an insulated wire bond plate positioned beside or behind the chip provides the cathode connection. The submount is then placed on a heat sink, which is often water-cooled (with a macro-channel or micro-channel cooler), allowing

for a high *fill factor* (ratio of emitter width to total width of emitting region) of e.g. 80% and thus provides for a high brightness module. Conduction-cooled bars (often used with a thermoelectric cooler) have a lower fill factor of e.g. 30%, because the heat cannot be removed as efficiently. Passive devices are cheaper to produce and their form factor allows them to be installed in systems more easily. In both cases, the diode bars are often produced in hermetically sealed packages.

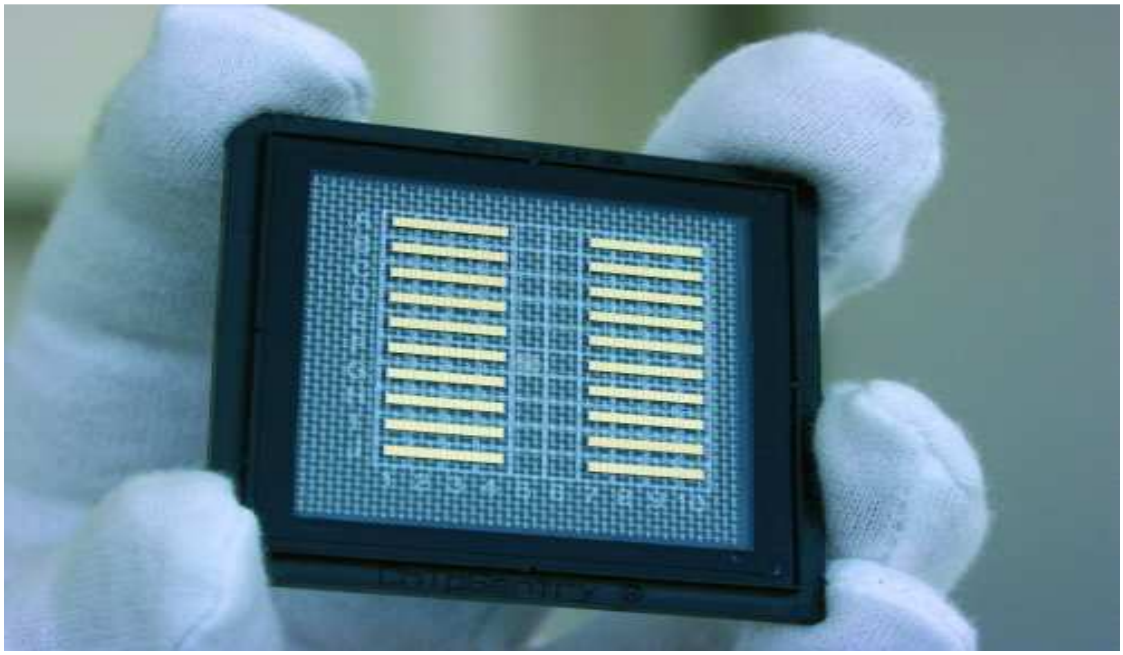

Figure 2-7: Unmounted laser diode bars in a gel pack (35).

Electrically, the emitters are all connected in parallel. This means that the overall drive current is substantial, of the order of tens or even hundreds of amperes. One obtains roughly 1 W of optical output power per 1 A of current; combined with the typical bias voltage of ≈2 V, this results in a wall-plug efficiency of the order of 50%. Crucial technological goals are to reduce the operating voltage by optimizing electrical contacts and layer structures, to reduce further the thermal impedance, and to improve methods for facet passivation, effectively allowing higher optical intensities without the risk of catastrophic damage. Improved power efficiency reduces the total electrical power demands and also the demands on the cooling system, and concomitantly allows for higher brightness. Often it comes with the additional effect of reducing the price per watt of output power.

Under ideal conditions, diode bars can have lifetimes of many thousands of hours. However, devices often fail long before the specified lifetime is reached. This is not necessarily a consequence of faults in the production or the design, but can be caused by a variety of factors outside the control of the manufacturer, such as short voltage spikes caused by a defective or ill-designed laser diode driver (often during switching the device on or off), or by

too high an operation temperature, which itself can be caused by too high a drive current or insufficient cooling. Water cooling is usually effective, see Figure 2-8, but its effectiveness can be strongly compromised by corrosion, which can occur when the specifications for the chemical condition of the cooling water (particularly its ion content) are not met. On the other hand, excessive cooling can cause problems via condensation, when the dew point is reached, creating short circuits or more serious consequences. The whole laser diode system has to be properly designed in order to exploit the full lifetime potential of the bars (36).

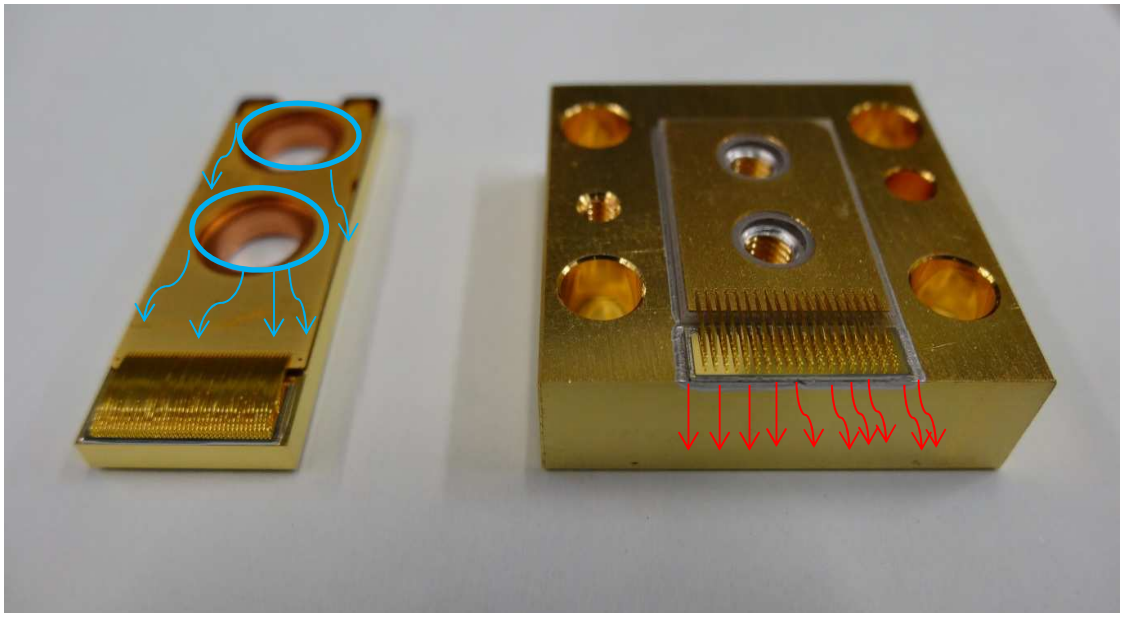

Figure 2-8: Multi-channel high power multimode laser (left) showing cooling water entry and (right) passively cooled laser showing thermal flow from the laser bar (37).

High-power diode bars are used in material processing (e.g. welding and certain surface treatments), in medical applications (e.g. photodynamic therapy, tattoo removal and laser surgery), or for pumping high-power solid-state lasers (bulk or fibre lasers) (33). Diode bars are also under development for military use as battlefield laser weapons. In the future, they may also increasingly be applied in large-volume consumer products such as cars (18).

2.4 Method of Manufacture

There are multiple fabrication techniques employed in the manufacture of laser diodes - liquid phase epitaxy (LPE), and metal-organic chemical vapour deposition (MOCVD), however only molecular beam epitaxy (MBE) is applicable to the devices used in this thesis.

2.4.1 Molecular Beam Epitaxy (MBE)

Scientists discovered the basic idea of quantum mechanics in the early 20th century; however it took nearly half a century for researchers to begin fabricating devices that could exploit the quantum mechanical behaviour of carriers in layers of epitaxially grown ultrathin

semiconductors. These devices brought together the basic quantum mechanical principles with advances in control of doping, layer thickness and band gaps of the layers. Only a small volume of the wafer is actually used for device manufacture - a device can be fabricated on a few microns of wafer surface, but only a few nanometres are needed to implement quantum well technology. Achieving such small scale was not possible until the development of thin-film semiconductor crystal growth techniques such as molecular beam epitaxy (MBE). The diodes used in this thesis are manufactured using this MBE technique.

A.Y. Cho and J.R. Arthur (38) (39) invented the MBE process in the late 1960s. The technology was used in the early 1970s to verify R. Tsu and L. Esaki's prediction that superlattices with interesting electron-transport properties could be fabricated (40).

Figure 2-9 below shows the basic components of an MBE system which usually consists of three ultrahigh vacuum chambers: an introduction chamber, a sample-preparation chamber, and a growth chamber. The introduction chamber, as the name implies, is used to transfer an appropriately prepared wafer, mounted on a molybdenum holder, into an MBE system. The preparation chamber then heats the wafer and holder to a temperature sufficiently high to drive off any atmospheric contaminants from the sample's surface.

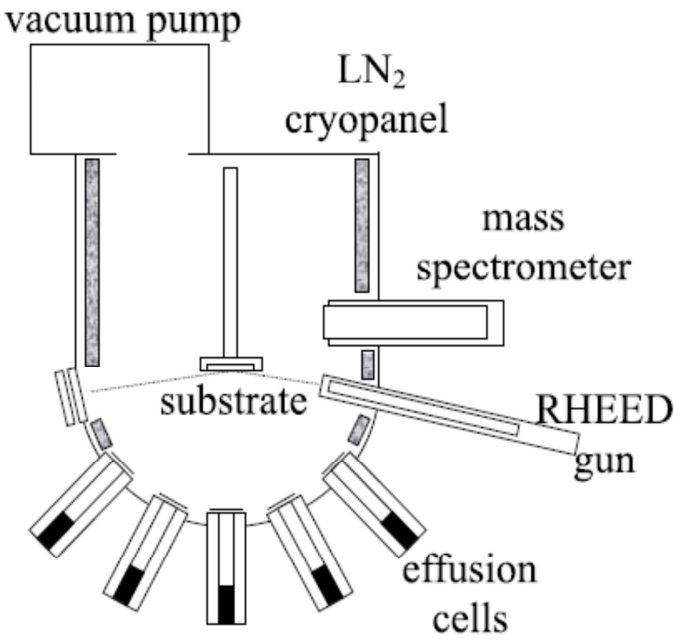

Figure 2-9: A typical MBE system (41).

The effusion cells, also known as Knudsen Cells (named after Martin Hans Christian Knudsen), are the source of the molecular beams. A source material is placed in a crucible within the cells and heated by radiation from a resistive heating source. The solid source material sublimates due to the increased temperature and high vacuum. The pressure of the vapour

can be controlled by varying the temperature of the solid phase, which in turn is controlled by variations in crucible heating. Because the beam intensity within the substrate chamber depends on the effusion cell pressures, the amount of material reaching the surface can be controlled by varying the source temperature.

The growth chamber with a base pressure of 10^{-11} Torr is the heart of an MBE system. In the growth chamber, samples are first rotated into a position that facilitates crystal growth. They are then heated to the appropriate temperature and bombarded with molecular beams of constituent and dopant materials. By directing appropriate fluxes of these beams onto the sample substrates, one can initiate epitaxial single-crystal growth.

A RHEED (reflection high energy electron diffraction) monitoring system is implemented in modern MBE equipment (42). The RHEED system is used to monitor the structure and/or composition of the growth surface during deposition. High energy electrons are incident upon the surface, producing a diffraction pattern upon the RHEED screen. The diffraction pattern can be analysed to determine material characteristics, like the structure, as well as composition. The intensity of the diffraction pattern has been found to vary predictably with the surface layer formation (42), and can be used to determine when a monolayer has been fully formed. This information can be used to control the effusion cell shutters to produce an atomically flat surface (42). During MBE growth, a very significant portion of the crystal is affected by its proximity to the surface. A greater amount of surface diffusion increases the rate of growth, as well as the surface quality. If atoms arriving can travel farther along the surface, they are more likely to arrive at the lowest energy, defect-free, state. The surface area must be heated sufficiently so that the thermal energy of the diffusing atoms is great enough to diffuse out defects.

Minimisation of surface energy is a major driving force for growth in MBE. When a single atom arrives on the surface, the total number of broken atomic bonds associated with the surface (in other words, its energy) increases. This atom on its own is not favoured to remain on the surface, and is likely to return to the vapour phase after diffusing along the surface. If another atom should arrive nearby, and the two interact while diffusing, the number of broken bonds associated with the two atoms is decreased. The addition of a third atom leads to a further decrease in surface energy. This leads to the formation of groups of material on the surface. Figure 2-10 shows graphically that as more and more atoms arrive near the group, they tend toward the group, resulting in further localised growth.

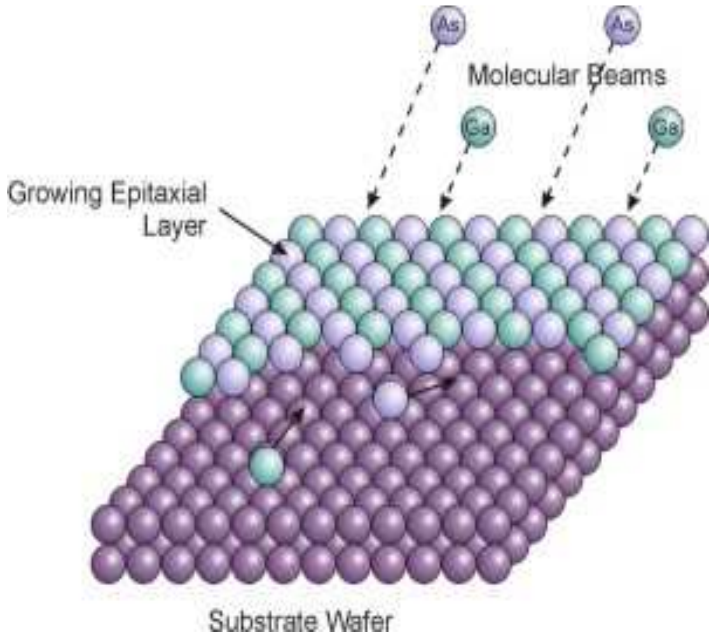

Figure 2-10: MBE growth mechanism of a heteroepitaxy layer GaAs (43).

Atoms that arrive on top of the group will tend to diffuse off the group over a ledge. This jump down is energetically beneficial. The number of broken bonds associated with the atom on top of the group is greater than that of an atom on the edge. Similarly, atoms will diffuse toward kinks in the ledge as opposed to open regions. No additional broken bonds are associated with joining the kink, whereas the formation of a new section of ledge involves the creation of many new broken bonds. This results in the growth of relatively circular groups. Due to the slow rate of growth in typical MBE applications, the rate of diffusion across the surface is great enough that atoms landing on top of an island on an incomplete layer will diffuse across the group, joining the incomplete layer (44).

In the GaAs materials system, GaAs epitaxial layers will grow on a GaAs substrate at a rate of 1 *µm/h* under the following conditions: substrate surface temperature of 580 °C; Ga-beam equivalent pressure of 5 x 10^{-7} Torr, corresponding to a Ga furnace temperature of about 1185 °C; and an As-beam equivalent pressure of 5 x 10^{-6} Torr, corresponding to an As furnace temperature of about 310 °C (45).

Control of the composition and doping of the growing structure at monolayer level is via computer controlled shutters. Growth rates can be shuttered in a fraction of a second allowing nearly atomically abrupt transition from one material to another. Independent heating of material sources allows more control of the process. The RHEED gun is used for monitoring the growth of the crystal layers and a mass spectrometer is installed for monitoring the residual gases and checking source beams for leaks. A cryogenic screening around the substrate acts as a pump or cold trap for residual gases. (46)

2.5 Conclusion

Chapter 2 has covered the basics of the laser diode in single chip form, but has gone into greater detail on laser bars; the description of modes and resonator types, and showing the difference between a multiple longitudinal mode and single mode laser. It has explained the concept of emitter spacing “pitch” and its effect on the laser efficiency and reliability along with the contribution this makes to the thermal effects of the module, and how this influences the package type used. The chapter has also explained the functionality of a laser, and how they are mounted and packaged as an end product. Finally, the fundamental ideas of the MBE process for fabricating these laser bars has been described.

3. Spectroscopy with Semiconductor Lasers

Semiconductor lasers were first introduced in the mid-1960s and found immediate application as much needed tuneable sources for high-resolution infrared laser absorption spectroscopy. All optical spectroscopy designs contain a radiation source, a detector, wavelength selector and the species under investigation in a closed absorption cell for the determination of gas concentrations according to Beer's law (47). To obtain the required specific optical frequency, wavelength selective elements (e.g., A Fabry-Perot interferometer) have to be inserted into the optical path.

In principle, laser spectrometers allow less complex opto-mechanical designs than analytical instrumentation, and semiconductor lasers modulation, if required, for example for phase sensitive detection, can be implemented electronically. Therefore, laser diode spectroscopy is an attractive and promising technique for analytical instrumentation. The most important research applications of **T**uneable **D**iode **L**asers (TDLs) in atmospheric field measurements require long-path absorption cells to provide high-sensitivity local measurements. In high resolution spectroscopy, a single narrow laser line usually scans over an isolated absorption line of the species under investigation (48).

Environmental monitoring of the air to assess its composition and to identify pollutants is important for health and environmental research and for the control of industrial discharges (e.g., in plasma processing of semiconductor materials). Many different techniques are available (49), and modern equipment includes portable instruments giving immediate warning of harmful contaminants, which are very useful in industrial and fire-fighting situations. For environmental studies, however, it is more important that the measurements are carried out consistently over a long time period, as they can then be used to assess the effectiveness of legislation and pollution-abatement programmes. As such, there remains a place for more traditional equipment and measuring techniques that comply with established standards (49). In this regard, the durability of laser diodes is an extremely attractive feature. If the difficulties in achieving a high power output along with a narrow spectrum could be overcome, this advantage could be extended and would allow significant improvements to standoff or remote measurements with TDLs.

This chapter will give an overview of the application of lasers, describing the role they play in spectroscopy. A synopsis of the different types of spectroscopy employing laser diodes will also be reviewed.

3.1 Types of Spectroscopy

In tuneable laser diode spectroscopy, the laser plays the most critical role as part of the spectrometry system. The ideal requirement is to force the laser to operate in a single longitudinal mode, in the milliwatt (mW) power range and with little noise. Single mode operation is required to prevent absorption signals from other nearby transitions, close in wavelength or equivalent optical frequency to the species under examination and to minimise noise.

An important aspect of any gas-sensing device is the limit-of-detection. It is determined ultimately by the signal-to-noise (SNR) ratio and signal-to-background (SBR) ratio attainable. Accordingly, much effort has been devoted to developing detection methods over the past decade to increase the sensitivity of laser diode absorption spectroscopy instruments. Wavelength modulation spectroscopy (WMS) with second-harmonic detection, WMS-2*f*, is a type of absorption spectroscopy best known for its ability to make sensitive measurements and reject noise (50). In this technique, laser light is passed through the sample gas as the wavelength is modulated electro-optically by a crystal with high frequency (51). The detection sensitivity is improved by shifting the detection to higher frequencies where laser generated excess noise and detector thermal noise are both much smaller, and the flow-generated noise that lies outside the detection bandwidth is suppressed by the phase-sensitive detection.

3.1.1 Direct Absorption Spectroscopy

Direct Absorption Spectroscopy, or DAS, is the simplest of the laser based absorption techniques. In a DAS system, a tuneable laser beam is fired through a gas sample and the transmitted intensity is measured with a single element detector such as a photodiode or photomultiplier tube. If the intensity of the transmitted light decreases, this indicates the frequency of the transmitted light is close to, or centred on, an atomic or molecular transition. The concentration of the absorbing molecule can be calculated via the relative change in intensity according the Beer-Lambert Law (47).

Absorbance of a sample, A, is given by:

$$A = log_{10} \frac{I_0}{I} \tag{3.1}$$

where I_0 is the initial intensity of light and I is the measured intensity exiting the sample (52).

The Beer-Lambert law takes into account the path length through the sample to be measured:

$$log_{10}\frac{I_0}{I} = \sigma nl \qquad (3.2)$$

where σ is the absorption cross-section (in MB or MegaBarns where 1 MB = 10^{-18} cm^2), n is the gas density in units of cm^{-3}, and l is the absorption path length in cm. Figure 3-1 shows a basic schematic diagram of the functionality of a direct absorption system.

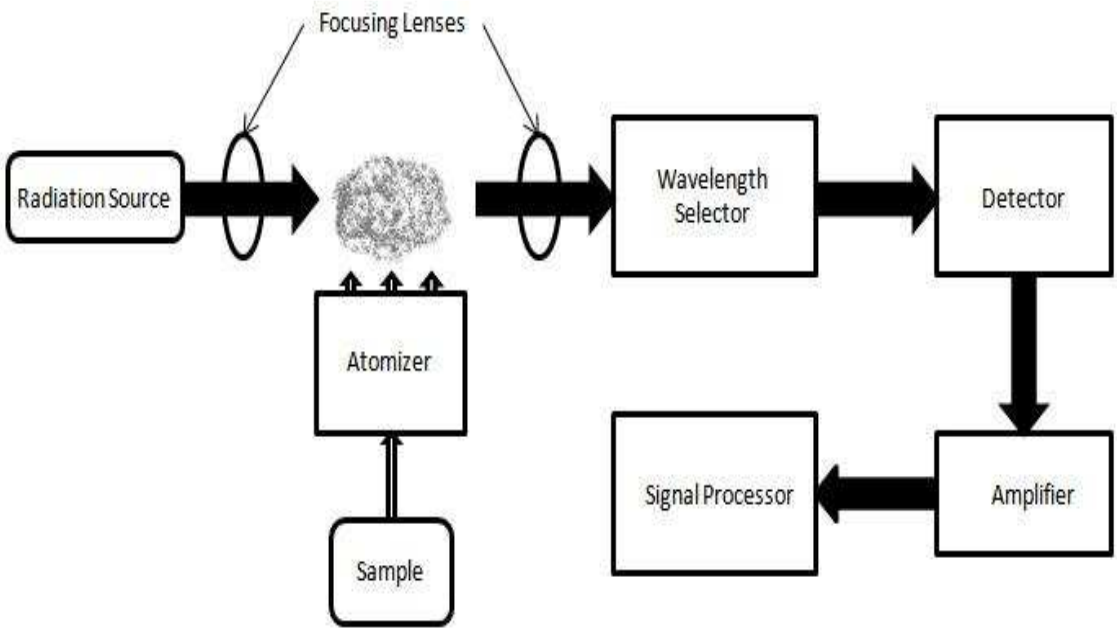

Figure 3-1: Schematic of a general spectroscopy system (53).

3.1.2 Wavelength Modulated Spectroscopy

The drawback of direct absorption spectroscopy is the limited sensitivity, due to low frequency interferences in the measurements coming from mechanical instabilities in the laser and mirrors. This noise is referred to as 'flicker' or 1/*f* noise. The influence of this noise can be reduced by shifting the detection to higher frequencies with the use of modulation techniques, the most common being Wavelength Modulated Spectroscopy (50). The frequency of the laser light is modulated electro-optically, usually in the 100's of kHz range, which leads to a modulation of the transmitted intensity in the vicinity of the transition. The resulting periodic detector signal is then demodulated at a multiple integer of the modulation frequency with the use of a lock-in amplifier. This greatly increases the sensitivity; DAS can detect in the 1000 parts per million (ppm) range, while WMS can do so in the ppm range.

3.1.3 Frequency Modulated Spectroscopy

Frequency-Modulation Spectroscopy or FMS is a powerful technique that can achieve a high signal-to-noise ratio with a relatively simple experimental setup. In a typical FMS experiment, the wavelength of a continuous-wave laser is modulated at a particular frequency. This frequency modulation is much higher than in WMS. As the centre wavelength is scanned across the atomic transition of the target species, the wavelength modulation is converted into amplitude modulation, giving rise to a modulation in the optical absorption of a sample with species that absorb at the laser frequency. Narrow-band demodulation techniques, such as phase-sensitive detection using a lock-in amplifier, then allow the absorption information to be extracted as a DC signal. Because the signal has been moved to a high frequency via modulation, FMS avoids the typical limitations of absorption measurements such as laser-intensity noise, which peak for direct current drive (CW operation) and fall off roughly as *1/f (f* here the frequency of the target transition), hence the name *1/f* noise. Using this technique, absorption sensitivities can reach limits of detection at parts per million (ppm) levels. For example, H_2S has been detected at the ppm level in air (54).

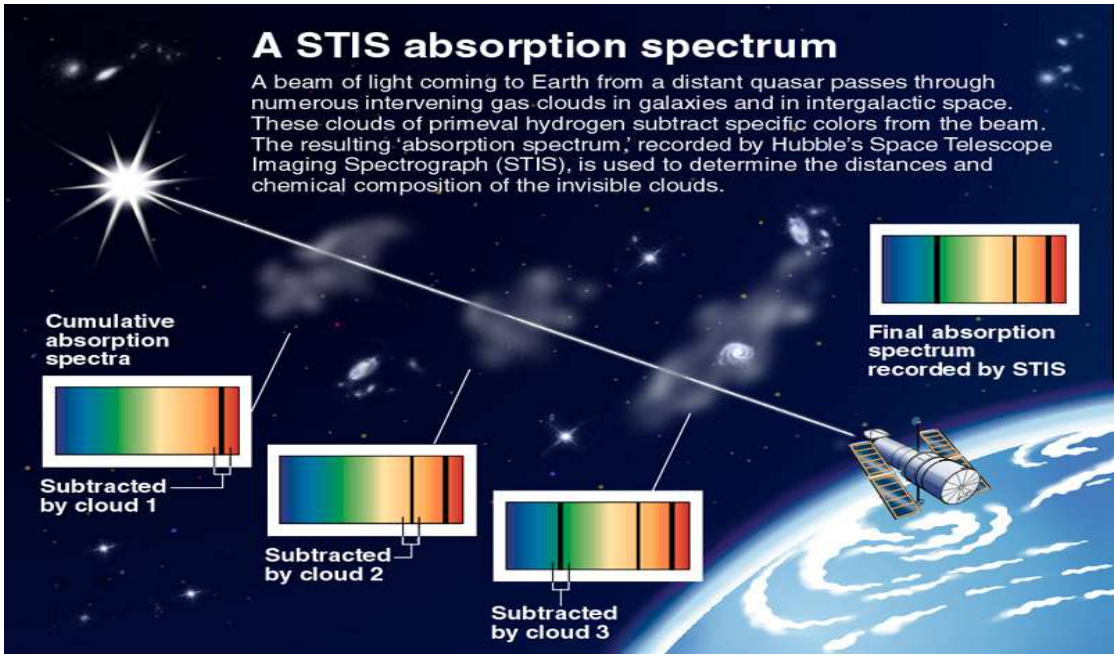

Figure 3-2: Example of remote absorption spectrometry (55).

The principal differences between FMS and WMS are slight, as in both cases it is the frequency of the laser that is modulated. They are two limiting cases of the same technique. In FMS the ratio of modulation frequency to the absorption line width is large, and as a result the absorption feature of interest is probed by a single isolated sideband. In WMS the modulation ratio to absorption line width is small; as a consequence the features are probed

with a large number of sidebands. In both cases the laser diode frequency is modulated via the drive current (56).

3.1.4 Recent developments

The use of tuneable laser diodes is attractive since they are compact, readily available, robust, and compatible with optical fibre technology. Single mode laser diodes are mostly used in spectroscopic applications since their narrow line width provides the necessary high spectral resolution. However, some intrinsic properties of single mode laser diodes can impair their suitability (57). For example, the central wavelength of the single mode laser diode might change with thermal or mechanical fluctuations. Hence, measurements with single mode lasers over an extended period of time will not be systematic and reproducible in a complex ever changing industrial environment. To cope with these problems, a further development of laser absorption spectroscopy using tuneable multi-mode diode lasers (TMDLs) as the light source has recently been reported (58) (59). *Hamilton et al.* (58) reported the use of a multimode laser diode based correlation spectroscopy (COSPEC) to measure oxygen in ambient air, thereby employing a laser diode having an emission spectrum that overlaps the oxygen absorption lines of the *A*-band. A sensitivity of 700 ppm was achieved with good accuracy (2%) and linearity ($R2$=0.999). For comparison, measurements of ambient oxygen were also performed by tuneable diode laser absorption spectroscopy (TDLAS) technique employing a vertical cavity surface emitting laser (59). They demonstrated that, despite slightly degraded sensitivity, the multimode laser diode COSPEC-based oxygen sensor has the advantages of high stability, low cost, ease-of-use, and relaxed requirements in component selection and instrument build-up compared with the TDLAS-based instrument.

3.2 Wavelength and Power Stability

The discussion in this thesis focuses on the wavelength and absorption spectra of target materials. To function consistently and repeatedly, the wavelengths emitted by the laser diodes employed in these spectroscopy applications must be stable, and a multitude of factors can influence this wavelength stability.

3.2.1 Laser Bar Smile

One of the biggest factors affecting emission quality is laser bar smile. This is a bending of the laser bar relative to it's soldered metal contact or submount. In this regard, the coefficient of thermal expansion plays an important role in determining the performance and degradation time of the laser diode product in terms of its output power and wavelength. Materials usually expand with increasing temperature. Even a small degree of Coefficient of Thermal Expansion (CTE) mismatch could cause "smile" which results in poor power and spectral

performance of lasers. A “smile” is a non-linearity of the near-field of emitters. However, external optics can be used to correct, or at least improve, the beam profile (60). Figure 3-3 shows an example of a corrected emitter array. Copper Tungsten (CuW) and Gold Tin (AuSn) are common solder materials used due to their (61):

- high tensile strength of any solder
- High melting point is compatible with subsequent reflow processes
- Lead-free construction
- Superior thermal conductivity
- Resistance to corrosion
- Superior thermal fatigue resistance
- Good joint strength
- Excellent wetting properties
- Resistance to oxidation

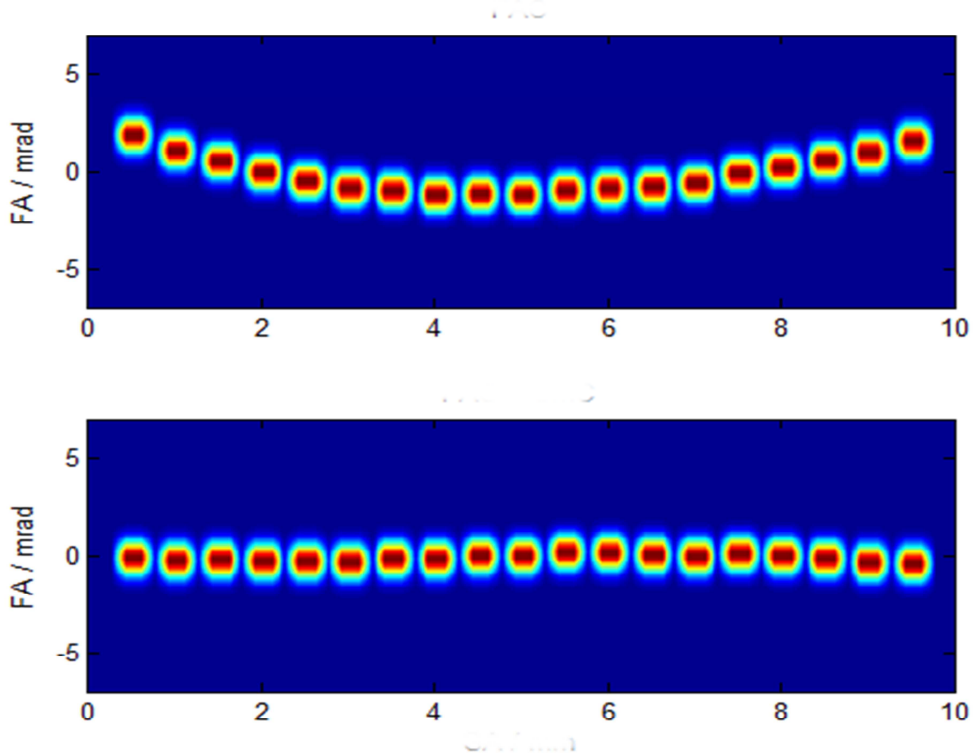

Figure 3-3: Illustration of laser bar smile and offset created (top), with correction lens in place (62).

Recent developments in soldering techniques indicate that low temperature silver sintering will become a much more widely used technology for the soldering of dies allowing a far more reliable soldering process and therefore a more stable heat dissipation (63).

3.2.2 Thermal Crosstalk

The thermal cross-talk is defined as the relative variation of the chip's output power for a given injection current, if all other emitters are switched on and off simultaneously, i.e.,

$$\boldsymbol{Thermal\ Crosstalk} = \frac{\boldsymbol{Power_{all} - Power_{one}}}{\boldsymbol{Power_{one}}} \qquad (3.3)$$

Thermal crosstalk also affects the wavelength of emitters as the heating of a laser causes drift in its output wavelength. Two different cross-talks can be calculated. The first describes the situation when all emitters are switched on ("cold emitters") and one waits until a steady-state temperature is reached (maximum temperature). This is called the "dynamic cross-talk". The second situation starts from one emitter at steady-state temperature and all other emitters are switched on later. Then the power drop is measured after waiting until all chips have reached the steady-state temperature distribution. This is called the "static cross-talk".

Much research goes into the design of the cooler body in order to maximise the transport of heat from the bar. For example, it is important to ensure the right type of flow of water passes through the cooler. In literature a value of about 400 W/(m^2K) for the laminar heat-transfer coefficient compared to about 4000 W/(m^2K) for a turbulent flow of the water is found.

3.2.3 Modelling of Thermal Effects

Recent simulation work (64) gives a good insight into the importance of thermal effects when planning for the design of a laser bar. Figure 3-4 shows the effect of emitter spacing/pitch and the resulting thermal effects on the emitter Current – Power curve obtained from (64). It portrays clearly the correlation between the pitch of the emitters and the effect on output power. The greater the pitch the more efficient the laser becomes, due to a reduction in thermal effects from neighbouring lasers. Thermal "rollover" occurs at high emitter densities as is seen with the spacing of 0 µm. This pitch effect also has an influence on wavelength.

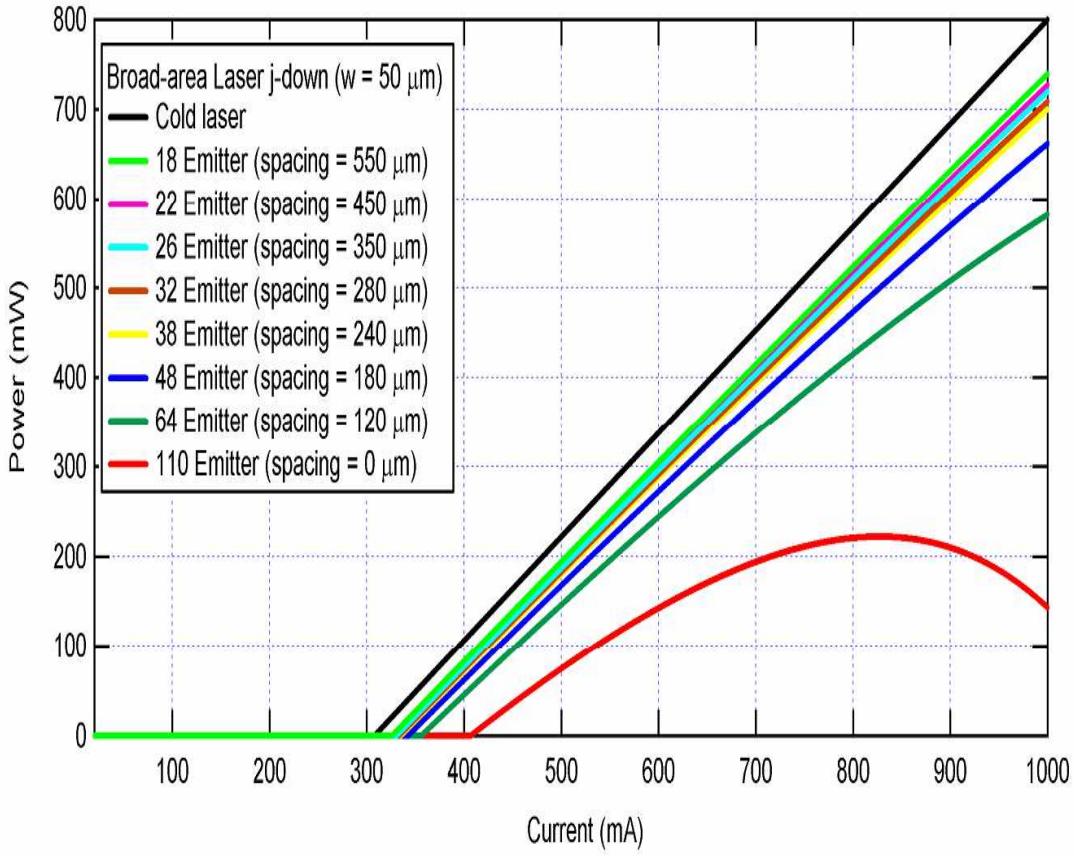

Figure 3-4: Effect of emitter spacing on output power shows emitter proximity plays a big role in efficiency (64).

Simulations of the thermal influence of neighbouring emitters on a lasing emitter were also undertaken in (64). Figure 3-5 shows the results for different cooler body design types where the peak temperature in the first emitter as function of the distance between both emitters can be seen. It is clear that nearest neighbours have the greatest effect. The maximum temperature impact decreases from ≈0.42°C to ≈0.375°C, for the closest 5 emitters reaching an almost constant value for an emitter to emitter separation of around 5 emitters or more.

The plateau defines the thermal resistance of a single emitter, if all other emitters are switched off. Values between single R_{th}^{single} = 23.3 °C/W and R = 24.3 °C/W for the three different cooler designs can be seen. The thermal cross talk is independent of the cooler design. It can be defined as the difference in the peak temperature between two directly neighbouring emitters and a single emitter. The difference value of about 0.047 °C leads to a thermal cross talk of 3.0 °C/W, when the heat load of both emitters is set to 1 W.

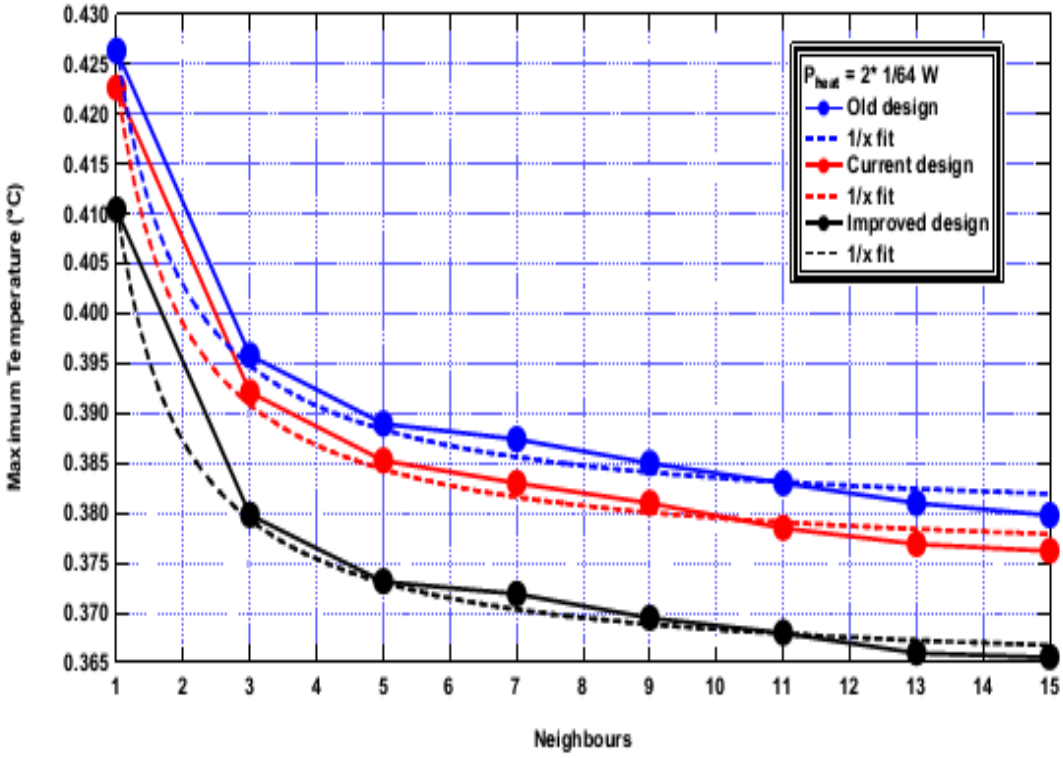

Figure 3-5: Comparison of build designs to show the effects of neighbours on an emitter (64).

Recent work has focused on determining the optimum design of the laser and also on eliminating defects. High resolution thermography is a well-established method for investigating thermal effects in semiconductor devices (65). The method has been successfully used for various analyses of the thermal properties of laser diodes including steady-state and transient characterization of laser bars (66), defect detection and reliability screening (67). Application of the method for characterisation of high-power laser diodes allowed for precise thermal profiling and hot spot detection in high-power laser diodes providing important information about the device performance (67).

The work of *Kozlowska et al.* (68) shows that by changing the structure of the laser waveguide, namely introducing an asymmetric double barrier separate confinement heterostructure, results in lower temperatures. Their work also revealed hotspots at the mirrors detected by thermal imaging as seen in Figure 3-6. These hotspots most probably come from inconsistency in the mounting (soldering) process leading to mirror defects. The laser systems require efficient thermal management which becomes particularly important in the case of high-power operation. Effects such as migration of point defects, or generation of extended defects, can be accelerated by temperature and mechanical stress.

(a)  (b) 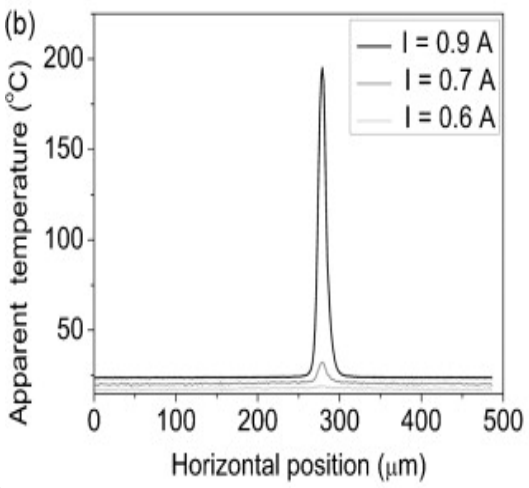

Figure 3-6: CCD image of laser bar, showing (a) a defect on the facet due to a failure of the solder material under the emitter. (b) Shows the temperature profile for different drive currents (69).

It has also been demonstrated that the thermal effects from emitter to emitter are confined to the laser structure rather than the solder/heatsink section of the package. Having measured the transient thermal crosstalk between an emitter and its nine neighbours, the work shows that it has a critical effect on laser performance (70). For the purpose of the experiments carried out as part of this project, there should be no difference in thermal activity between the bar mounted on a passive cooler or the water cooled custom built package.

3.2.4 Effect of Modulating (Pulsing) the Laser Diode

Pulsing (quasi Continuous Wave Mode, qCW) of the diode can limit the thermal effect on the output beam by switching the device off before it reaches an affective thermal state. However, even doing so will still introduce a spectral spread as demonstrated by *Kozlowska et al*. (71). Using wide-stripe laser diode arrays of 0.7 mm cavity length, they used Schottky isolation for the stripe definition. Each array contained 26 x 100 µm wide stripe emitters, with an array pitch of 150 µm. CrPt and AuGeNi metallisations were used as p- and n-contacts, respectively. The facets were high and low reflectivity coated with AlN–Si/AlN multilayers. The arrays were mounted epi-side down with array dies bonded using In-based solder. By using a simple monochromator, *Kozlowska et al.* (71) examined the constituent components of a pulsed diode and Figure 3-7 shows graphically the component wavelengths. It can be clearly seen from the figure; that a thermal shift over the duration of the pulse pushes the dominant central wavelength rom 811 nm to 816 nm.

Even in the case of a laser diode, there is still a relatively broad distribution of wavelength components around the central wavelength. In addition, while pulsing allows for higher peak powers to be reached, as will be demonstrated in the results section, the overall degree of stability of the central wavelength and the overall spectrum remains unchanged.

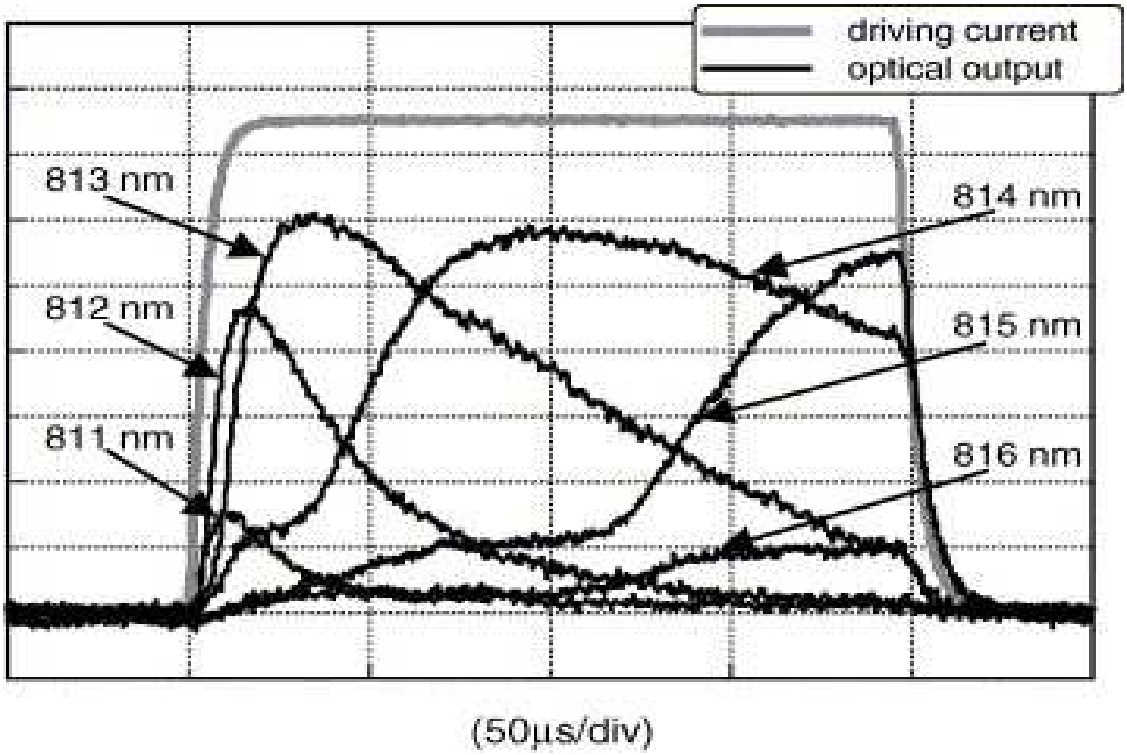

Figure 3-7: This screen shot of multiple sweeps using different wavelength filters shows constituent wavelengths of a pulsed laser diode source (71).

Over the duration of the pulse, as thermal equilibrium is reached, there is still a drift in the dominant output peak wavelength and, as a result, side-nodes appear when the traces in Figure 3-8 are integrated into a single spectrum. Shorter pulses reduce this effect, but this can impact the suitability for a measurement.

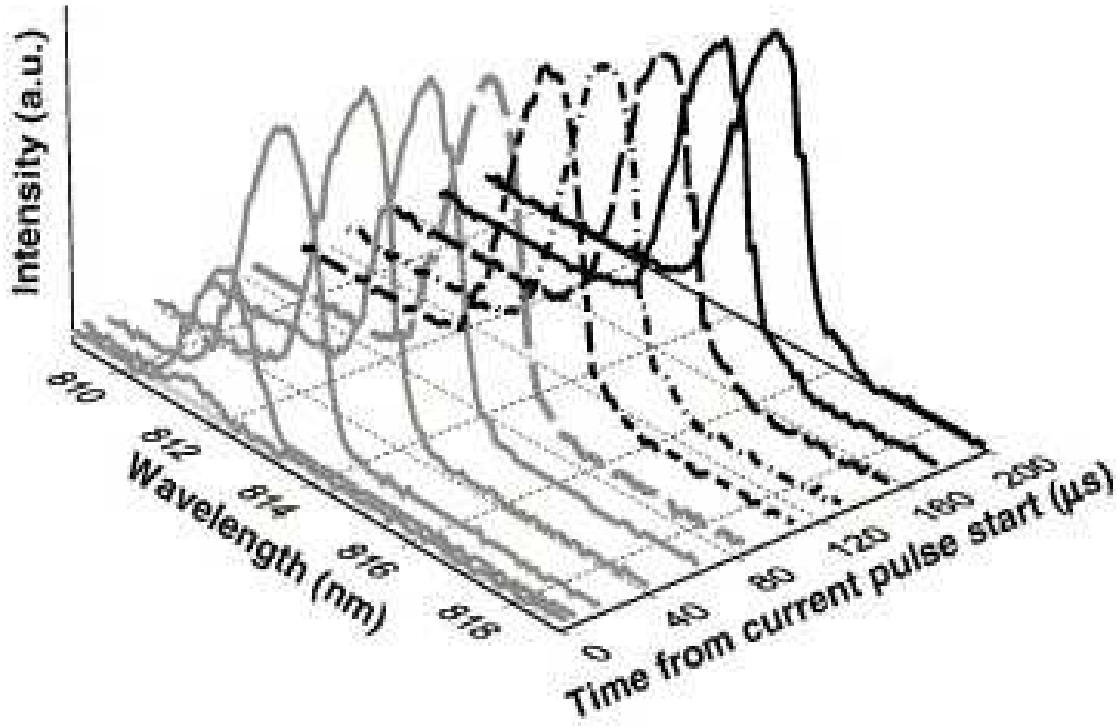

Figure 3-8: Time resolved evolution of the spectral distribution of a pulsed source. It clearly shows the shift in wavelength against time (71).

3.3 Conclusion

This chapter has shown the various spectroscopic techniques used; their advantages and measurement limit. The concept of thermal crosstalk was introduced and the influence of its effects from neighbouring emitters using modelling techniques employed during development of the laser bar was also discussed and explained. There is a brief description of the effects of solder quality and how the correct thermal expansion matched material is critical on the laser bar output, in terms of power.

It has shown that laser diodes are sensitive to external effects such as drive current in continuous wave mode and quasi continuous wave mode and by showing such susceptibility they can be manipulated to our advantage i.e. control of the spectrum by adjustment of the input current.

4. Laser Bars used in Testing

This chapter will provide an insight into the type of laser bar used and how it was mounted to the two types of heatsink. It will provide information on the chip dimensions, features and functions available to the user of the individually addressable laser bar.

4.1 Devices under Test

The lasers used in these experiments were AlGaAs devices, fabricated using Molecular Beam Epitaxy or MBE by II-VI laser Enterprise in Zurich. The aluminium profile of the device can be seen in Figure 4-1. The quantum well size is in the order of nanometres with the graded index doping layer in the order of approximately 100nm. There is a beryllium (Be) graded doping on the N side and a silicon (Si) step graded doping on the P side.

Layer		Width (nm)	Material	x
Start	0.0	0.1	AlGaAs	0.000
Contact	0.1	25.0	AlGaAs	0.000
Contact	25.1	35.0	AlGaAs	0.000
Ramp	60.1	70.0	AlGaAs	0.100
P2	130.1	1000.0	AlGaAs	0.350
P1	1130.1	500.0	AlGaAs	0.350
P-GRIN (Graded Index)	1630.1	100.0	AlGaAs	0.350
P-GRIN	1730.1	0.0	AlGaAs	0.200
Active	1730.1	12.0	AlGaAs	0.090
N-GRIN	1742.1	100.0	AlGaAs	0.200
N3	1842.1	100.0	AlGaAs	0.330
N3	1942.1	150.0	AlGaAs	0.330
N3	2092.1	1000.0	AlGaAs	0.330
N3	3092.1	150.0	AlGaAs	0.330
N2	3242.1	1000.0	AlGaAs	0.330
N1	4242.1	100.0	AlGaAs	0.330
Ramp	4342.1	100.0	AlGaAs	0.330
Buffer	4442.1	500.0	AlGaAs	0.000

Table 4-1: Layer widths and material content of a 830nm 64 emitter laser bar (33).

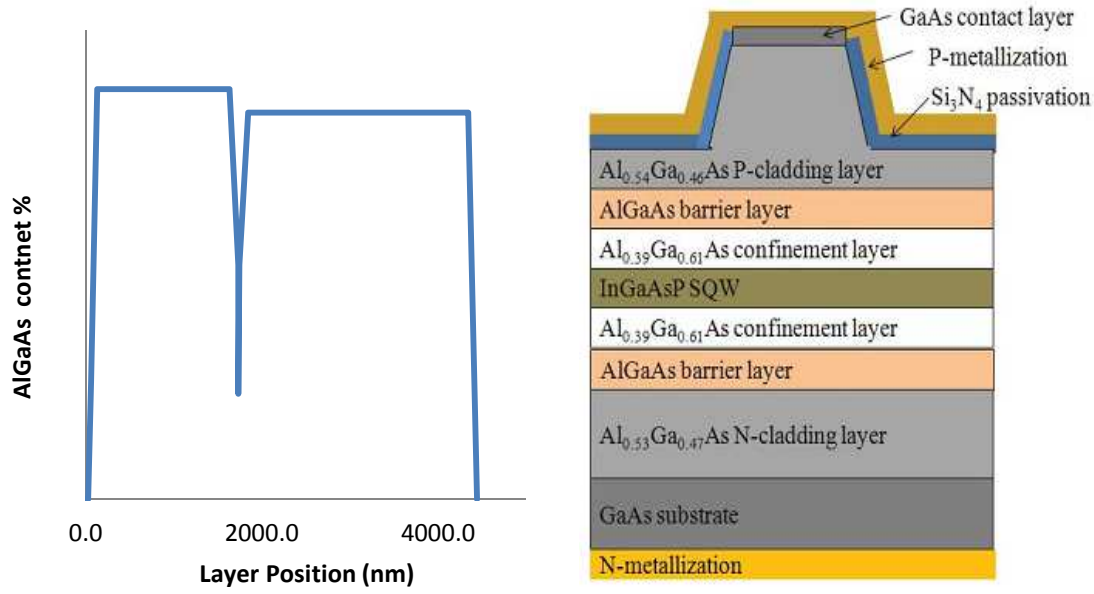

Figure 4-1: Left panel, Graphic showing the layers and aluminium content. The active region is in the order of 10s of nm. Right panel, Typical layers of a single Quantum well laser (33).

For the purpose of the project, a number of 64-emitter, narrow stripe laser bars were measured. The commonly wire-bonded devices were soldered to a standard "passive mount" copper block. The standard production module is an actively cooled (single water channel) copper block which also contains electronics enabling individual addressability of the lasers. All devices were water cooled to an operating temperature of 25°C.

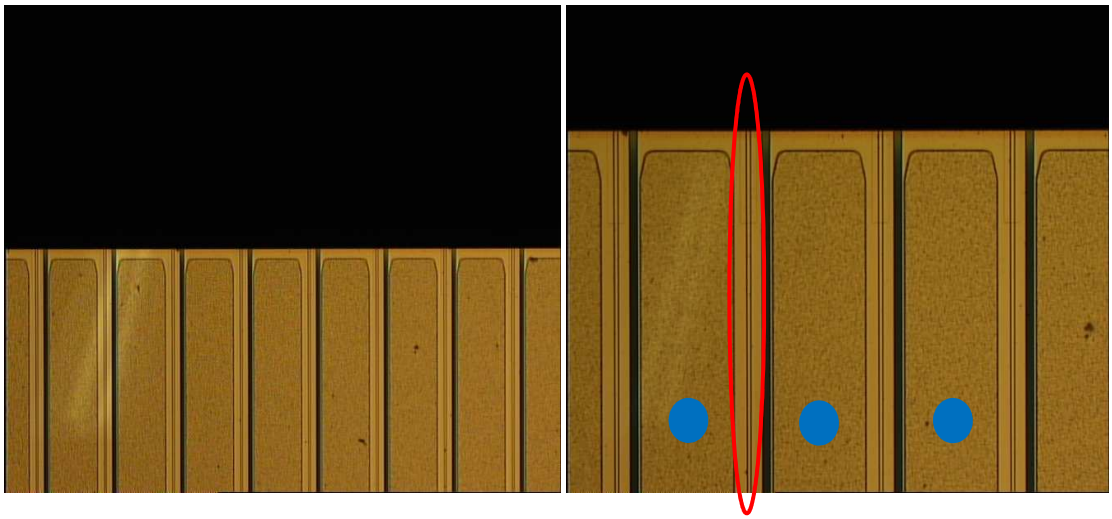

Figure 4-2: Top of laser bar at 10x (left panel) and 50x (right panel) magnification. The waveguide is marked by the red oval; the blue spots are the areas where wire-bonds contact the device (37).

The emitter design is based on an established ridge-waveguide design with V-grooves separating each laser to limit propagation of defects. Figure 4-2 shows the view from the top of the bar. The waveguide is marked in red with the ridge both sides and the area where the gold wire bonds form the anode contact are also marked in blue. Figure 4-3 provides a facet

facing view of the laser. The small waveguide is just visible in the red circle. The interface between substrate wafer and the cooler body is also visible. As mentioned in the section on fabrication, 2.4.1, only a very small portion of the wafer is used for the active region. It is not entirely visible in the smaller photos but there is a distinct border transition approximately 2% from the top of the chip.

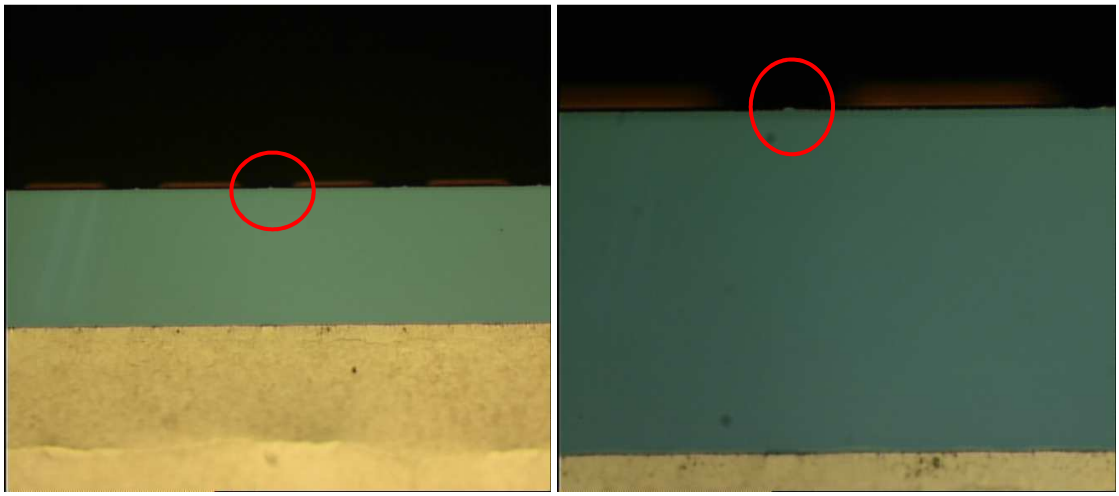

Figure 4-3: front view of the facet at 50x (left panel) and 100x (right panel) magnification. The active region is marked by the red oval (37).

To achieve single lateral mode operation, the high order cavity modes must be eliminated. This can be achieved with the use of internal Diffractive Bragg Gratings in the cavity of the device, external filters and optics, and/or by the design of the chip dimensions. The devices used in this thesis have neither internal nor external wavelength selection mechanisms. It is entirely due to the narrow width of the waveguide that single lateral mode lasing occurs. *Zhen et al.* (32) calculated the dimensions of a ridge waveguide laser fulfilling these single mode criteria:

$$W = \frac{\lambda}{2\sqrt{n_{eff2}^2 - n_{eff2}^2}} \tag{4.1}$$

where W is the width of the ridge, n_{eff2} is the refractive index of each layer. For the purpose of testing, a laser bar with an emitter width of 2 µm, bar length 1200 µm and a pitch (emitter spacing) of 170µm was used. The overall width of the bar is 10.7 mm.

4.2 Bar Mounting

This bar was mounted in two ways. The first method was to solder the bar to a gold-plated copper block. The gold plating is used to prevent corrosion of the copper without losing its thermal transport properties. This is a passive cooler with limited heat dissipation abilities,

but with a simple form factor and convenient installation possibilities. It has a standard contact point; with the bar soldered P-up and gold wire bonds connecting to the anode contact. This contact is soldered to the copper block but is isolated to prevent a short circuit. The current leaves the diodes through the underside of each diode and into the copper block. Isolation is paramount in the configuration to prevent short circuits. In Figure 4-4, flat strip-line cabling is used to connect the power supply (72) (Make: Directed Energy, Model: PCO 6131 Quasi-Continuous Wave Laser Diode Driver) to the module to limit the effect of inductance on the cable which would induce a voltage spike and therefore current spikes. A steady current creates a steady magnetic field (Oersted's law) (73) and a time-varying magnetic field induces voltage in nearby conductors (Faraday's law of induction). According to Lenz's law, a changing electric current through a circuit that contains inductance, induces a proportional voltage, which opposes the change in current (self-inductance). The varying field in this circuit may also induce an *e.m.f.* in neighbouring circuits (mutual inductance). This is critical when pulse shape is important.

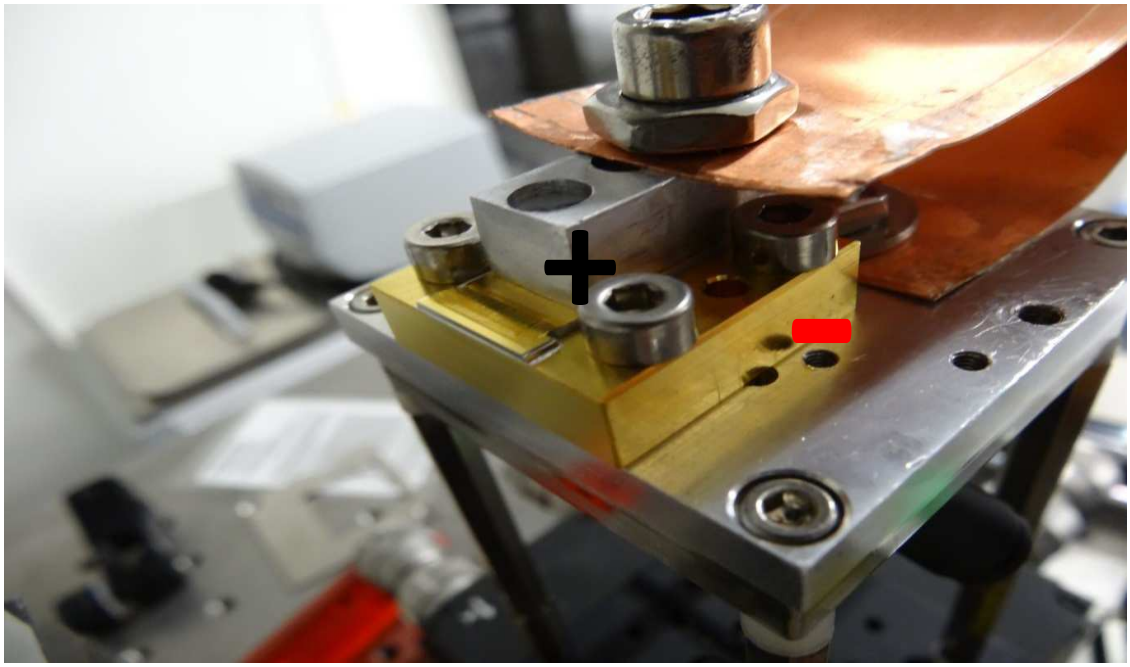

Figure 4-4: Cabling contact of passively cooled device (37).

The second mounting technique is an actively cooled module which is specifically designed to a customer request. This device has a water channel running directly beneath the laser bar in order to enhance the thermal load transfer. As can be seen in Figure 4-5, there are 3 screw contact points for the external current driver electronics which records the serial number and Power-Current (PI) data of the module the first time it is measured. The device itself contains on board micro-electronics to allow addressability of the emitters individually. It was a key component of the customer specification to control the laser diodes for printing applications.

The external driver board is used to perform a PI (Power Vs. Current) curve analysis of each individual emitter and then set each emitter to the appropriate output power. For this thesis, this aspect is critical in enabling the fine tuning of the wavelength spectrum which has not been done before. It has not been done to date due to a broader spectral requirement in the printing industry of ± 3 nm, a key customer of this laser diode array. In practical user terms, in the printing industry, the individual addressability allows pixel precision printing of computer-to plate presses.

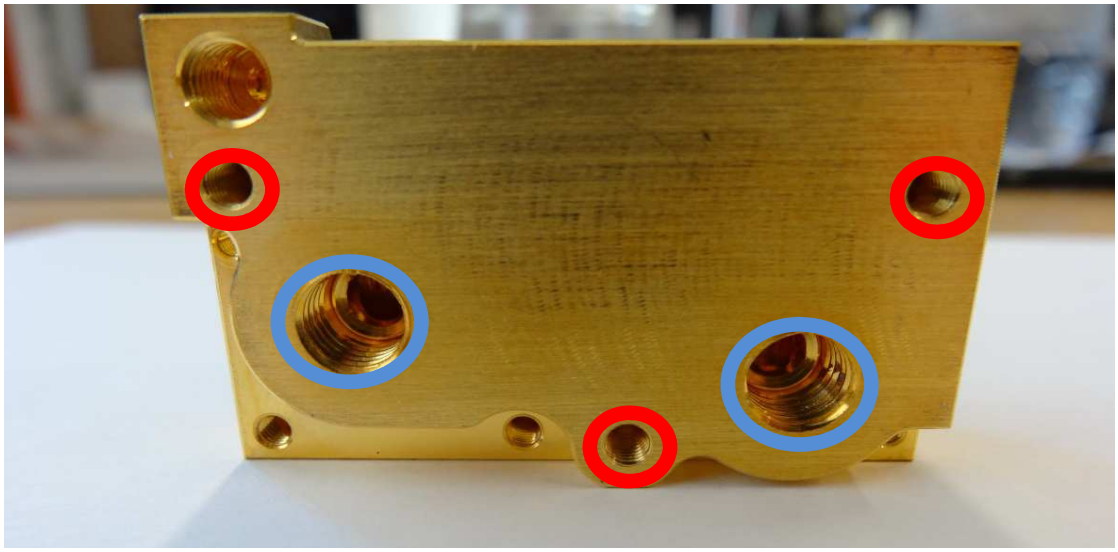

Figure 4-5: Underside of Actively cooled module showing water inlets (blue) and bolt fixing points to the measurement chuck (red) (37).

The top side of the actively cooled module, shown in Figure 4-6, shows the laser bar and the connecting gold wire bonds which lead back to the Application Specific Integrated Circuit or ASIC (via a jumper). The power bar, as the name implies, is the connection to the current source and has wire bonds connected individually to each emitter switch on the ASIC.

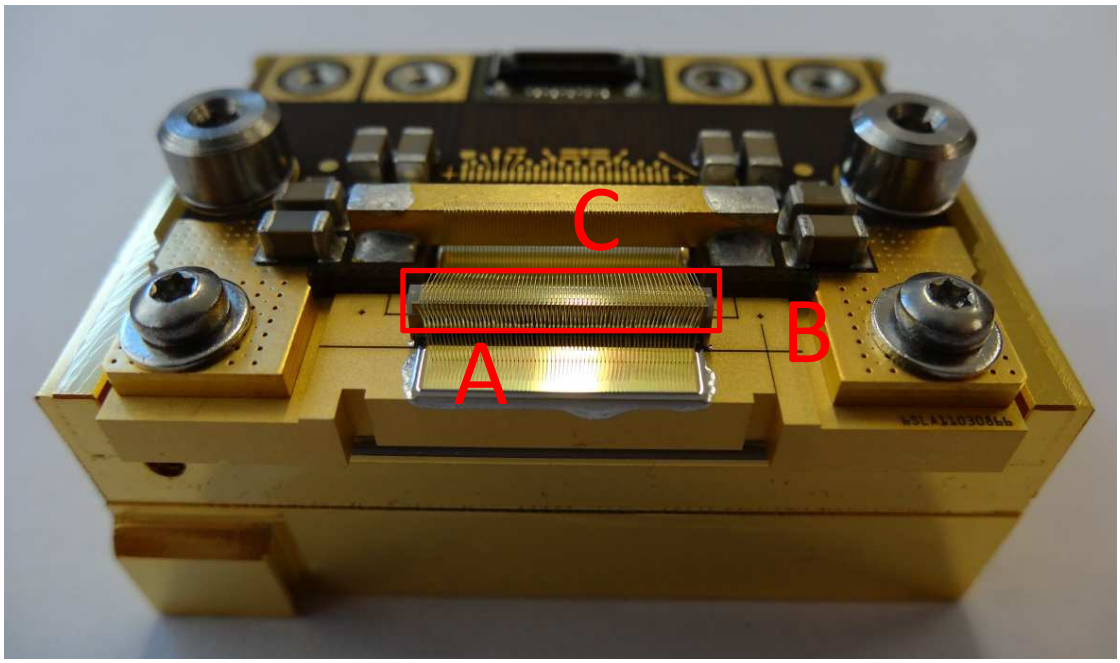

Figure 4-6: Front facing view of the module showing (A) the laser bar, (B) the submount and (C) the ASIC beneath the power bar. The jumper block is the link from ASIC to laser diode and photo diode and is contained within the red rectangle.

The ASIC is the control centre of the module, allowing the user to switch individual emitters or groups of emitters to varying power levels, and varying a whole host of parameters e.g. switching time. It also provides feedback to the user in terms of temperature and diode health. From the ASIC, gold wire bonds are connected to the jumper block, where a pair of gold pads for each emitter is positioned. From here, wire bonds connect to the photodiode and lasers. Positioned directly at the back facet of the lasers is a photodiode array which also provides information on the internal stability of the cavity and the mirrors. A spike in photodiode feedback current usually indicates damage to the front facet, and conversely a reduction in photodiode current indicates a failed laser and/or lack of sufficient emission power.

4.3 Conclusion

This chapter has explained the laser bar used in this thesis and given detail on its structure and doping methods. It has gone on to explain the ways the laser bars were mounted on the two types of cooler body and the functionality of the actively cooled module, including detail on the ASIC and the control it allows the user to have over the module.

5. Basic Characterisation of Laser Bar

5.1 Quasi Continuous Wave or qCW Tester

A tester used for quasi-Continuous-Wave (qCW) measurements was used initially to characterise the passive module. Quasi-continuous-wave operation of a laser means that its pump source is switched on only for certain time intervals, which are short enough to reduce thermal effects significantly, but still long enough that the laser process is close to its steady state, i.e. the laser is optically in the state of continuous-wave operation (where the current source is always on). The duty cycle (percentage of "on" time) may be a few percent of the total pulse duration (including on and off time), thus strongly reducing the heating and all the related thermal effects, such as thermal lensing and damage through overheating. Therefore, qCW operation allows the operation with higher output peak powers at the expense of a lower average power.

Figure 5-1: Quasi Continuous Wave or qCW developmental tester set up (33) where "A" is the optical spectrum analyser, "B" is the Newport power meter for calibration, "C" is the Thermoelectric Cooler, "D" is the Oscilloscope for power signal readings, "E" is the Beratron current source, "F" is the PC, "G" is the water cooling for the current source, "H" is the water cooling for the laser mount.

This tester, as shown in Figure 5-1, is equipped with a water cooled power supply (74) (Make: Beratron, Model: Beryllium) with a range of 400 A and pulse widths of 20 µs and upwards.

The test device is clamped in place on a copper Atotec MC-1 microchannel cooler (75) which is also thermoelectrically cooled with a Newport Temperature Controller (Model 3150). The test head can be seen in Figure 5-2. The polarity of the test set up also requires changing as normally laser bars are soldered p-down. Industrial bars are robust enough that the p-contact, which is not as close to the active region, can be soldered to the cooling block to maximise heat dissipation. The lasers used in these tests are not so robust, with the active region closer to the p-contact, and they were also designed to allow individual control of the emitters so the p-contact had to be up-facing.

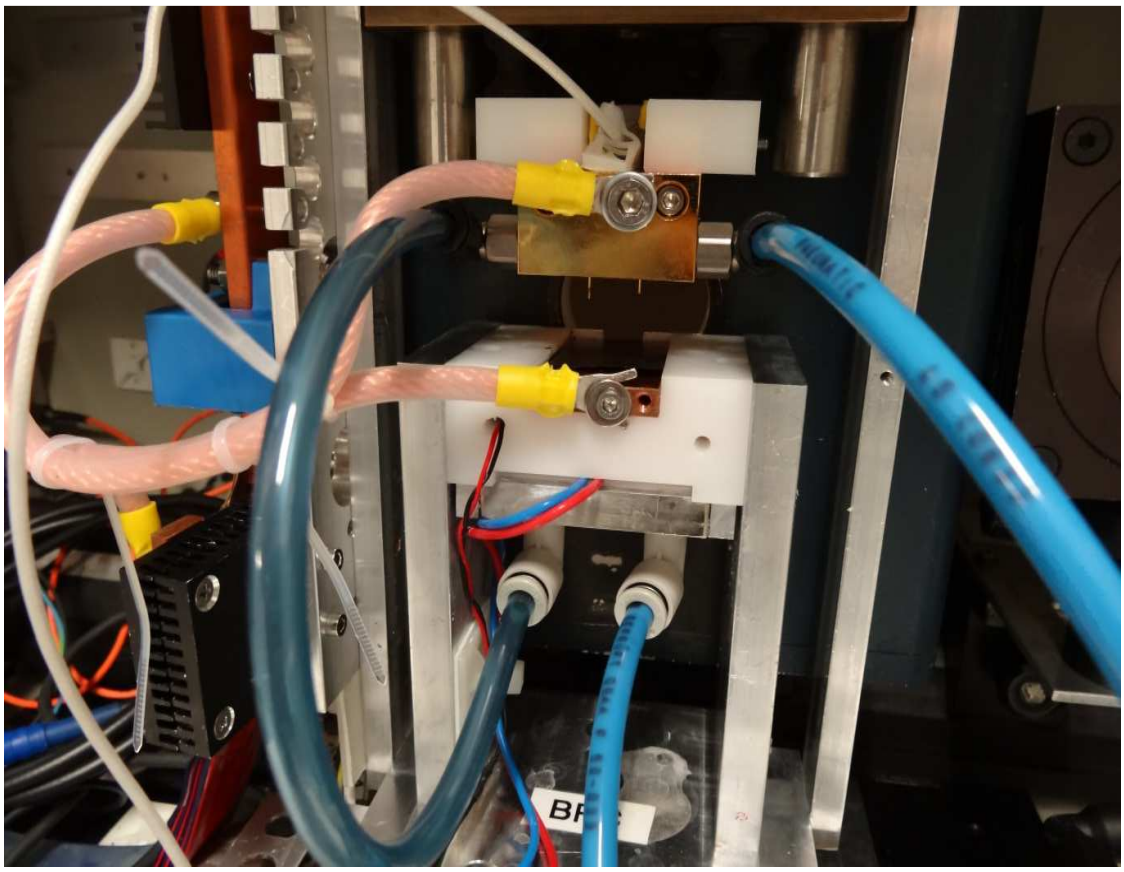

Figure 5-2: qCW tester module mount designed for internal testing of qCW devices (33)

The device facet is orientated towards an integrating sphere which has a Silicon photodiode connected to a Hewlett Packard (Model 54600B 150 MHz) oscilloscope, used to measure the power signal. The integrating sphere also has a fibre optic output to the Hewlett Packard 70951B Spectrum analyser. The optical power signal values recorded on the oscilloscope are calibrated against a certified thermopile and the calibration factor is stored in the software. The software also calculates the peak power based on the duty cycle.

The tester employs Labview software allowing full control of current step, ramp speed, cooling and data capture criteria. All data is recorded automatically and saved for later analysis.

5.2 Measurements on qCW tester

5.2.1 Initial Measurements

The majority of laser diode bars produced are multimode broad area emitters. However, for this thesis, an 830 nm, 64 emitter narrow stripe laser bar was used. This particular laser bar was designed to be actively cooled, so this was the first attempt at mounting it on a passive copper cooling block. The device was soldered p-side up for a few reasons. It allowed individual control of the emitters with distinct electrical contacts while the soldering of a device p-down would destroy the active region due to its proximity to the high soldering temperature required. Some tests with p-down devices were carried out but a fully working stable device could not be produced without expending too much time and money. These tests were done to copy the form of multimode broadband laser bars. The broadband devices are far more robust than their narrow stripe counterparts so this allows them to be soldered p-down to allow for better heat dissipation.

In order to make an initial characterisation of the laser bar mounted on a passively cooled device, it was mounted on a production tester. Normally, these devices are ramped to approximately 24 A (≈ 250 mW x 64 = 16 W output power) but for the purpose of this investigation, the device was ramped to 34 A due to the inability of the thermoelectric cooler to maintain a stable temperature at higher currents. All measurements were carried out at a cooling water temperature of 25°C.

Figure 5-3 shows the Power/Current/Centre wavelength plot for a narrow stripe 64 emitter module ramped to 34 A. It produces a maximum output power of 37.3 W at 34 A, with a threshold current of approximately 1.8 A. The tester didn't permit smaller current steps, so this is an estimate based on similar devices (33). It is known, for example, that an emitter on the ASEAL (Assembly Single Emitter Addressable Lasers) module has a threshold of 25 mA, so for 64 emitters this equates to 1.6 A. Looking at the fitted trend line on the graph, an intercept of 1.78 A is calculated. In parallel, the centre wavelength of the device was measured, and, as can be seen in Figure 5-3, there is deterioration in stability with increasing current above 25 A. The wavelength spans from 831 nm at threshold to 839nm at 34 A. As the current increases, the rate of increase in wavelength accelerates indicating more rapid heating effects on the laser.

To ensure as accurate results as possible, the CW measurement was recorded using the thermopile so a raw power value was generated. With thermopile measurements, a waiting

time of a minimum 30 seconds per measurement point is required to allow stabilisation of the thermal interaction.

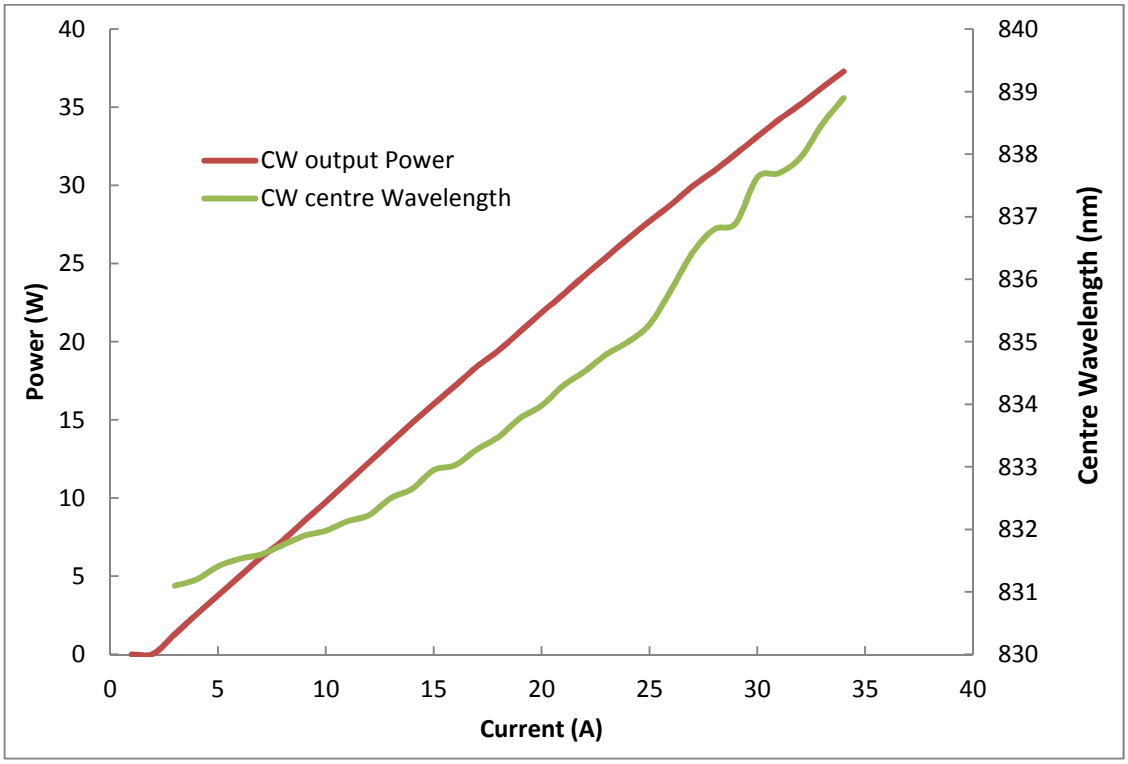

Figure 5-3: Output power and centre wavelength as a function of drive current of a passively cooled 64 emitter module operating in continuous wave mode.

5.2.2 Pulsed Measurements

In the following set of measurements, the Power/Current (PI) characteristic of the device was measured at various pulsed duty cycles, ranging from 5% to 65%. The device was pulsed so that the pulsed peak drive current could be increased to values up to 50 A. As with the continuous wave measurement above, the thermoelectric cooler (TEC) lost the ability to maintain a stable temperature at a duty cycle of 65%. The measured temperature of the thermal contact is displayed on the TEC controller. Table 5-1 summarises the power and wavelength results in CW mode and a selection of qCW modes levels for comparison. It can be seen from the summarised data that pulsing of the device has a stabilising effect on the wavelength but with the loss of average power. The main purpose of the pulsed measurements is to show the heating effects on the wavelength of the device.

Measurement Type	Operating Current Point (A)	Measured Wavelength Shift from CW (nm)	Peak output power (W)	Average output power (W)
Continuous Wave	30	0.00 (837.63)	33.14*	33.14*
65% Duty cycle	30.22	-2.41 (835.22)	33.8	22.11
30% Duty cycle	30.23	-3.97 (833.66)	33.7	10.11
5% Duty cycle	30.2	-5.09 (832.54)	34.4	1.71

Table 5-1: Comparison of measured wavelength and output optical power values in different measurement modes. *In the CW case the peak and average powers are clearly equal.

For completeness, the Average Power/Current curves are shown in Figure 5-4 and the Peak Power/Current curves are shown in Figure 5-5 for different duty cycles. It shows distinct pattern of curves as the duty cycle was incrementally increased. Thermal effects on output power were negligible up to the maximum duty cycle of 65% when the cooling equipment could not dissipate the thermal load effectively.

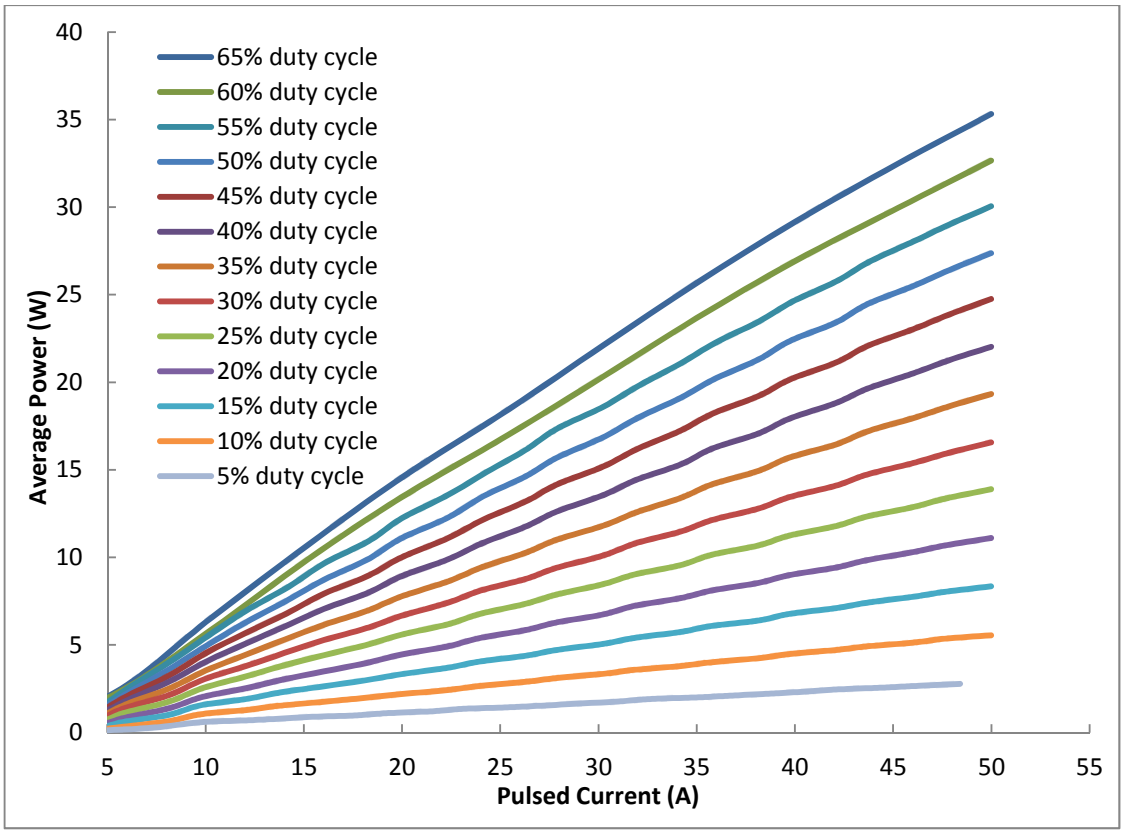

Figure 5-4: Average Power-Current (PI) characteristic of a passively cooled 64 emitter module operating at various duty cycles.

The purpose of the qCW tester is to find the maximum peak power of the devices while maintaining a stable wavelength which is ordinarily not possible in CW mode. It can be seen from the averaged power plot (Figure 5-4) that power increases linearly with increasing duty cycle indicating little thermal effect on the output.

The data in Figure 5-5 can be displayed to show the calculated peak powers. However, there is not much difference in the peak power performance except for the 5% duty cycle which outperformed the other duty cycle settings. This would indicate a possible lack of a thermal effect on the power output compared to higher duty cycles where thermal effects have an impact. It can also be seen in Figure 5-5 where there is little difference in peak power between the duty cycles except for a step from 5% to 10% and from 65% to continuous wave mode.

The Peak Power is calculated quite simply as follows:

$$\boldsymbol{Peak\ Power} = \frac{\boldsymbol{Average\ Power}}{\%\ \boldsymbol{Duty\ Cycle}} \tag{5.1}$$

The effects of varying the duty cycle are more pronounced when the wavelength measurements are viewed in Figure 5-6.

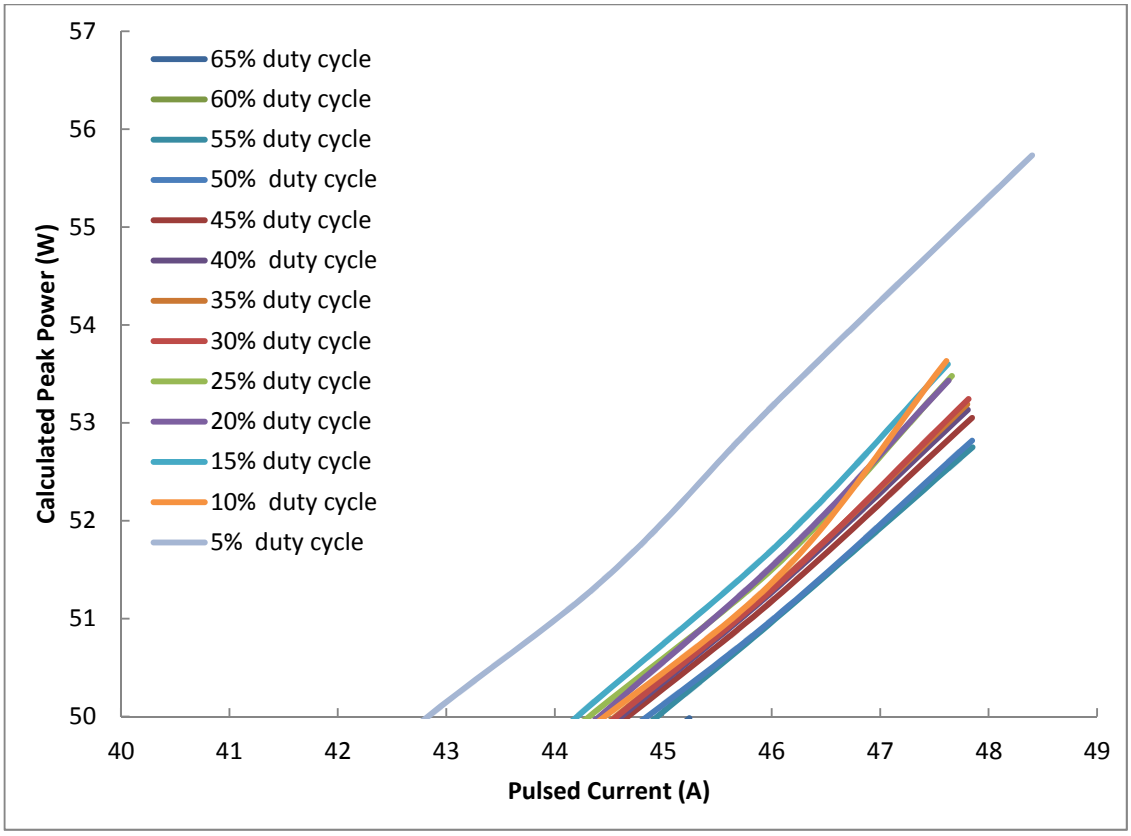

Figure 5-5: Calculated Peak Power-Current PI zoomed into the higher current range.

In parallel to measuring the peak power, the tester also takes a scan of the spectrum at each current set point and outputs the peak wavelength. This data is presented graphically in Figure 5-6. As can be seen in the data, a 3 nm shift at 30 A occurs between a duty cycle of 1% and 65% without a significant loss in peak output power (as shown in Figure 5-5). To compare

this to the continuous wave measurement seen in Figure 5-3 with data taken at the 30 A measurement point, there is a 5.5 nm shift from 1% duty cycle to continuous wave mode.

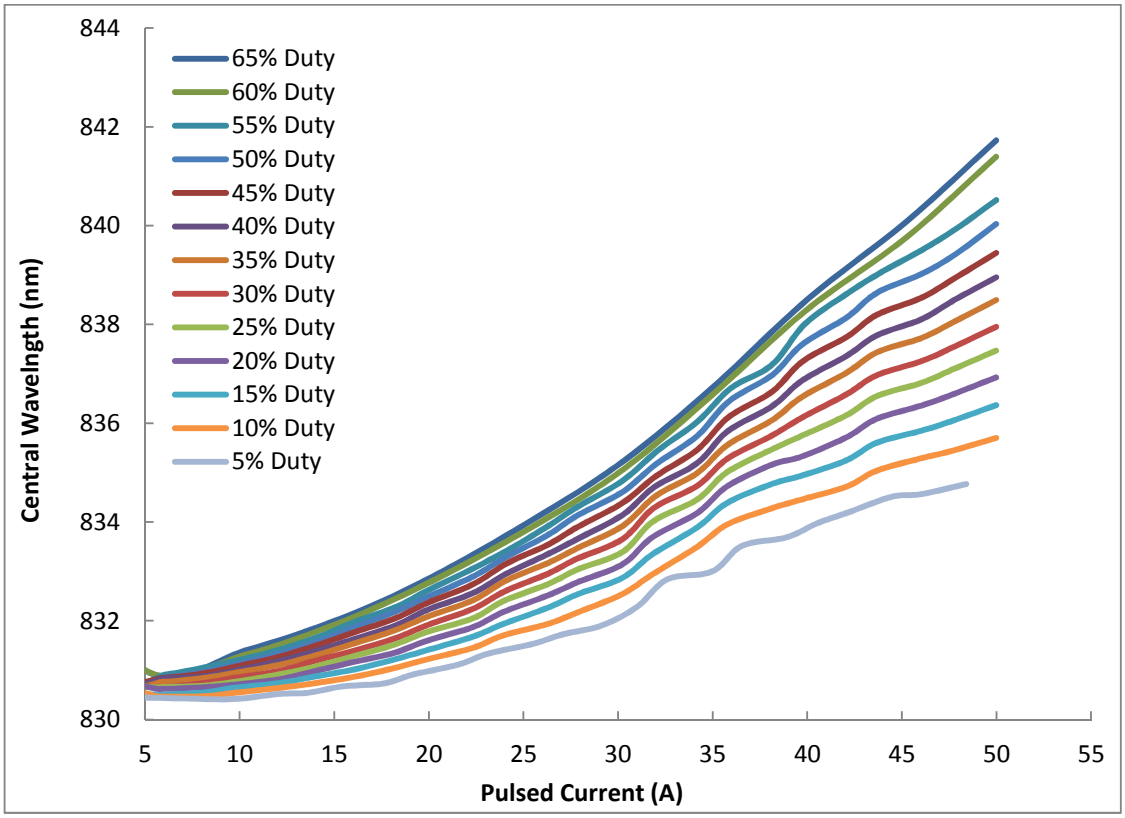

Figure 5-6: Centre wavelength measured vs duty cycle.

Figure 5-6 also shows that as the duty cycle increases the rate of wavelength shift increases with increased current. The heating effect is multiplied at higher currents due to the neighbouring emitters contributing to the greater thermal load. What is also noticeable are kinks in the curve which occur at 32 A, 36 A, 40 A, 43 A and which are repeated at every duty cycle. These kinks become less obvious at higher duty cycles, due to thermal stability, a saturated thermal effect and smoother transition from wavelength to wavelength, i.e. less mode hopping.

5.3 Conclusion

What is immediately apparent from this chapter is that pulsing of a device greatly enhances its spectral stability, albeit with the loss of average power. For some applications, this is acceptable where only a short burst of high intensity energy is required, for example in laser ablation applications. Having drawn the conclusion that there is strong thermal influence on the wavelength of the lasers with increasing current and increasing pulse duration, the next step was to look at individual emitters and their individual characteristics with and without influence from their neighbours. For these measurements different test equipment and module design was partly used.

6. Detailed Spectral Analysis of Individual Emitters on Laser Bar

In this chapter, the aim is to investigate how individual emitters are affected by the current ramp, especially focusing on the influence of neighbouring emitters and associated thermal crosstalk. The following section treats the same device which, was measured on the qCW tester, on the experimental tester, matching conditions as closely as possible to the qCW tester to make a comparable analysis. Later in the chapter, a separate module is measured on the ASEAL tester, whereby individual emitters can be controlled.

6.1 Lab Continuous Wave (CW) Tester

A test set-up was created to allow alignment of a laser cut lensed-fibre to the facet of the passively cooled module. A lensed-fibre is used to minimise capture of stray light from neighbouring emitters. In this set-up, a 120A pulsed laser driver from Directed Energy Corporation (72) (Model: PCO 6131) was used. However, it was only used in CW mode to allow direct comparison with the measurements on the ASEAL tester (section 6.2). As can be seen in Figure 6-1, the set up was quite developmental, although it was functional.

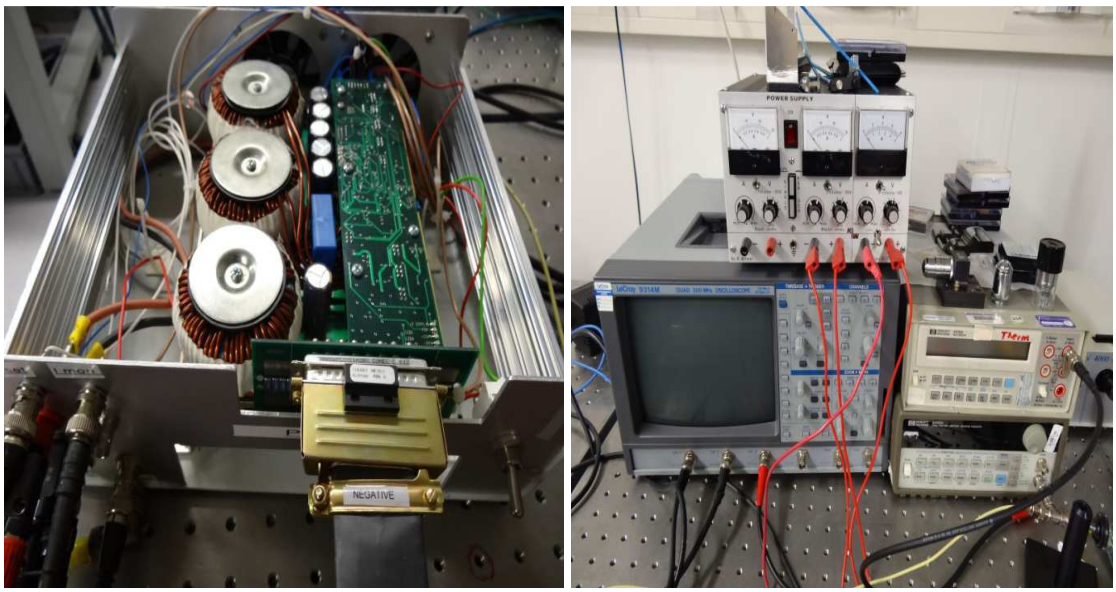

Figure 6-1: Laboratory CW tester set-up table, showing on the left the Directed Energy source, and right, the oscilloscope, wave generator and electrical bias for the power supply.

The directed energy power supply uses a strip-line layer cable approximately one metre in length, which is designed for pulsed applications. The power supply current is set by a potentiometer, but this can be made more accessible by applying an external voltage to the potentiometer circuit. This allows a scaling of the output current via the external voltage

source, e.g. setting 10V input to equal 100A power supply output. The power supply also has a current monitor which is connected to the oscilloscope for constant monitoring of the output voltage. In addition, an input gate of 5V is required to drive the power supply and this is provided for by the function (wave) generator.

Figure 6-2 captures the measurement point of the set-up, which shows the mount to hold a cleaved 105µm core, multimode lensed-fibre, which is secured to a moveable stage with micron scale incremental movements. This enabled a multi-directional positioning capability of the bare fibre with respect to the laser facets for alignment purposes. Initially, the lensed-fibre needs to be orientated to the correct axis of the laser, in this case the vertical fast axis, so it can capture as much emitted light as possible.

The passive device is bolted to a water cooled copper block, which in turn is attached to an Atotech, water-channelled cooling plate (Model Atotech MC-1) (75) which is also bolted to a micrometer-controlled movable stage. This gives multiple degrees of movement between the fibre and the laser.

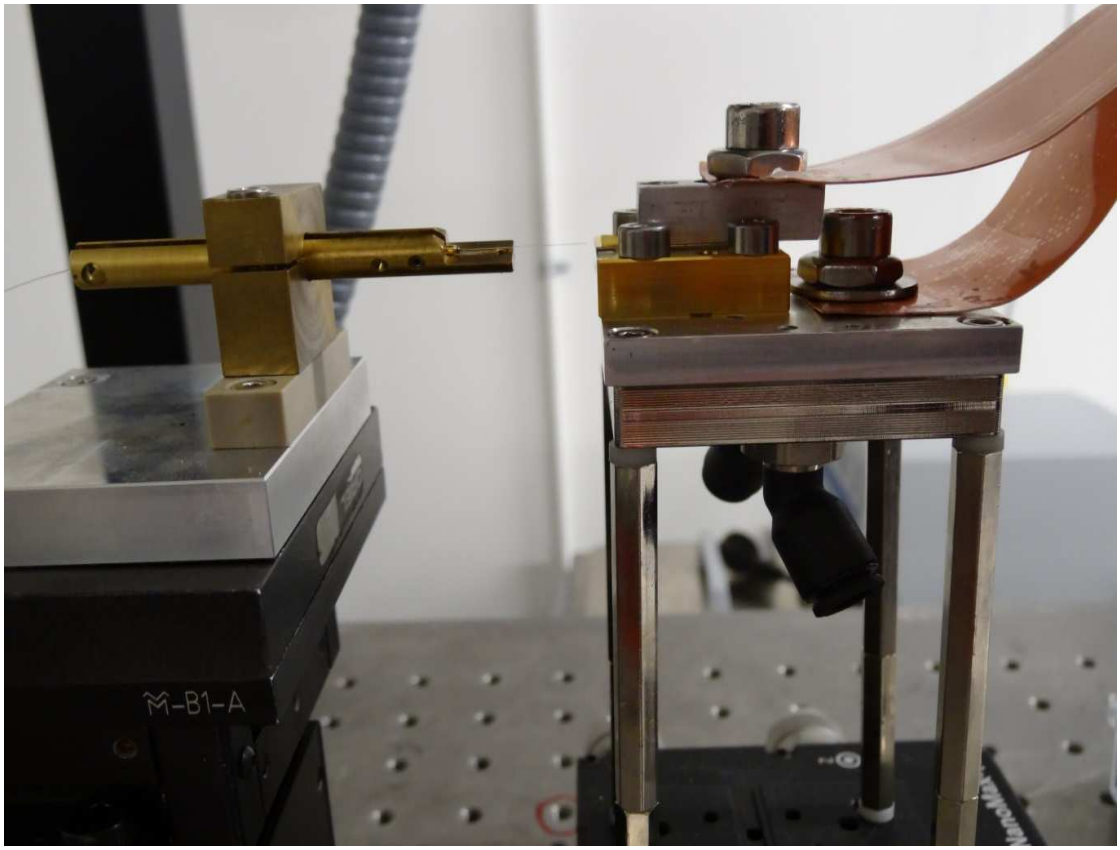

Figure 6-2: Fibre holder and device mount with connected strip-line current cables.

Like the qCW tester, this set-up operates with the basic labview software to capture spectra from the spectrum analyser, a Hewlett Packard 70951B, which is saved in comma delimited value format.

Figure 6-3 is a schematic of the test set up in its simplest form.

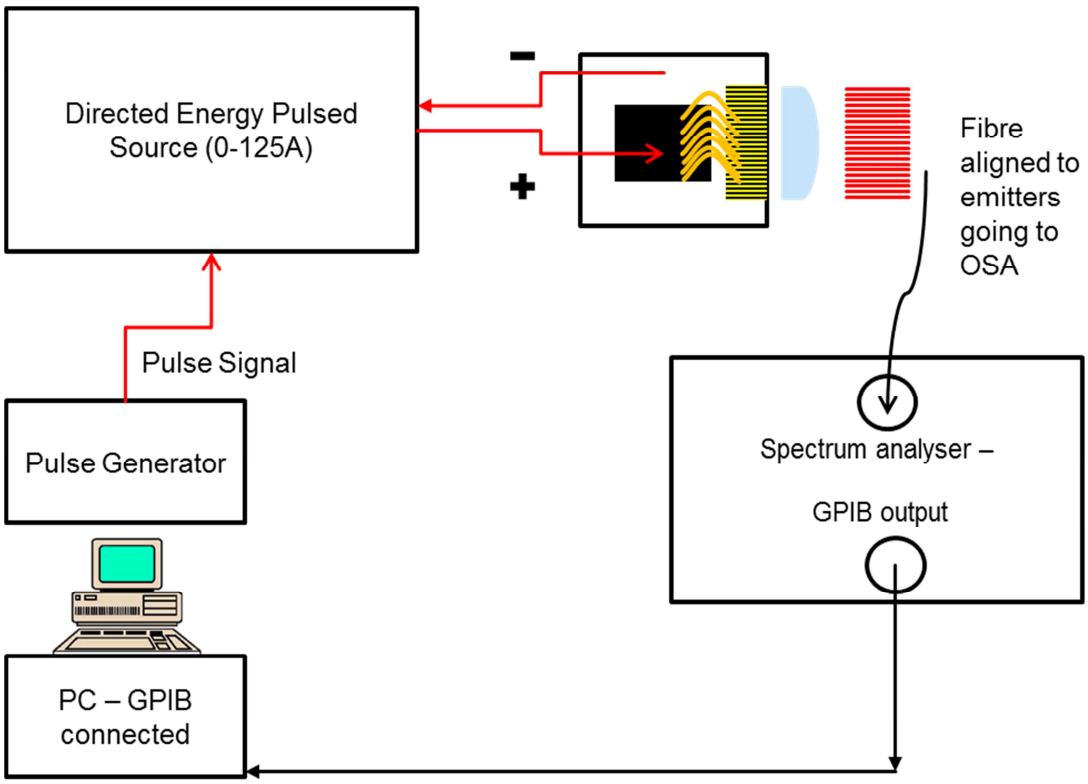

Figure 6-3: Schematic of CW lab tester assembled for the purpose of this research (37).

Alignment of the lensed-fibre was performed manually through a microscope. The fibre was initially rotated to orientate the lensed-fibre to the fast axis of the laser. Only then was the lens introduced to the laser facet. As can be seen in the left hand image of Figure 6-4, working distances of a few µm were used. This was required to ensure that no stray light from neighbouring emitters interfered with the spectrum of the emitter under examination. Further fine tuning by way of micron screw gauge was required once the lasers were on to maximise signal into the fibre core.

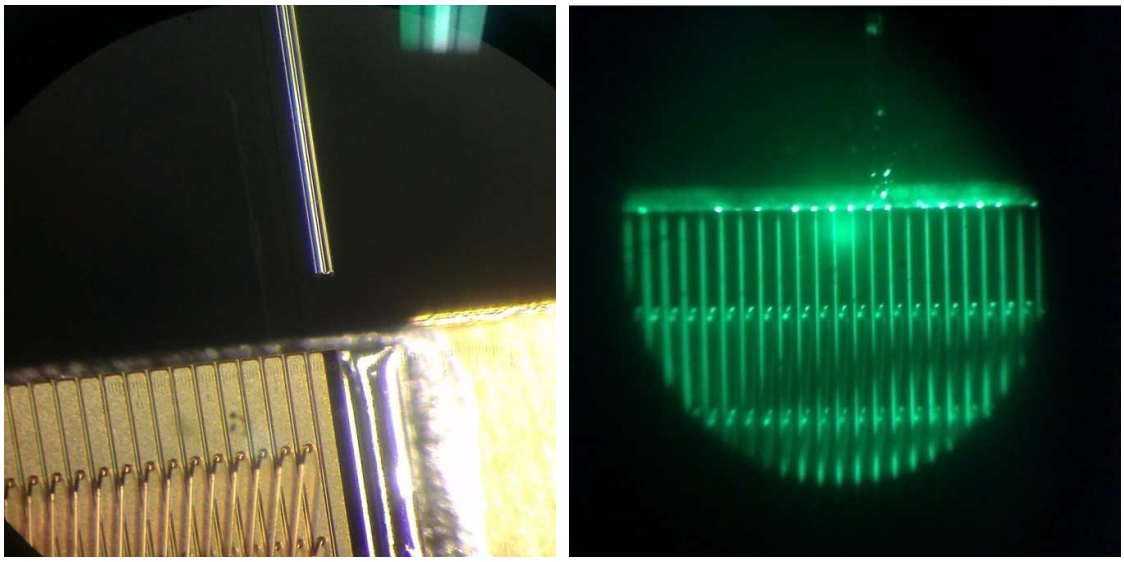

Figure 6-4: Alignment of a lensed-fibre to the emitters on the passively cooled module, and an infrared viewer captures the lasers running (37).

6.2 ASEAL Tester

A specific individually addressable laser bar was developed by Laser Enterprise for a laser printing client to be used in laser computer-to-plate (CTP) print applications. In order to function, the customer supplied the associated electronic circuit, and Application Specific Integrated Circuit (ASIC) chip, the laser diode driver hardware and associated software. As part of the specification, these devices are actively cooled with a water channel running through the cooler body, directly below the laser bar, allowing water with a flow rate of approximated 1.2l/min to pass.

The spectra of the modules are not measured at this tester under normal production test conditions. This measurement is performed at the Front End Of Line (FEOL) on the bare bars. The tester measures power, current and voltage, as well as thermal effects – specifically thermal crosstalk – by examining the effects on the output power signal. It also captures data from the ASIC in the form of ASIC temperature photodiode current read-back.

The images in Figure 6-5 show the positioning in the standard measurement set-up. The set-up is contained in a sealed box for safety purposes. The laser module with attached electronic circuit driver board is directed into an aperture of the integrating sphere which contains two photodiodes to record the optical power (P) - drive current (I) or PI curve of each emitter and also the thermal crosstalk of sections of the bar. This can be seen in Figure 6-5.

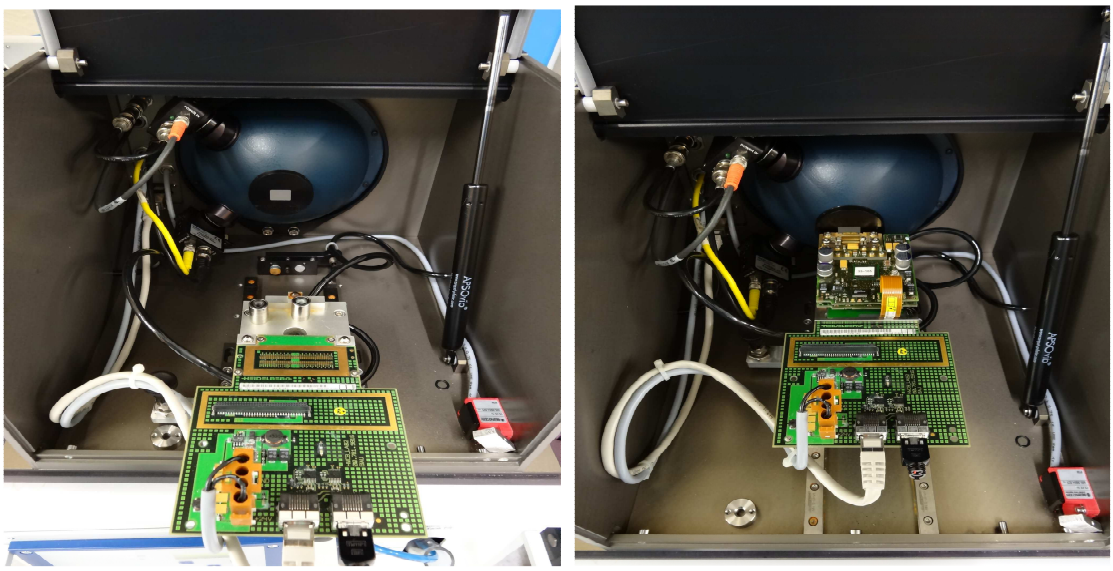

Figure 6-5: Unloaded and loaded standard set up of ASEAL Electro-Optical tester (33).

For the thermal crosstalk measurement, the module is switched to 200mW per emitter (all on) and the power recorded 100 µs after the rising edge of the drive current pulse. The module is then permitted to return to its quiescent state and the power recorded again after 10 seconds settling time. Secondly, the left side (emitters 1-32) of the device is powered on and the curve recorded, followed by the right side (emitters 33-64). The curves from each side are compared for transient/thermal effects at the rising edge overshoot.

In order to measure the spectra, a 2 inch Newport integrating sphere was inserted into the test enclosure as shown in Figure 6-6, and was used with the same Optical Spectrum Analyser (OSA) interfaced to a computer for data capture and analysis used in the CW Lab tester as described in section 6.1.

(a) 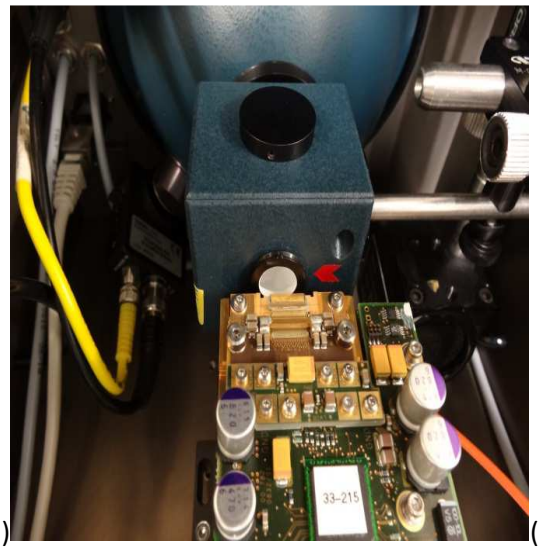 (b) 

Figure 6-6: Experimental set up used on ASEAL Electro-Optic tester, (a) shows the small integrating sphere inserted into the set up to capture light from individual emitters, and (b) shows the OSA and PC to capture the data (33).

6.3 Measurements on Lab CW Tester and ASEAL tester

The lab CW tester is a simpler piece of equipment compared to the ASEAL and qCW testers. Although its capabilities are limited, it still produced an interesting and informative array of results. There is a difference in the spectrum measured compared to the qCW tester, which can be attributed to the cooling mechanisms used. In contrast to the qCW tester, which used a single lever clamp to press and hold the module onto the test bed, the lab tester just used 4 screws at the corners of the module to secure it (cf. Figure 6-2). It is possible that the pressure applied, water flow and water pressure are different between the testers, resulting in some wavelength differences in the output spectra. Also, in order to compare data with the third and final set of measurements performed on the ASEAL tester, the input current was limited as the maximum power used in that tester is 250 mW per emitter. This tester performs measurements at a set power rather than a set current. The spectrum analyser used for all measurements had a resolution bandwidth of 0.08 nm – the best setting available on the device and the best device available for these measurements.

6.3.1 Spectral Analysis - Full bar spectrum

The first step is to capture an overview of the spectrum of the full bar which was carried out on the ASEAL tester. The laser bar was orientated towards the small integrating sphere and the power value set to 250 mW per laser diode resulting in the spectrum in Figure 6-7, which exhibits a spectral width of more than a nanometre at each power setting. Looking at a full spectrum of the entire bar, the spectral width of all merged emitters' spectra remains stable. However the centre of the spectrum shifts from 823.6 nm at 30mW to 827.5 nm at 250 mW.

The modes of the individual emitters can be seen in the overall spectrum resulting in quite a contrast of intensities and distribution of wavelengths. In this image there is no way to tell which lasers contribute to the different parts of the spectrum. This will be addressed in the following section where a separation of the emission spectra for each emitter will be examined.

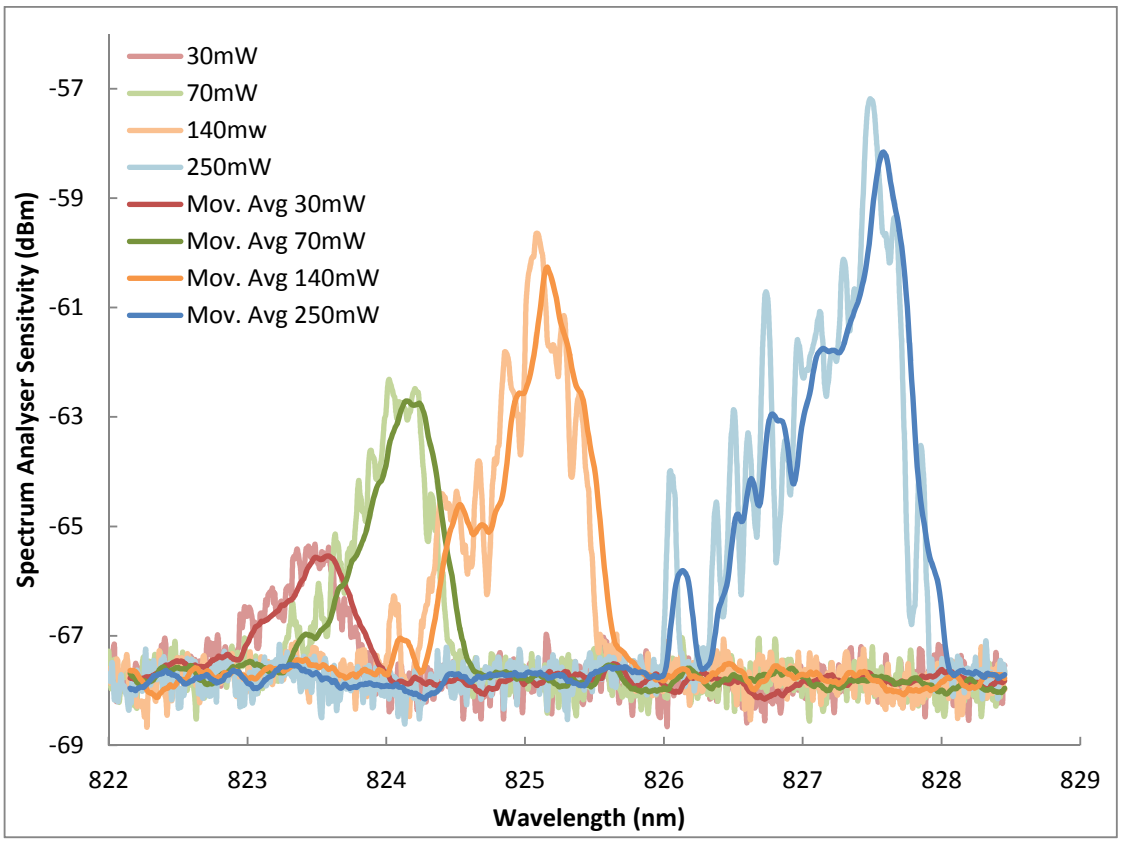

Figure 6-7: Spectra of full bar measured on CW tester at various optical power levels with averaged trend lines to provide clarity.

The total output power of the full bar during these tests ranged from 1.92 W to 16 W (250 mW x 64).

6.3.2 Spectral Analysis - Individual Emitters

The first detailed measurement carried out was to check the exact spectrum of each emitter when a common drive current was applied to the bar. All of the measurements performed were carried out in CW mode. Figure 6-8 below shows the spectrum of each emitter, while all other lasers are also running in parallel. The drive current used was 8A DC. A spread in peak wavelength is demonstrated, the first noticeable trait is that the overall wavelength spread (ignoring channel 64) would be around 0.8 nm. The smile effect is also in evidence, but this will be demonstrated in Figure 6-10. The emitters towards the edges of the bar are cooler and so produce a shorter wavelength. For example, the outlier in Figure 6-8 is channel 64 which has a peak wavelength at 827.2 nm, channel 1 has a peak at 827.5 nm while the middle

channels e.g. emitter 32 has a centre wavelength 827.9nm which is at the higher end of the spectrum.

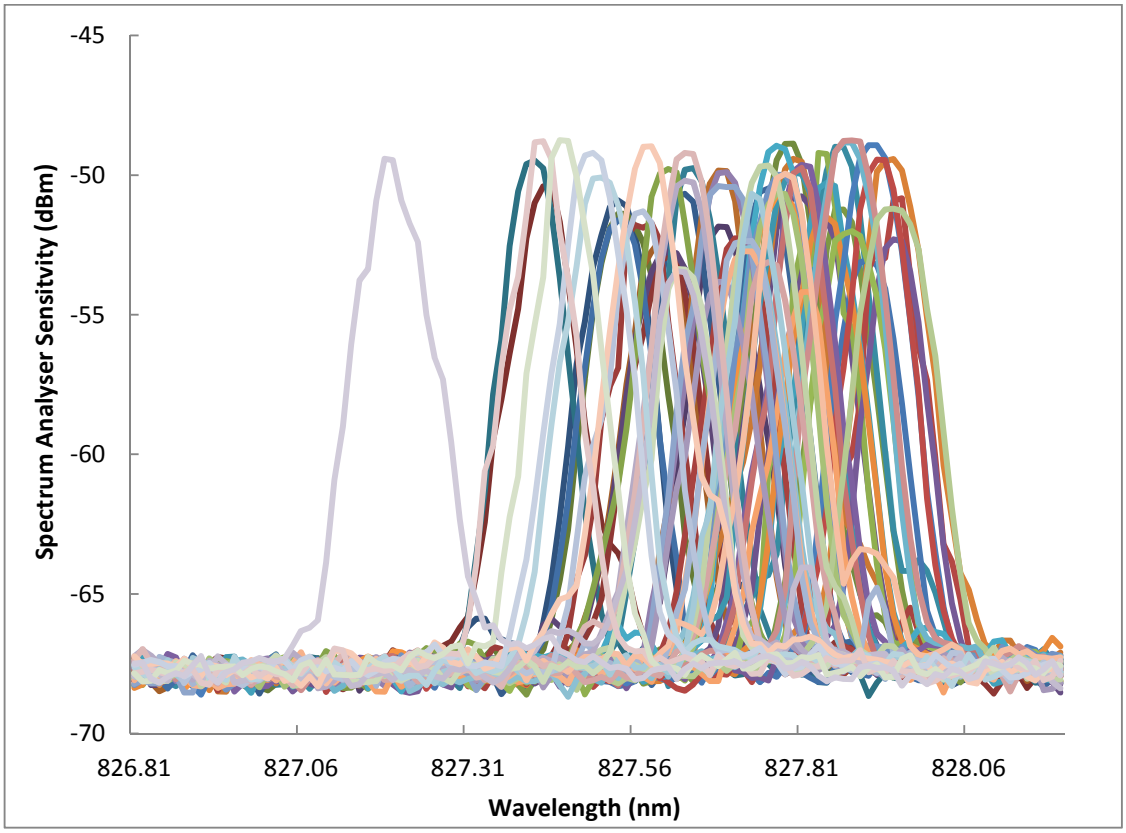

Figure 6-8: Spectra of each emitter, obtained via fibre alignment, while all emitters are powered on.

Given that the measured spectral width of an individual channel is approximately 0.1 nm at FWHM, from Figure 6-8, there is huge potential to narrow the spectral spread of the overall bar spectrum when compared to the full bar spectrum in Figure 6-7. The limiting factor of the spectrum analyser which has a resolution of 0.08 nm must also be taken into consideration. There are shoulders on the spectral profiles which could be longitudinal modes – as this is a single transverse mode laser. What can also be seen is a drop in intensity in the overall bar spectrum compared to the individual emitters. This occurs because of the attenuation in the integrating sphere compared to the light entering the lensed fibre on the individual measurements, where the fibre was aligned using a micrometre-controlled stage to maximise the captured light.

6.3.3 Spectral Analysis - Individual Emitters Running Independently

When one looks at each individual emitter running alone, with no thermal impact from neighbouring devices, a different picture emerges. As Figure 6-9 shows, the overall wavelength spread for the superposition of all individual spectra is approximately 0.8nm compared to when the whole bar is running as one (1.9nm FWHM in Figure 6-7). As

mentioned previously, the resolution of the spectrum analyser limits the accuracy of the result. The wavelength shift of the peak is 5nm i.e. 822 nm compared to 827nm. These are the individual attributes of each laser waveguide coming to the fore. Based on any differences in the epitaxy structure or doping content changes, effects during the soldering process (solder voids) may have reduced thermal efficiency in isolated regions under the bar, which would affect particular emitters. Also, in the spectral profiles of Figure 6-9, some profiles appear with a plateau which is a result of using a higher resolution band width to capture more signal. It's a limiting effect of the Spectrum analyser.

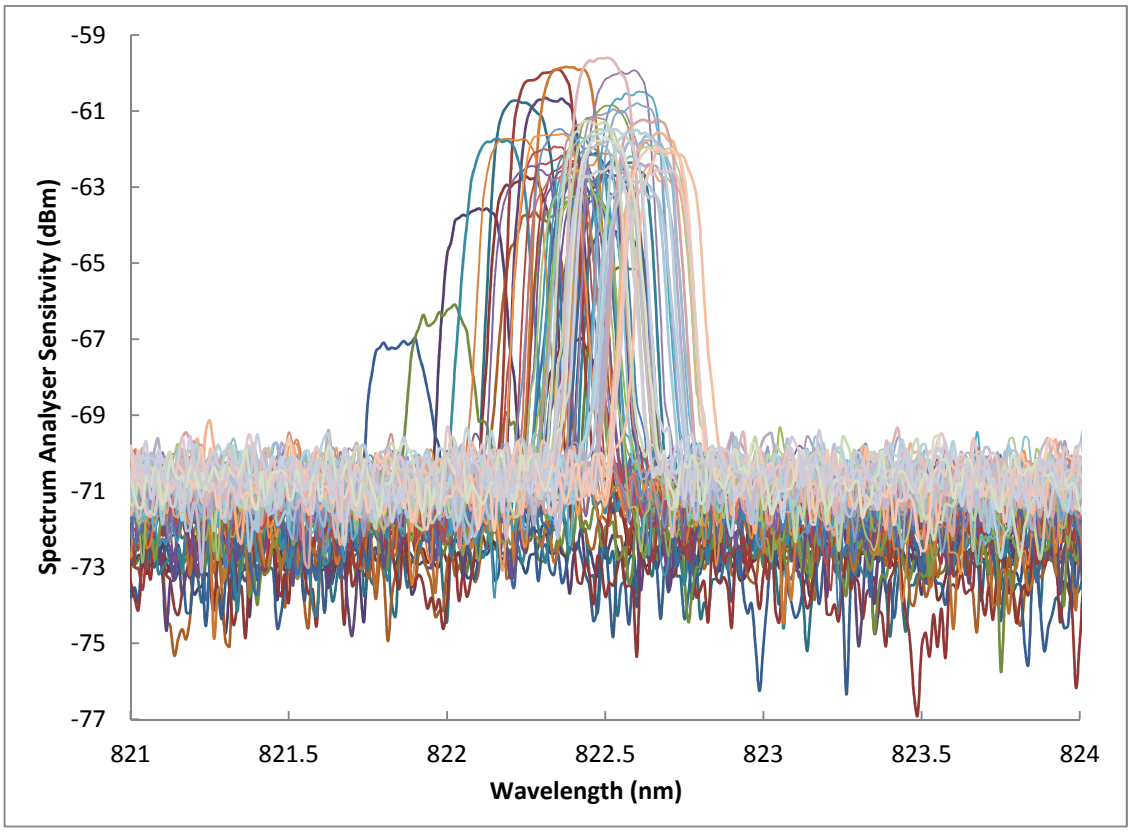

Figure 6-9: Individual spectra of the 64 emitters running one at a time on ASEAL tester.

When the data in Figure 6-8 and Figure 6-9 are compared, the behavioural difference of individual emitters can be seen. Once a thermal load is applied to an emitter by way of its neighbours running in parallel, this indicates that the thermal effect is not evenly spread across the bar and the shift in wavelength with emitter number or channel does not vary smoothly when all emitters are on. Based on the referenced modelling (64) presented in section 3.2.3, this would indicate that emitters at the edges do not shift in wavelength as much compared to emitters in the middle of the bar. The modelling suggests that the first five neighbours have maximum impact. This can be seen in Figure 6-10, in which the shift of each emitter running alone on the ASEAL module is compared to when all other emitters are running in parallel to the emitter under analysis on the passive module.

Figure 6-10 shows that the centre wavelength varies from emitter to emitter with all other emitters switched off (red curve). This, as explained previously, is the individual characteristic of the emitters. There is a slight slope on the curve which can be because of the soldiering process step misaligning the bar on the submount, as there appears to be an even gradient.

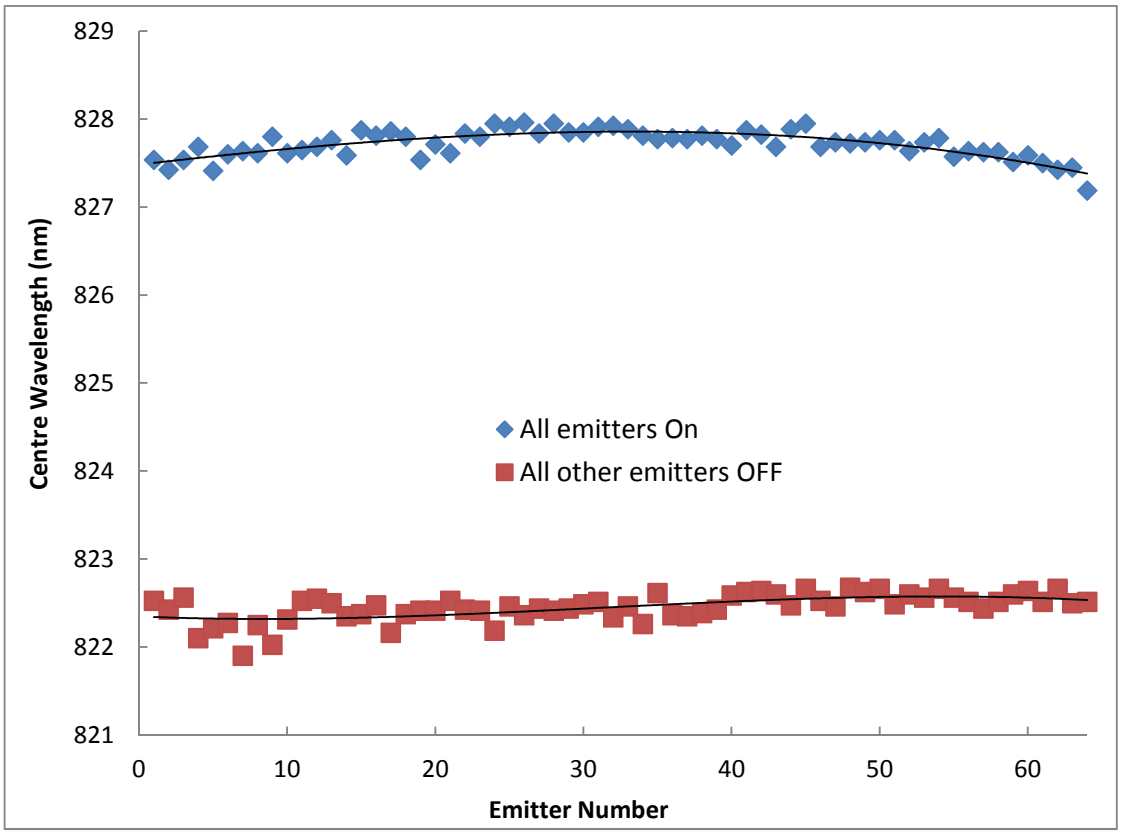

Figure 6-10: Centre wavelength of each emitter running alone (red) and with all others also on (blue).

Looking at the case where all other emitters are activated (blue curve) the wavelength varies rather smoothly across the bar and is more symmetrical with respect to the centre of the laser diode bar. This gives a clearer view along with the 3rd order polynomial trend lines of the spread of the wavelengths when the emitters run alone or in parallel with all others. Emitters 1-6 have an average centre wavelength of 827.53 nm, emitters 28-33 have an average centre wavelength of 827.9 nm and emitters 59-64 have an average of 827.44 nm.

Figure 6-10 shows that an overall shift of approximately 5 nm occurs between emitters running alone and compared to all emitters powered up simultaneously. A 5 nm shift would indicate a temperature shift of around 20°C at the laser junction as shown by Bowers and Pollack in 1988 (76). This is clearly a heating effect of having all emitters running simultaneously, and this needs to be addressed to be able to minimise the spectral spread from the laser bar. By controlling the individual input drive currents to the lasers, the wavelength of the emitters can be controlled, despite the thermal effects of neighbouring

lasers. Other methods such as gratings (internal and external) can of course be used to select a particular band of wavelengths, but the aim here is to demonstrate an ability to control the bar's spectral distribution externally via drive current control.

It must be noted that two different lasers mounted in different ways, as explained in Section 4.1 "Devices under Test", are used in these experiments due to compatibility issues with the testers, but as stated in section "3.2.3 Modelling of Thermal Effects", the mounting method of the lasers has a limited contribution to thermal effects on the laser bar. Any differences can be attributed to individual characteristics of the bars which occurred during the fabrication and mounting process steps.

An additional benefit of measuring at the wavelength of each individual emitter is that it provides an insight into the smile of the bar as described in the section on Laser Bar Smile, Section 3.2.1.

6.3.4 Determining the Wavelength to Power Setting

Now that the wavelengths of the emitters in relation to each other have been examined, the next step is to look at how the wavelength changes as a function of the input current to the emitter itself. It is necessary to take both individual drive current and thermal effects from neighbouring emitters into account when determining the appropriate drive current at which to switch the emitters in order to achieve the narrowest possible full bar spectrum.

In the following experiments, two emitters were selected at two contrasting positions on the bar, i.e., emitters 1 and 32. This experiment was done initially on the ASEAL tester, switching on the emitters alone to determine the spectral spread as output power increased. On the CW tester, these lasers were switched on manually, their current ramped up in 1A steps and the corresponding spectra recorded from emitters 1 and 32. During this time all other emitters were also running at the same current steps as this measurement was done on the passive bar with no individual current control.

Firstly, looking at the ASEAL data in Figure 6-11, spectra were measured in 10 mW intervals from 30 mW to 250 mW output power. The spectra had a wavelength span of 0.9 nm extending from 821.8 nm to 822.7 nm or a temperature difference of around 2°C. On average, the width of each peak is 0.2 nm. At higher powers, the peaks definitely become better defined and less noisy.

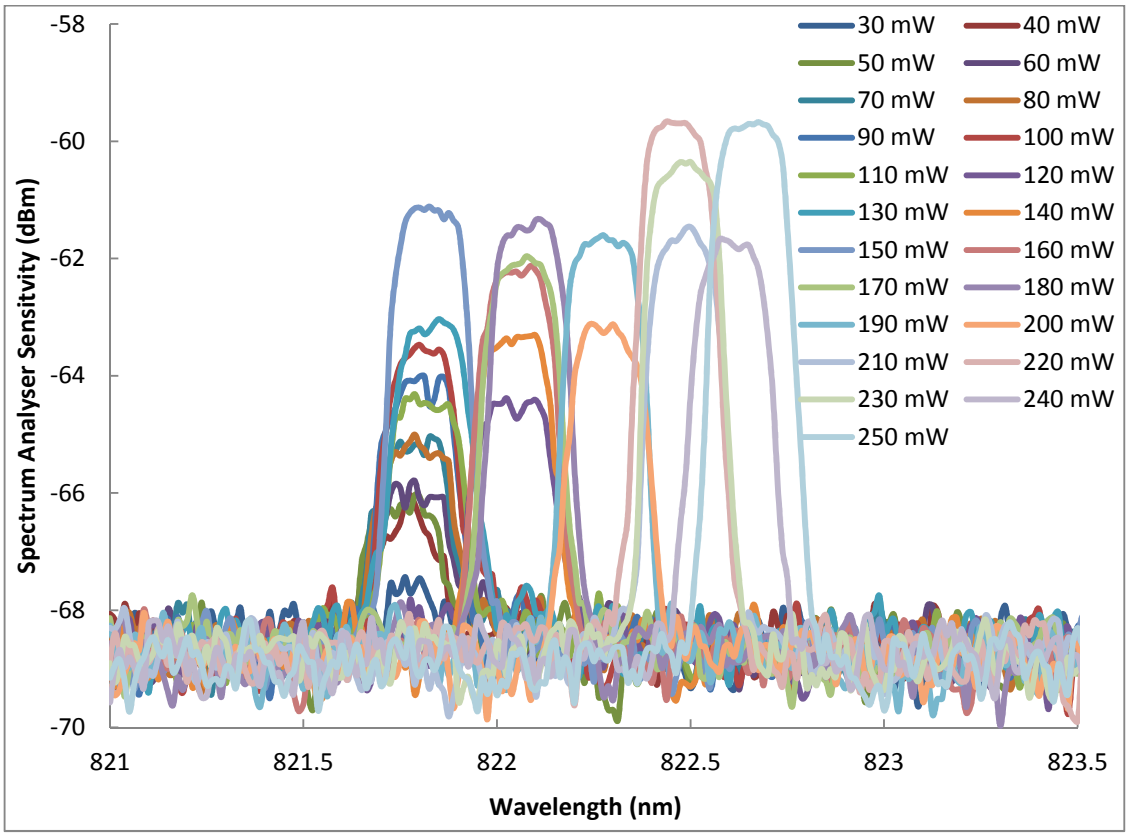

Figure 6-11: Output spectrum as a function of output power from channel 1 when running alone.

What is noticeable is how the wavelength shifts in steps as seen in Figures 6-11 and 6-13, appearing to be a mode hopping effect. Mode hops are often provoked by external influences. For example, a drift in the temperature of the gain medium will shift the wavelength of maximum gain while not shifting the frequencies of the resonator modes to the same extent (this can happen in laser diodes, where temperature changes usually affect the gain more than the cavity resonances) (77). The previously lasing mode may then no longer be the mode with highest gain, so that the power of a competing mode with higher gain can quickly rise. Essentially the same phenomenon can occur for length drifts of the laser resonator, which shift the resonator mode frequencies without also shifting the gain maximum (77).

Both origins of mode hops often result from attempts to tune the wavelength of a laser (78). The external influences can of course also just be random noise, e.g. mirror vibrations, temperature fluctuations or changes of pump power, or external optical feedback. That may be the case here where, as the temperature increases in the cavity, the wavelength shifts from mode to mode.

Figure 6-12 shows the same information for channel 32 as Figure 6-11 showed for channel 1. There is a similar grouping of wavelength at various power bands, i.e. from 50 mW to 140

mW and then a step to 150 mW. A wavelength shift from 821.9 nm to 822.7 nm is observed on emitter 32. This is done for comparison between the two emitters from the same bar to demonstrate their individual characteristics, which would have to be taken into account before even considering thermal effects from other lasers. The span of the FWHM at each power level is similar to channel 1 i.e. ≈ 0.2 nm. The peak widths remain consistent during the power ramp increase. The spectral curves are sharper here due to a better alignment of the laser into the small integrating sphere thus, capturing all the power meaning a smaller bandwidth resolution can be used.

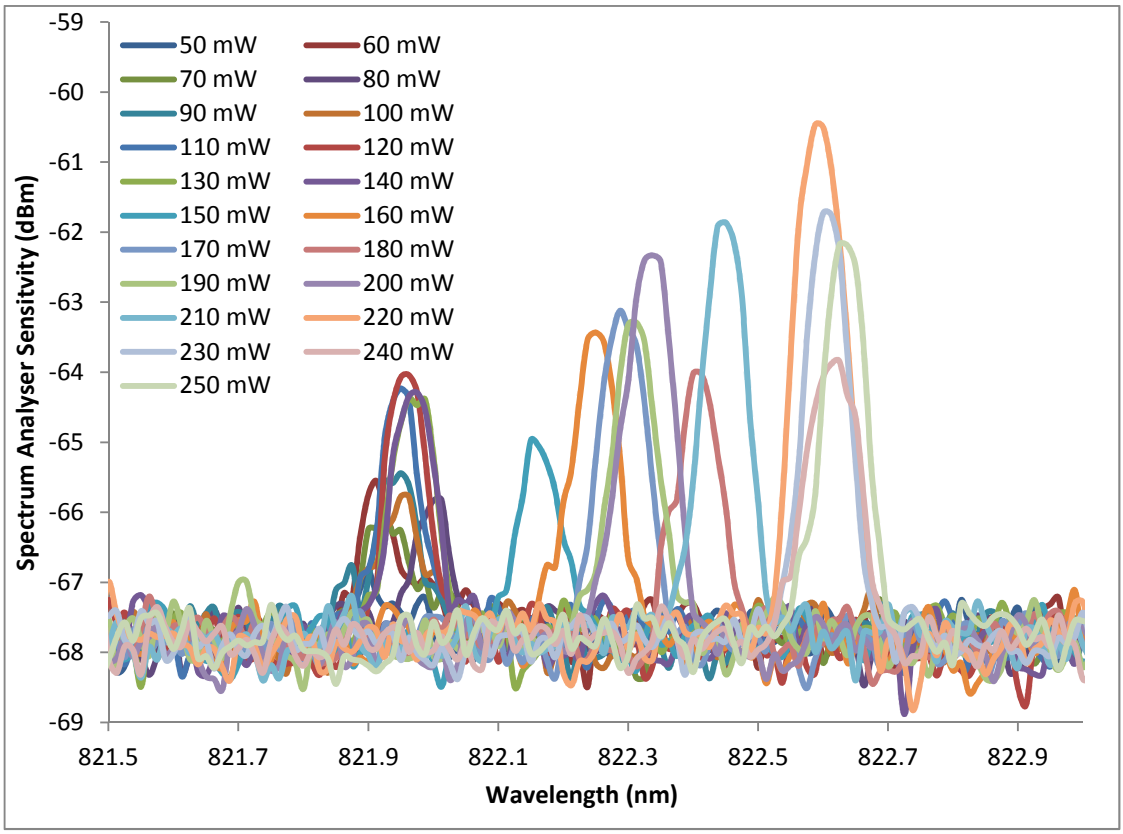

Figure 6-12: Output spectra as a function of output power from channel 32 when running alone.

The wavelength progression of both emitters is more visible in a direct plot of central wavelength as a function of output power as seen in Figure 6-13. There are a number of outliers which do not follow the more linear path and this can be due to mode hopping. It is a difficulty which would have to be factored into any system design i.e. that wavelength shifting may not be smooth or entirely linear.

The central wavelength remains very stable up to 130 mW output. At this point, the shift is continuous but hopping occurs at discrete points. From 140 mW and higher, the wavelength shifts in line with the output power indicating that heating effects occur in the laser.

Both emitters 1 and 32 show similar characteristics in their power-wavelength curves in Figure 6-13. There is a step in wavelength progression rather than a clean linear curve, which indicates some modal activity as temperature begins to play a role. The heat dissipation works well up to 150 mW when it begins to drift. The wavelength settles at various plateaus until the next modal transition occurs at 210 mW.

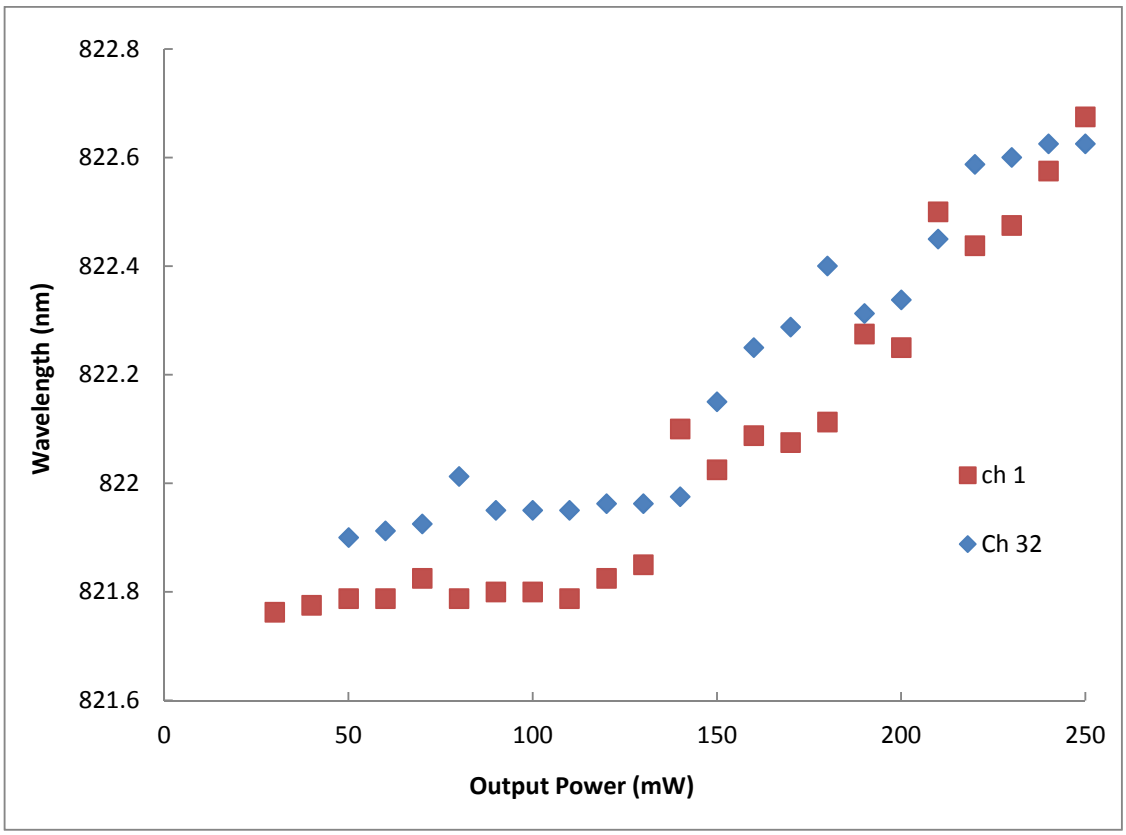

Figure 6-13: Centre wavelengths as a function of output power from channels 1 and 32 when running alone.

To enable the direct comparison of a single emitter running alone as opposed to running in parallel with all its neighbours, a second set of results from the passive module on the CW tester is presented in the next paragraphs and in Figure 6-14, Figure 6-15 and Figure 6-16.

Channel 1 had a fibre aligned to the facet and the power source was ramped in 1 A steps from 3 A to 15 A. All other lasers on the bar were operating at the same input current levels. As expected, a spectral spread, greater than for the case of the emitter running alone on the ASEAL tester (Figure 6-11), is observed. A total range of 3 nm over the input current ramp (828.2 nm at 3 A input compared to 831.6 nm at 15 A) can be observed in Figure 6-14.

There are a number of differences between the two lasers, firstly, the longer wavelength emitted from the passive module compared to the actively cooled ASEAL module. This occurs as all lasers are running, therefore producing heat. There is a much greater shift in

wavelength from lower currents to higher - 3 nm in the passive module compared to 0.8 nm in the ASEAL. The wavelengths are more evenly spread and follow a linear increase, as can be seen in Figure 6-16. The two main reasons for this wavelength behaviour are the effect of thermal crosstalk from neighbouring lasers and the passive conductive cooling compared to the active water cooled ASEAL module.

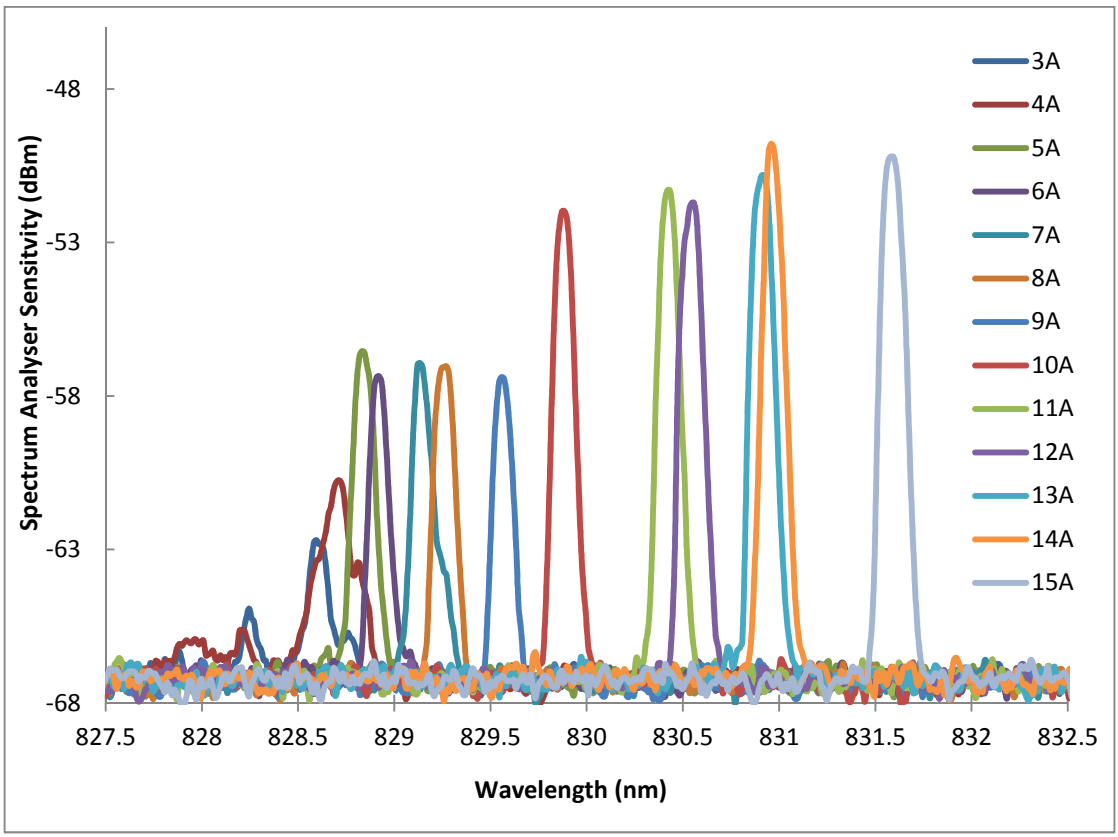

Figure 6-14: Output spectra as a function of input current from Channel 1 of passive module with all emitters on.

Moving to look at the spectra of the middle channel, 32, on the laser bar, the spread increases even more drastically. This can be seen in Figure 6-15 where an input current of 4 A gives a peak wavelength of 828 nm – the same as channel 1, but at higher currents, such as 15 A, the centre wavelength is now at 832.6 nm compared to 831.6 nm for channel 1.

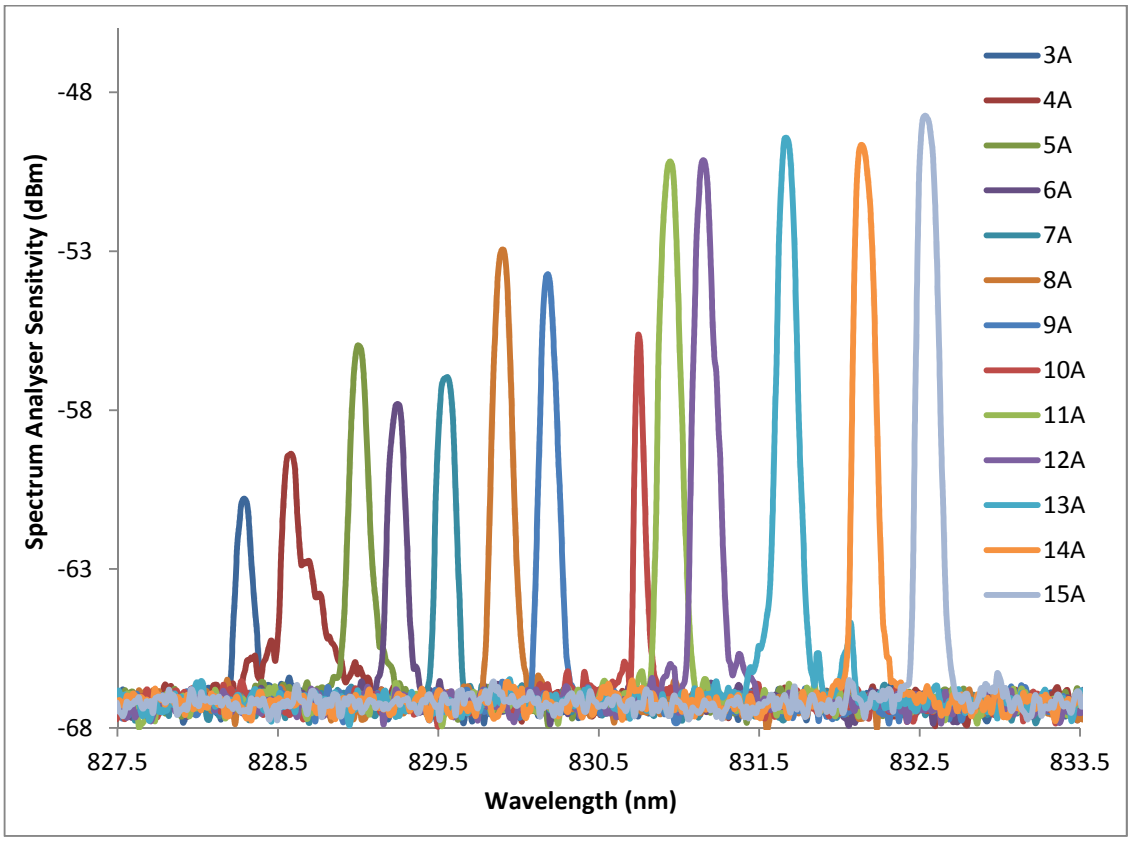

Figure 6-15: Output spectrum as a function of input current from Channel 32 of passive module with all emitters on.

The fact that there is a more linear increase in centre wavelength as current increases (Figure 6-16) indicates a stable thermal equilibrium, where the cavity of the laser under investigation is already thermally activated so that there is not the same “shock” in moving to higher powers/currents. It results in a smoother transition from one input current set point to the next. The slope of channel 32 is almost linear compared to channel 1. With less thermal impact on channel 1 - due to having neighbours on one side only - there is a more gradual progression in increasing wavelength until it reaches approximately 9 A, from which current point it starts to increase more rapidly. This is similar to the two channels in the ASEAL module in Figure 6-13. As can be seen, there is less mode hopping and a more linear increase in wavelength. This is due to the thermal influence of neighbouring emitters, aiding the heating of the emitter under test. The wavelengths are already longer, approximately 10nm at maximum output power indicating a strong thermal effect.

The influence of the neighbouring emitters clearly pushed the wavelength of any of the centrally positioned lasers on the bar to higher values. This larger drift in centre wavelength for the middle channels is what needs to be considered and then corrected in order to achieve a narrow spectrum.

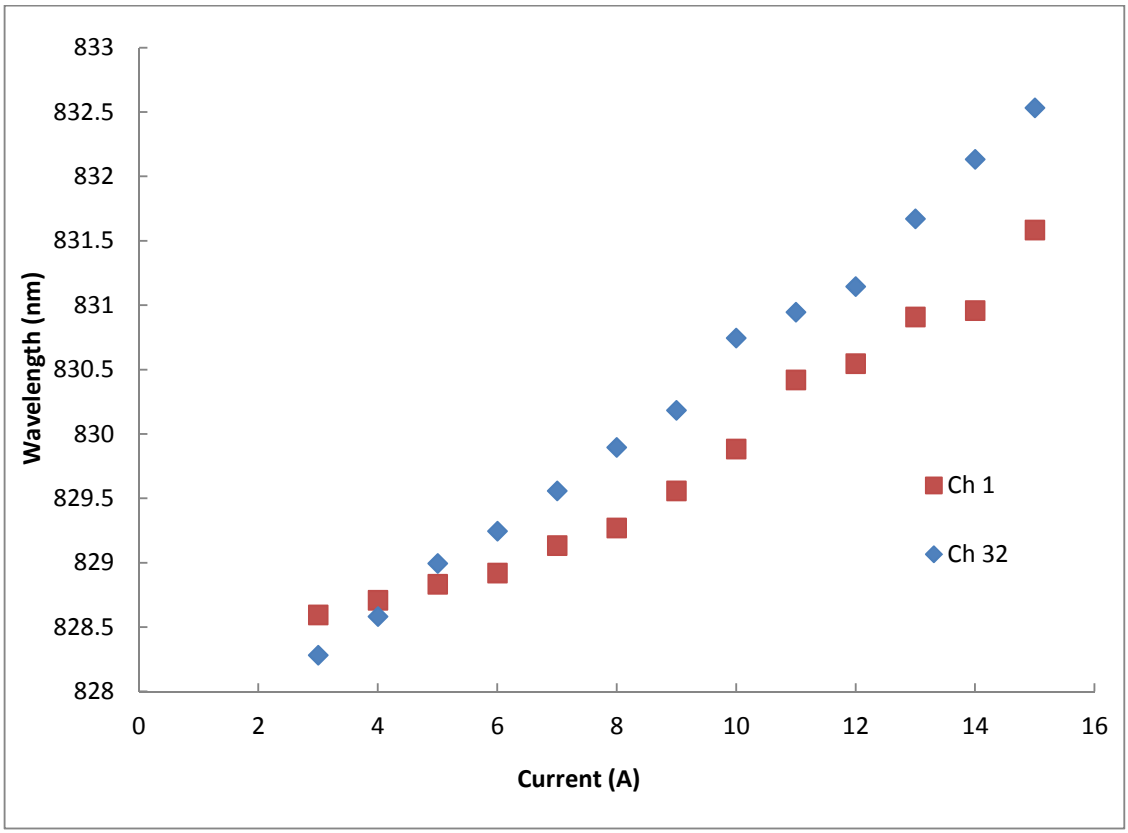

Figure 6-16: Centre Wavelength as a function of output power from channels 1 and 32 of the passive module with all emitters on.

The overall shift in wavelength is best seen in Figure 6-17, which demonstrates very clearly how the central wavelength of an emitter increases with output power and therefore temperature. The graph shows the difference in wavelength behaviour of a selection of channels (1, 8, 16, and 32) depending on their position on the diode bar, including the emitters discussed previously in this section. A single emitter (emitter 1 from Figure 6-11) from the ASEAL module is also included for reference and comparison.

In Figure 6-17 it can be clearly seen that heating affects all emitters and that from approximately position 8 there is a step up in thermal effect which correlates to the cited modelled data (64) in Section 3.2.3 that neighbours up to five positions away have an effect on a laser's output wavelength.

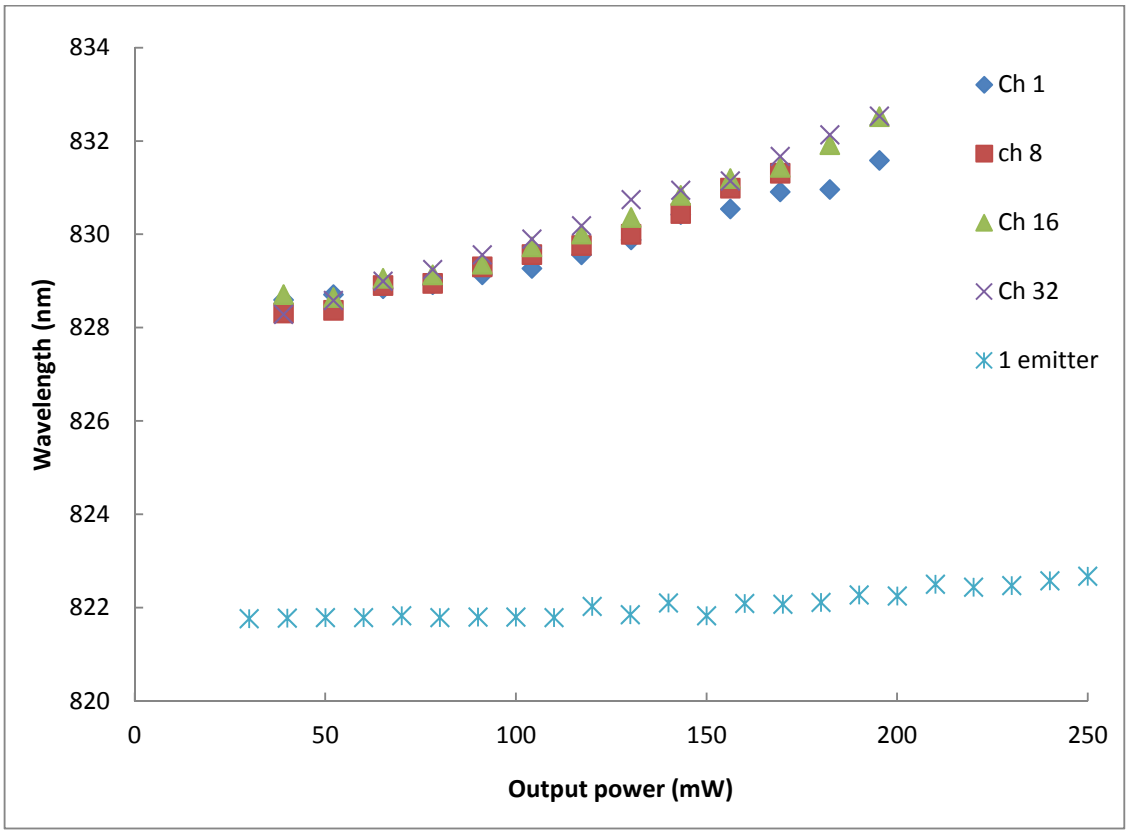

Figure 6-17: Centre wavelength as a function of operating power of channels 1, 8, 16, 32 on the passive device with all emitters running, and 1 emitter running alone on actively cooled module.

Now that extensive analysis of the behaviour of the lasers has been undertaken, the next step is to see if a tuning of a group of emitters is possible.

What also must be considered is that reducing the power to achieve a certain wavelength in one emitter will have a knock-on effect. As that laser is then producing less power, it is consequently producing less heat; therefore its effect on its neighbours is lessened, thus affecting that output wavelength.

6.4 Spectrum of tuned emitters

To finish the experimental section, an attempt was made to spectrally align or overlap the outputs from a group of emitters. This was attempted on the ASEAL tester as it allows individual drive current control of the emitters. The only drawback to this tester is that it is impossible to align a fibre to the facets of the lasers to probe the wavelength of each emitter individually. This is due to the tester construction and set up, which is shown in Figure 6-6. This makes the task all the more difficult as the current inputs must be blindly manipulated while observing changes to the spectrum on the spectrum analyser.

Channels 32 to 37 were selected to be the test population. All other emitters were powered off while the experiment was in progress. Initially, the individual spectra of the channels were recorded at an operating power of 200 mW and are graphed in Figure 6-18. The purpose of this exercise was to check the total wavelength spread and the minimum potential spectral width achievable.

The overall spread of the emitters is 0.5 nm, from the rising half max of emitter 36 to the falling half max of emitter 33.

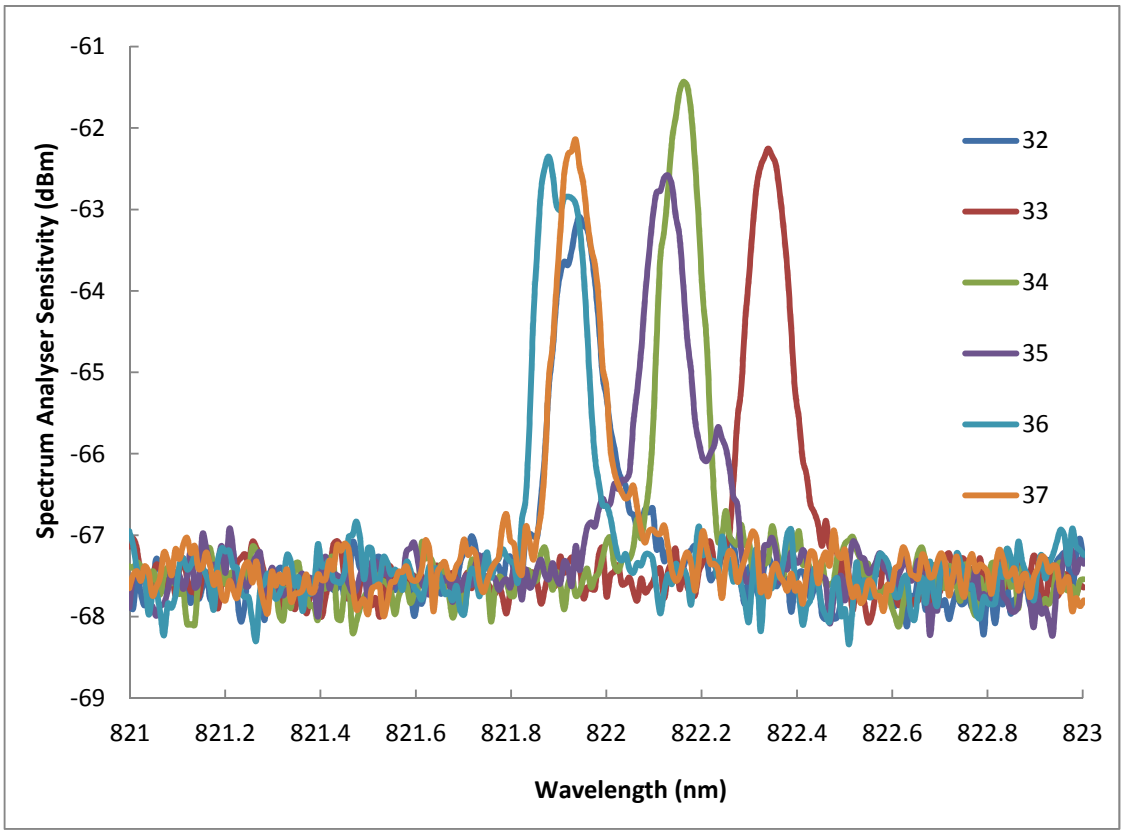

Figure 6-18: Individual spectra of channels 32-37 each operating individually at 200mW.

To see what the starting point of the tuning process would be, a spectrum of the emitters running together was recorded and can be viewed in Figure 6-19. In comparison to the individual spectra viewed as a cluster in Figure 6-18 to the overall spectrum, there is a wavelength shift, whereby the rising half max occurs at 822.4 nm in the combined spectrum, compared to 821.9 nm in the individual spectrum. The FWHM of the combined spectrum is 0.6 nm. Therefore there is a 0.1 nm increase in the spectral width, which comes about because of the heat generated. It is for the same reason that a shift to higher wavelengths in the entire spectrum occurs. This is an interesting observation because, as mentioned in previous sections, the influence of the nearest five neighbours is greatest and, by using only six emitters, a shift in wavelength can already be seen.

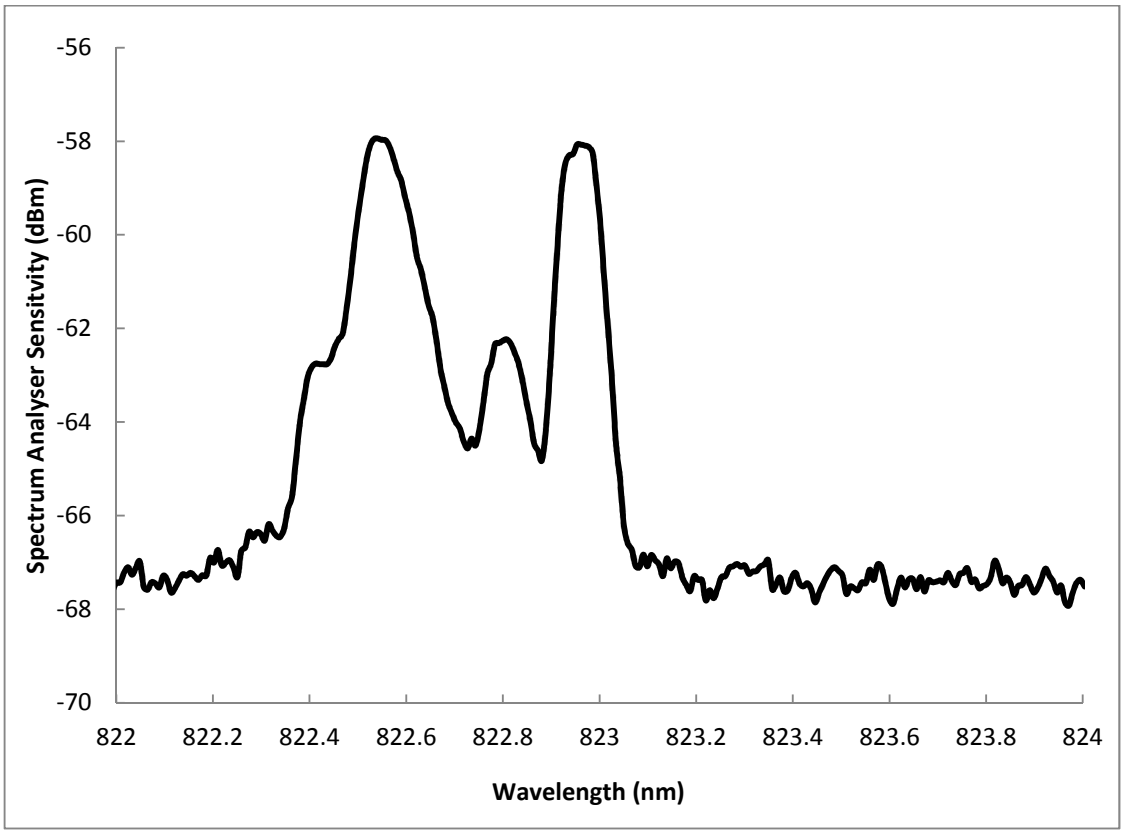

Figure 6-19: Spectrum of emitters 32-37 each running at 200mW output power (1.2W total power).

The task of tuning the emitters was a slow process. The simplest method was to switch on one emitter, in this case emitter 32, at 200 mW, then add emitter 33 also at 200 mW. To reduce these two emitters combined spectrum was straightforward. Adding the third emitter, 34 made the scenario more complex and the spectrum is shown in Figure 6-20. The emitters were set at 230 mW, 220 mW and 150 mW output power respectively. 150 mW would be on the limit of creating a thermal impact, so increasing it to higher levels would have required changes in lasers 32 and 33 inputs. A FWHM of 0.26 nm was achieved at a peak wavelength of 823.01 nm. The following emitters were then switched on in turn and tuned as closely as possible to merge with the already established peak.

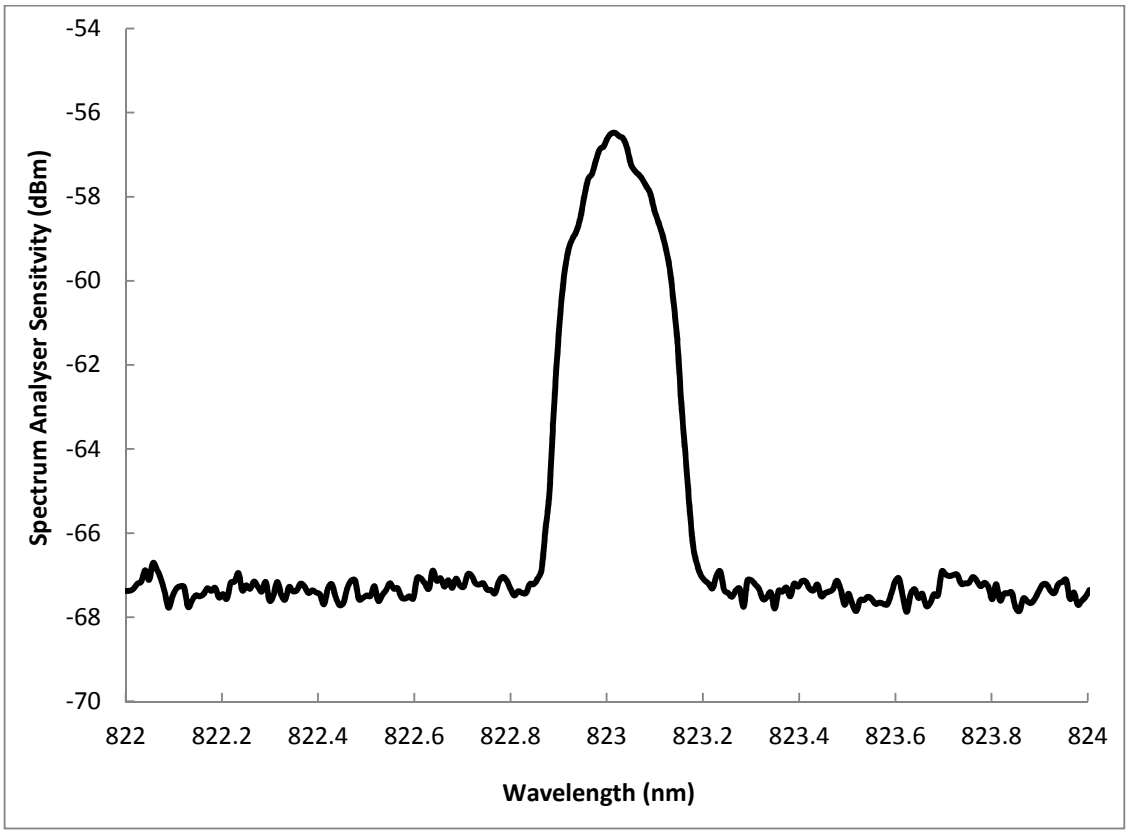

Figure 6-20: Spectrum of emitters 32, 33, 34, tuned.

The previously switched emitters, i.e. 32 – 34, also required retuning as thermal effects from the newly powered-on lasers caused heating effects to propagate to neighbouring lasers. It was mainly the most recent laser which required retuning, e.g. if emitter 35 was turned on then emitter 34 required manipulation. Eventually, emitters 32 to 36 were running and the tuning process became more complex with minute adjustments required and the process had to be restarted a number of times. The end result of the tuning, as best as manually possible, is displayed in Figure 6-21.

The output powers of the lasers, 32 – 36 used in the final tuning were as follows: 205 mW, 200 mW, 210 mW, 205 mW, and 230 mW respectively. Compared to the previous configuration in Figure 6-20 with only three lasers, the five laser array maintained wavelength at 823.01 nm and a FWHM of 0.26 nm, so there was no change, even with added power. Total output power at 823.01 nm was 1.05 W.

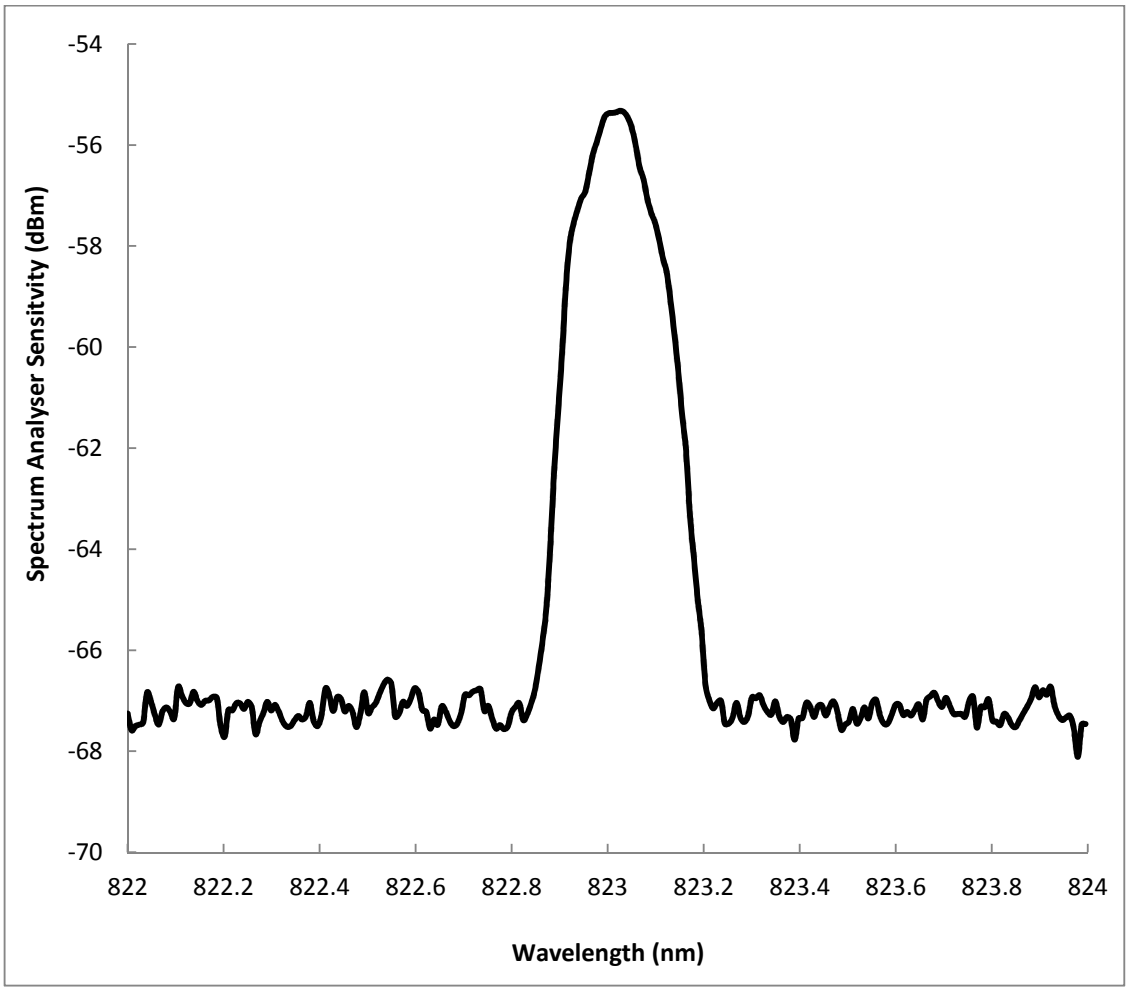

Figure 6-21: Spectrum of emitters 32 -36, input current tuned.

As the lasers were in a settled thermal state, adding another laser disturbed the equilibrium. Lasers had to be added slowly, by ramping up the current in small increments. If a laser was added suddenly, as is the case in Figure 6-22, it disturbed the entire spectrum and the tuning would have to start again, or at powers around 100 mW, where there is still minimal thermal impact, and slowly ramped up again to have a constructive contribution to the spectrum.

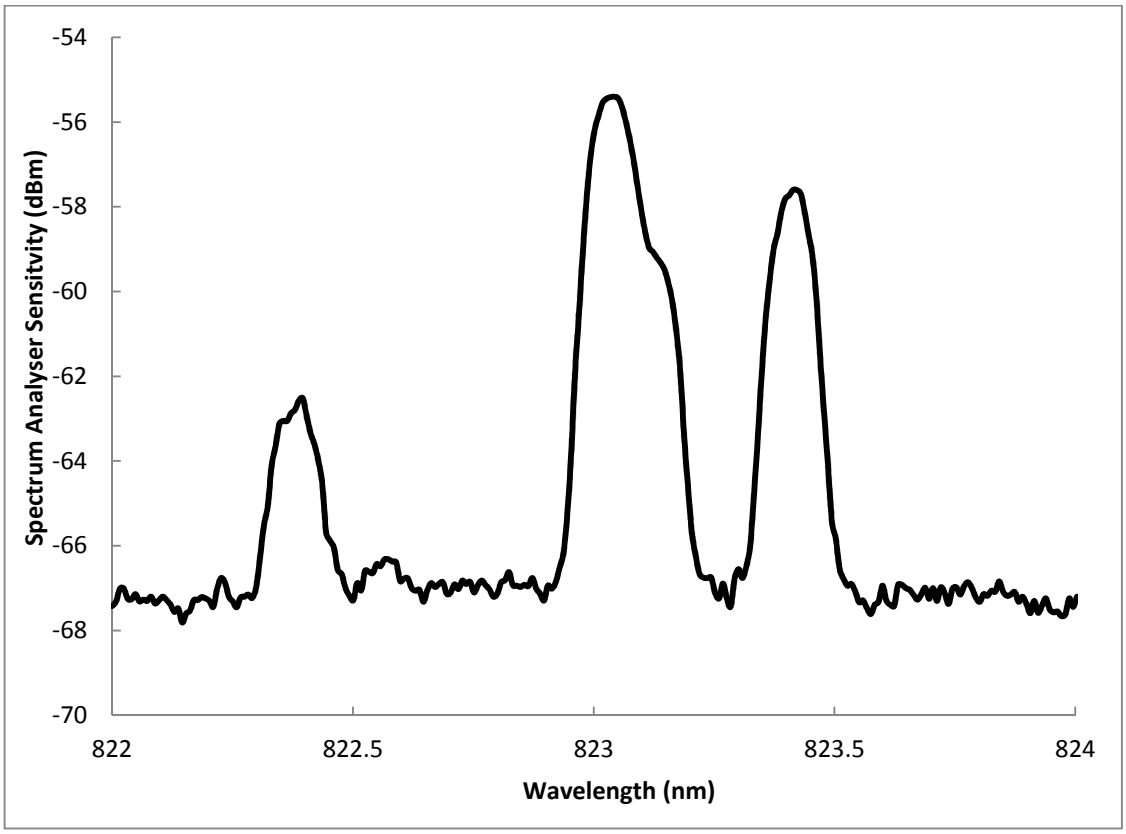

Figure 6-22: Spectrum of emitters 32-36, tuned and then emitter 37 powered on at 230 mW.

6.5 Conclusion

This chapter has gone into greater depth on the individual characteristics of the lasers on the two modules. The spectrum of the full bar, with all emitters active, was examined and compared to the spectra of each of its individual emitters while running in an independent state. This showed the individual traits of the lasers, their peak wavelength, spectral width and intensity, and how they contributed to the overall spectrum profile of the bar.

Comparisons were made to a laser bar where emitter spectra were captured from each laser with all other emitters also running. The influence of the thermal crosstalk from neighbouring active lasers on wavelength shift per emitter was examined giving a wavelength profile for the bar. This demonstrated the areas of highest thermal load and where wavelength shifted most. It can be clearly seen that thermal impact on emitters in the middle of the bar plays a huge role in the wavelength shifts seen in comparison to those on the edges.

With this information, the possibility to tune the individual lasers was possible. A number of emitters, grouped together, were switched on to create a mini laser bar. The tuning of this group of emitters required several adjustments as modes hopped with changes in input current and therefore thermal load. As seen in Figure 6-13, the lasers had a tendency to jump at certain points in their Wavelength-Current curves so low increments of 5 mW steps were

used to adjust each laser. It's also known that AlGaAs lasers can be ramped to higher temperatures thus enabling temperature tuning to adjust the wavelength and increase the range.

Five lasers would be the maximum that is possible to adjust by hand. Beyond this, a fast scanning fibre with wavelength feedback to the power source would be needed to make swift precise changes. However, these results show that it can be done.

7. Conclusion and Future Perspectives

From the outset, the goal of the thesis was to tune individual emitters of a laser diode bar to align and overlap their emission spectra to form a high powered, narrow bandwidth signal with a view to their potential use in the field of remote or stand-off spectroscopy. It set out to find a way to harmonise the spectrum of a laser diode bar using control of the current source to tune the wavelengths of each individual emitter. The idea is to substitute the use of external gratings to select a wavelength band but to also minimise power losses.

The main findings were broken into two specific chapters, 5 and 6, and are discussed briefly by way of conclusion at the end of the chapters. The main question was: could the individual emitters on laser bar be tuned by way of current control to greatly reduce the spectral width of the overall output signal?

By looking at a standard, simple, single current source multi-emitter device and examining the wavelength fluctuations, a method to address individual lasers by selecting a unique current source per emitter provided the opportunity to investigate the interaction between the emitters. By individually addressing the lasers, the element of control over the bar increased, allowing manipulation of the wavelengths. The work carried out measured the differences in wavelength across a 64 emitter, single lateral mode laser bar mounted in two different ways and operating under different conditions. Having investigated the characteristics of the lasers running individually - and also alongside other emitters - it can be clearly seen that the mount used, i.e. passive block or actively water cooled, the position of the laser on the bar, and the source current all play key roles in determining the output wavelength of each emitter.

It was clearly demonstrated that emitters lying near the edge of the bar were far less affected by thermal impact from other lasers, compared to emitters at or near the middle section of the diode bar. This was shown through the shift in wavelength and then compared to all emitters across the bar. A side feature of this data resulted in a demonstration on detecting the “smile” of a laser diode.

As individual emitters, the lasers provided a narrowed spectrum of ≈ 0.1 nm but, once merged within a full bar, this resolution was impossible to maintain with a common current source powering all lasers. Various methods could be used to filter for the desired band of

light but with the loss of much optical power. The aim was to maintain optical power, but at the same time obtain a narrow spectral range of signals emitted from the laser bar. The lasers on both modules exhibited their individual wavelength characteristics, while all lasers (across both modules) were similar in terms of peak wavelength position and intensity. The interaction with neighbouring lasers changed the way they operated drastically. Emitters operating alone showed a step-wise increase in wavelength after a certain thermal threshold was reached. This did not occur in the emitters under thermal influence from its neighbours.

The limitation of the research was the inability to align a fibre to the tuneable module. The tuning could only be performed blind by hand, with feedback via the integrating sphere to the spectrum analyser, checking for changes in the spectrum while changing input currents of the emitters. Going forward, to execute the alignment of the emission spectra, the mounting of a fibre on a pre-programmed positional stage is required. The fibre would then scan each emitter, providing feedback on wavelength so the drive current to the emitter can be adjusted to ensure maximum wavelength overlap with all other emitters.

As shown in chapter 6, varying the power from one emitter has a thermal impact on neighbouring emitters, so multiple iterations of scanning and current adjustments would need to be made to achieve the desired result. An even better approach would employ multi-fibre fixture to probe several emitters in parallel, a tentative suggestion of ten fibres fixed equidistant, matching the pitch of the diode bar, returning ten wavelength signals could work. The suggestion is ten, based on the thermal information gathered from the modelling research cited (64), and the experimental work carried out where the five closest neighbours have the main thermal impact on a particular emitter. As seen in the results, even manual adjustment works with a smaller number of emitters, by carefully and slowly increasing or reducing the input current to shift the emitters spectra into a narrowed spectral width.

While the use of such a laser module for long range spectral applications would require further examination in terms of beam stability and shaping, with the use of an optical corrector mounted to the front facet of the module to account for the high divergence from a laser diode, it is hoped that this work at least shows the possibility of achieving that aim.

As mentioned in the introduction, the 0.1 nm spectral width range of these lasers would enable them to be used for materials processing and plasma analysis. As the devices here are multiple longitudinal mode, a much narrower line width is not possible; however using single longitudinal mode lasers would enable atmospheric (cold) gas detection if the required power can be achieved by using a similar method to tune wavelengths of multiple emitters. The

lasers used in this thesis could still be used with analysis of the returned spectrum showing absorption dips as a result of scatter from particular molecules.

References

1. **Hering, Peter, Lay, J.P. and Stry, Sandra.** *Laser in Environmental and Life Sciences.* s.l. : Springer, 2004.

2. **Faber, Sandra M.** *Spectrometer.* s.l. : World Book Multimedia Encyclopedia, 2004.

3. **D.C. Hanna, M.A. Yuratich, D. Cotter.** *Nonlinear Optics of Free Atoms and Molecules.* New York : Springer-Verlag, 1979.

4. **Siegman, A. E.** *Lasers.* s.l. : University Science Books, 1986.

5. **Griem, Hans R.** *Principles of Plasma Spectroscopy (Cambridge Monographs on Plasma Physics).* s.l. : Cambridge University Press, 2005.

6. *Empirical fits to the Voigt line width: A brief review.* **Olivero, J.J. and Longbottom, R.L.** 2, s.l. : Cambridge University Press, 1977, Journal of Quantitative Spectroscopy and Radiative Transfer, Vol. 17.

7. *Temperature dependence of atomic spectral line widths in a plasma.* **Zmerli, B., Nessib, N. Ben and Dimitrijevic, M.S.** Tunis : Springer-Verlag, 2008, The European Physics Journal, Vol. D.

8. *Experimental determination of the Stark widths of Pb I spectral lines in a laser-induced plasma.* **Alonso-Medina, A.** 5, s.l. : Elsevier, May 2008, Spectrochimica Acta Part B: Atomic Spectroscopy, Vol. 63, pp. 598-602.

9. **Lichtgarm, Fred.** *Trace Gas Sensor. US 4235690 A* USA, 11 May 1979. Grant.

10. *Frequency-agile, rapid scanning spectroscopy.* **Truong, G.-W., et al., et al.** 7, 28 April 2013, NATURE PHOTONICS, pp. 532–534.

11. **Weber, Marvin J.** *Handbook of Laser Wavelengths.* Berkeley, California : CRC Press, 2010. 142005015X.

12. **Waynant, Ronald W. and Ediger, Marwood N.** *Electro-optics Hanbook.* Rockville, Maryland : McGRAW-HILL, INC., 2000. ISBN 0-07-068716-1.

13. **Hollas, J. Michael.** *Modern Spectroscopy.* s.l. : Wiley, 2004.

14. **Harris, Daniel C. and Bertolucci, Michael D.** *Symmetry and Spectroscopy: An Introduction to Vibrational and Electronic Spectroscopy.* s.l. : Courier Dover Publications, 1989. 9780486661445.

15. **Bernath, Peter F.** *Spectra of Atoms and Molecules.* s.l. : Oxford University Press, 2005. ISBN 978-0-19-517759-6.

16. **Housego, Gooch and.** Narrow linwidth DFB lasers. *Gooch and Housego.* [Online] http://goochandhousego.com/product/narrow-linewidth-dfb-laser-modules/.

17. *A Method of Adjusting Wavelengths of Distributed Feedback Laser Arrays by Injection Current Tuning.* **Hou, Jie, et al., et al.** 6, December 2012, IEEE photonics Journal, Vol. 4.

18. **Rüdiger, Paschotta.** *Encyclopedia of Laser Physics and Technology.* Berlin : Wiley-VCH, 2008. 978-3-527-40828-3.

19. *Differential Absorption Lidar Using NH3-CO2 Laser.* **Vasil'ev, Boris I. and Mannoun, Oussama M.** Long Beach, California : Optical Society of America, 2006. Conference on Lasers and Electro-Optics. p. CThT2. ISBN: 1-55752-813-6.

20. **Silfvast, William T.** *Laser Fundamentals.* s.l. : Cambridge University Press, 2008.

21. **Weber, Marvin J.** *Hanbook of Lasers.* Boca Raton : CRC Press LLC, 2001.

22. **Schubert, E.F.** *Light Emitting Diodes.* s.l. : Cambridge Univserity Press.

23. *Optimised Fabry-Perot (AlGa)As quantum well lasers tunable over 105 nm.* **Mehuys, D., Mittelstein, M. and and Yariv, A.** 143, 1989, Vol. 25.

24. *Laser oscillations from quantum states in very thin GaAs-Al0.2Ga0.8As multilayer structures.* **van der Ziel, J.P., et al., et al.** 1975, Applied Physics Letters, Vol. 26, pp. 463-465.

25. *A model for GRIN-SCH-SQW Diode Lasers.* **Chinn, Stephen R., Zory, Peter S. and Reisinger, Axel R.** 11, November 1988, IEEE Journal of Quantum Electronics, Vol. 24, pp. 2191-2214.

26. **Goldwasser, Samuel M.** resonators. *Sam's Laser FAQ.* [Online] 1994. www.repairfaq.org/sam/laserfaq.htm.

27. **Paschotta, Rüdiger.** *Field Guide to Lasers.* [ed.] John E. Grievenkamp. Washington : SPIE, 2008. Vol. FG12.

28. *A single ion as a nanoscopic probe of an optical field.* **Guthöhrlein, G. R., et al., et al.** s.l. : Nature Publishing Group, 1 Novmeber 2001, Nature, Vol. 414, pp. 49-51.

29. **Newport.** Laser Diode Technology. *Newport.com.* [Online] http://assets.newport.com/web600w-EN/images/1225635.gif.

30. **Moss, S. J. and Ledwith, A.** *The Chemistry of the Semiconductor Industry.* s.l. : Springer, 1987.

31. **Baca, Albert G. and Ashby, Carroll I. H.** *Fabrication of GaAs Devices.* s.l. : IET, 2005.

32. *High Power single mode 980nmAlGaAs quantum well lasers with very low threshlold current.* **Dong, Zhen, et al., et al.** 11, Beijing : s.n., November 2013, Journal of Semiconductors, Vol. 34, pp. 114011-1 - 114011-4.

33. II-VI homepage. *Laser Enterprise.* [Online] [Cited: 15 07 2014.] http://www.laserenterprise.com/.

34. *High power diode laser arrays.* **Endriz, John G., Vakili, Mitral and Gerald S., Browder.** 4, s.l. : IEEE, 1992, IEEE Journal of Quantum Electronics, Vol. 28, pp. 952-965.

35. **Graydon, Oliver.** Laser diode bars break 400W barrier. *Optics.org.* [Online] 25 August 205. http://optics.org/article/22991.

36. **Diehl, R.** *High Power Diode Lasers: Fundamentals, Technology, Applications.* Berlin : Springer, 2000.

37. **Sheehy, Brian.** Original work. s.l. : Laser Enterprise gmbh, 2014.

38. *Growth of III-V Semiconductors by Molecular-Beam Epitaxy and their properties.* **Cho, A.Y.** 1983, Thin Solid Films, Vol. 100, p. 291.

39. *Molecular Beam Epitaxy.* **Cho, A.Y. and Arthur, J.R.** 1975, Progress in Solid State Chemistry, Vol. 10, p. 157.

40. **Esaki, L. and Tsu, R.** *"Superlattice and Negative Conductivity in Semiconductors.* IBM. 1969. Note RC-2418.

41. **Rinaldi, Fernando.** *Basics of Molecular Beam Epitaxy (MBE).* Optoelectronics Department, University of Ulm. Ulm : s.n., 2002.

42. **Ledentsov, Nikolai N.** *Growth processes and surface phase equilibria in molecular beam epitaxy.* New York : Springer, 1999.

43. **Instruments, Veeco.** Veeco Instruments. *http://www.veeco.com .* [Online] 2008.

44. **Porter, D.A. and Easterling, K.E.** *Phase Transformations in Metals and Alloys.* s.l. : Taylor & Francis Group, 1992.

45. **Dhanaraj, Govindhan, et al., et al.** *Springer Handbook of Crystal Growth.* s.l. : Springer Science & Business Media, 2010.

46. **Chambers, Austin.** *Modern vacuum physics.* Boca Raton : Chapman & Hall/CRC, 2005.

47. **Lakowicz, Joseph R.** *Principles of Flouresence Spectroscopy.* 3rd. Baltimore : Springer, 2006. pp. 59-61. ISBN-13: 978-0387-31278-1.

48. *Near- and mid-infrared laser-optical sensors for Gas analysis.* **Werle, Peter, et al., et al.** 27, s.l. : Elsevier Science Ltd, 2002, Optics and Lasers in Engineering, pp. 101-114.

49. **Connolly, Christine.** Environmental monitoring of the air to assess its composition. *Sensor Review.* 2008, Vol. 28, 4, pp. 294-298.

50. *Frequency-modulation spectroscopy for trace species detection: theory and comparison among experimental method.* **Silver, J.A.** 1992, Applied Optics, Vol. 31, pp. 707–717.

51. *Fast Electro-Optic Wavelength Selection and Frequency Mdulation in Solid State Lasers.* **Schulz, P.A.** 3, 1990, The Lincoln Laboratory Journal, Vol. 3.

52. **Clarke, Jim.** Chemguide.co.uk. *Chemguide.* [Online] 2007. http://www.chemguide.co.uk/analysis/uvvisible/beerlambert.html.

53. **K05en01.** wikipedia. *wikipedia.* [Online] http://commons.wikimedia.org/w/index.php?title=User:K05en01&action=edit&redlink=1.

54. *Detection of H2S at the ppm level using a telecommunication diode laser.* **Modugno, G., et al., et al.** 76, 1998, Optics Communications, Vol. 145.

55. STIS absorption spectrum at work. *Hubble Site.* [Online] http://hubblesite.org/the_telescope/nuts_.and._bolts/instruments/stis/stis_a.php.

56. *A review of recent advances in semiconductor laser based monitors.* **Werle, P.** Garmisch-Partenkirchen : Elsevier, 1998, Spectrochimica Acta Part A, Vol. 54, pp. 197-236.

57. *Temporal correlation scheme for spectroscopic gas analysis using multimode diode lasers.* **Somesfalean, G., et al., et al.** 18, 2005, Applied Physics Letters, Vol. 86, pp. 184102–184103.

58. *Multi-mode absorption spectroscopy, MUMAS, using wavelength modulation and cavity enhancement techniques.* **Hamilton, M.L., et al., et al.** 3, Applied Physics B, : s.n., 2010, Vol. 100, pp. 665–673.

59. *Oxygen measurement by multimode diode lasers employing gas correlation spectroscopy.* **Lou, X., et al., et al.** 5, 2009, Applied Optics, Vol. 48, pp. 990–997.

60. **Photonic, Power.** Smile corrector for laser diode bar. *Power Photonic.* [Online] 2013. http://www.powerphotonic.com/wp-content/uploads/2014/01/Smile-Corrector-Data-Sheet.pdf.

61. Gold Based Solder Paste. *Indium.com.* [Online] Indium Corporation, 2014. http://www.indium.com/solder-paste-and-powders/gold-based-solder-paste/.

62. **powerphotonic.** Laser Bar Bonding. *Powerphotonic.* [Online] 2014. http://www.powerphotonic.com/products/smile-corrector/.

63. *Evaluation of Thermal Cycling Reliability of Sintered Nanosilver Versus Soldered joints by Curvature Measurment.* **Jiang, Li, et al., et al.** 5, s.l. : IEEE, 6 May 2014, IEEE transactions on components, packaging and manufacturing technology, Vol. 4, pp. 751-761.

64. **Matuschek, Nicolai.** *Internal report on Thermal Cross Talk of A-SEALs.* Bookham R&D. Zurich : s.n., 2007. Internal Project.

65. **McDonald, J. and Albright, G.** Microthermal Imaging in the Infrared. *Electronic s Cooling.* [Online] January 1997. http://www.electronics-cooling.com/2002/02/high-resolution-real-time-micro-thermal-imaging-steady-state-and-pulse-measurements-on-microscopic-semiconductor-targets/.

66. *Transient thermal properties of high-power diode laser bars.* **Ziegler, Mathias, et al., et al.** 263506, s.l. : American Institute of Physics, 2006, Appl. Phys. Lett., Vol. 89.

67. *Screening of high power laser diode bars in terms of stresses and thermal profiles.* **Tomm, J.W., et al., et al.** San Jose : s.n., 2008. High-Power Diode Laser Technology and Applications VI. Vol. 687619 .

68. *Thermal properties of high-power diode lasers investigated by means of high resolution thermography.* **Kozłowska, Anna, et al., et al.** 2012, Materials Science and Engineering B, Vol. 177, pp. 1268–1272.

69. *Thermal properties of high-power diode lasers investigated by means of high.* **Kozłowska, Anna, et al., et al.** 2012, Materials Science and Engineering B, Vol. 177, pp. 1268–1272.

70. *The thermal properties of AlGaAs/GaAs laser diode bars analyzed by the transient thermal technique.* **Qiao, Yanbin, et al., et al.** 2013, Solid-State Electronics, Vol. 79, pp. 192-195.

71. *Investigations of transient thermal properties of conductively cooled diode laser arrays operating underquasicontinuous-wave conditions.* **Kozlowska, Anna and Malag, Andrzej.** Warsaw : s.n., 2006, Microelectronics Reliability, Vol. 46, pp. 2079-2084.

72. **Colorado, IXYS.** http://www.directedenergy.com. [Online]

73. **Sears, F. W. and Zemansky, M. W.** *University Physics.* Reading MA : Addison-Wesley Publishing Company, Inc, 1964.

74. **Gmbh, Beratron.** Beratron Gmbh - Beryllium. *Beratron Gmbh.* [Online] http://www.beratron.de/en/beryllium.html.

75. *Atotec Germany Gmbh.* [Online]

76. *Semicondictor Lasers for Telecommunications.* **Bowers, J.E. and Pollack, M.A.** San Diego : Academic Press, 1988, Optical Fiber Telecommunications II, p. 512.

77. *Continuously tunable single-mode erbium fiber laser.* **Ball, G. A. and Morey, W. W.** 6, East Hartford, Connecticut : Optical Society of America, 1992, Optics Letters, Vol. 17, pp. 420-422.

78. *Mode-hop-free tuning over 80 GHz of an extended cavity diode laser without antireflection coating.* **Petridis, C., et al., et al.** Fife, Scotland : American Institute of Physics, 21 July 2001, Review of Scientific instruments, Vol. 72, p. 3811.

79. **Balembois, François and Forget, Sébastien.** Optical resonators and Gaussian beams. *http://www.optique-ingenieur.org/.* [Online] [Cited: 28 07 2014.] http://www.optique-ingenieur.org/en/courses/OPI_ang_M01_C03/co/Contenu_13.html.

80. **Hanson, Heather, McGill, Matt and Yorks, John.** *CATS: Measuring Clouds and Aerosols from the International Space Station.* s.l. : NASA, 2007.